SAND2013-10261C

Part 1: A finite-element formulation for general polyhedra in nonlinear solid mechanics
Part 2: Understanding material variability and the accuracy of homogenization in polycrystalline materials through direct numerical simulations

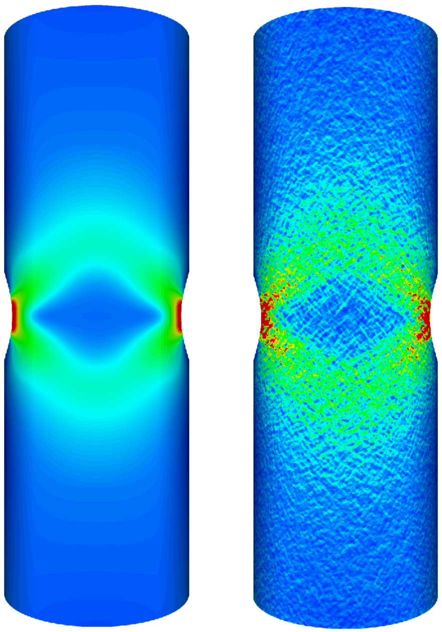

Sandia National Laboratories

Joe Bishop
Computational Structural Mechanics
Sandia National Laboratories
Albuquerque, NM

Seminar at The Institute for Computational Eng. and Sciences (ICES)
University of Texas
Austin, TX
December 5, 2013

U.S. DEPARTMENT OF ENERGY

NNSA National Nuclear Security Administration

Sandia National Laboratories is a multi-program laboratory managed and operated by Sandia Corporation, a wholly owned subsidiary of Lockheed Martin Corporation, for the U.S. Department of Energy's National Nuclear Security Administration under contract DE-AC04-94AL85000.

Outline

1. Polyhedral finite elements
    - motivation
    - harmonic shape functions
    - patch test
    - verification
    - future work
2. Multiscale modeling and material variability
    - review of homogenization theory
        a. weak convergence
        b. effective vs. apparent material properties
        c. type 1 and type 2 material variability
    - direct numerical simulations
3. Summary

Why Polyhedral Elements?

1. Facilitate mesh creation in complex geometries

Bishop, J., 2003, *Computational Mechanics*, 30, 46-478

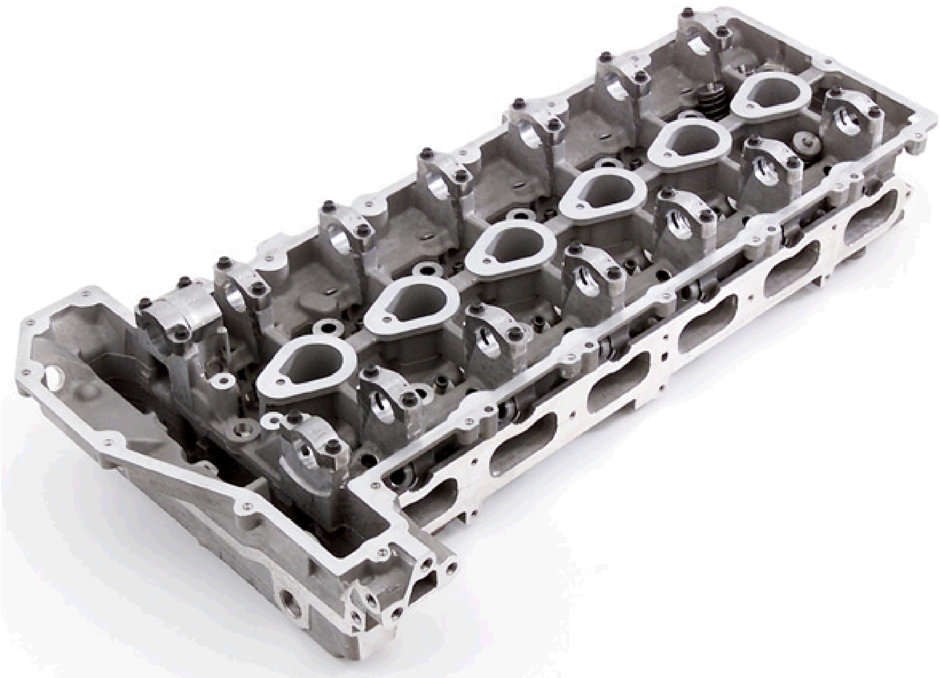

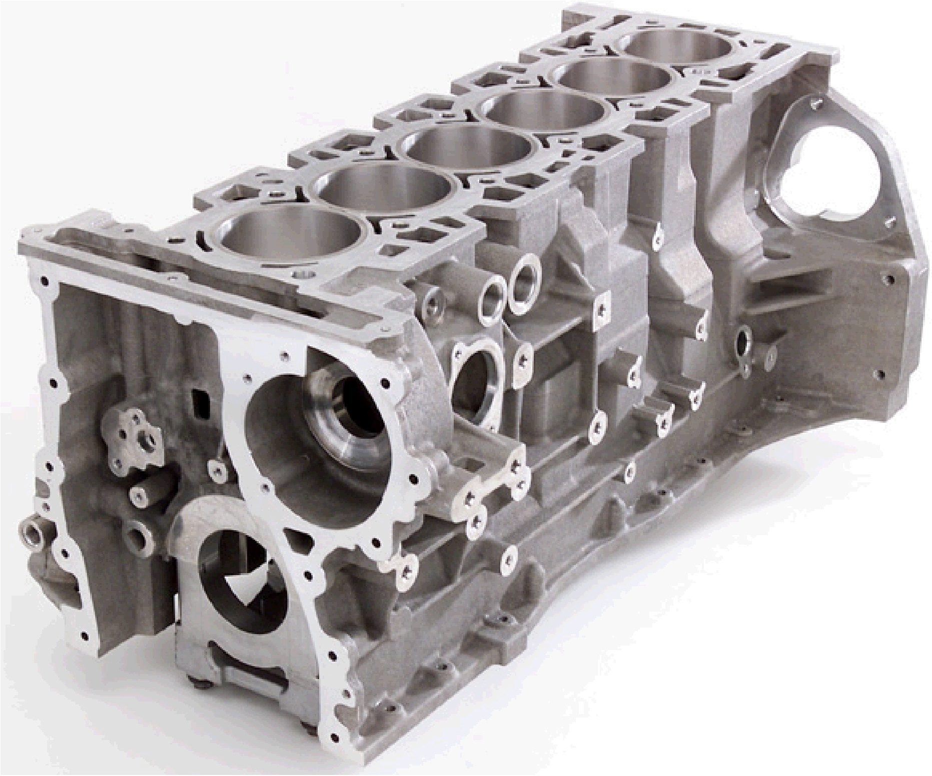

Conventional Meshing

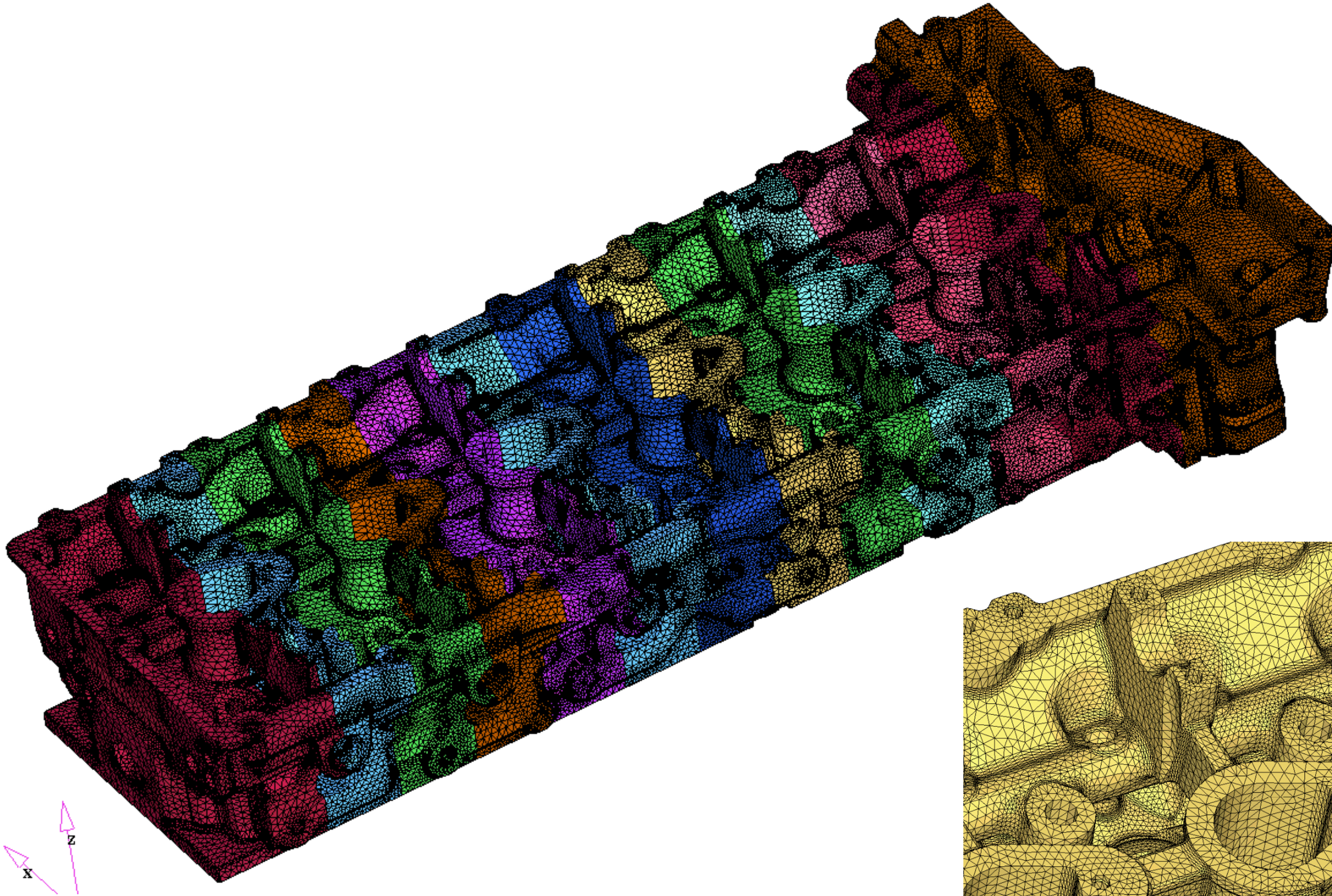

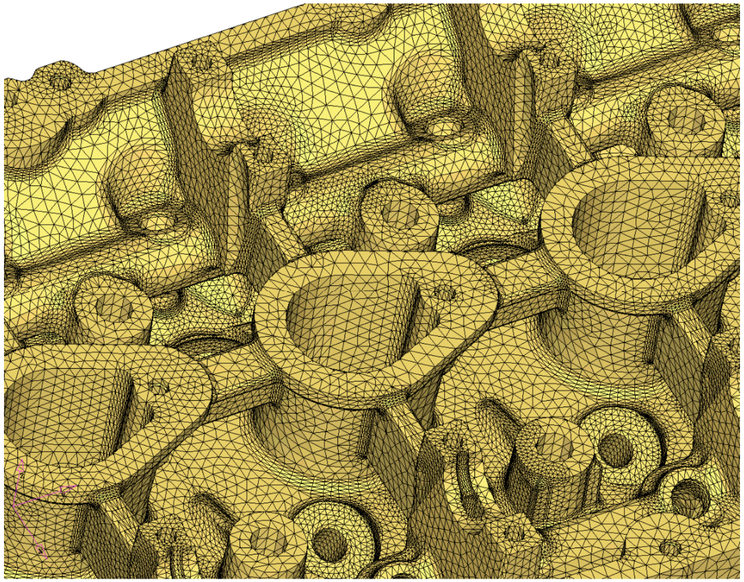

equiv. of 3 man-months of labor

Global-scale hexahedral mesh

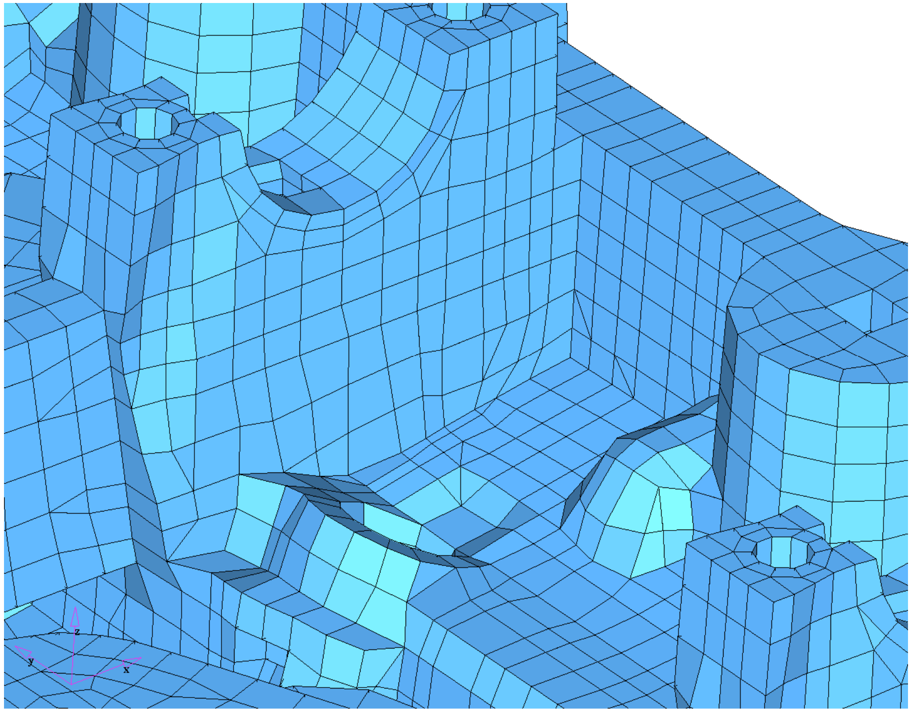

Stress-capable tetrahedral mesh

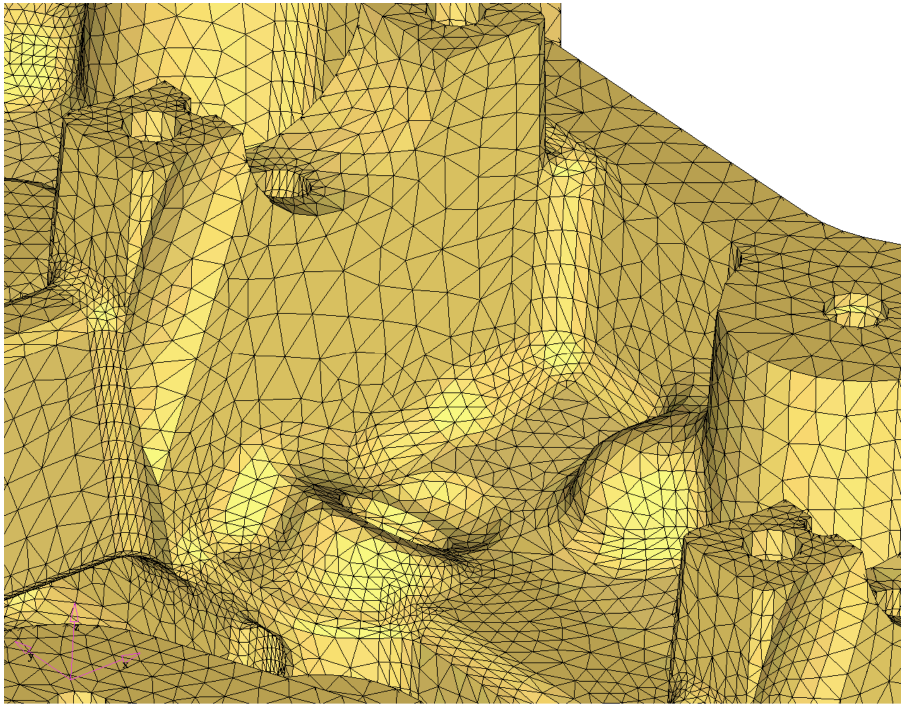

- time intensive
- no adaptivity (heuristics only)

Why Polyhedral Elements?

2. Pervasive fracture modeling on random meshes

Bishop, J., 2009, *Computational Mechanics*, 44, 455-471.

Bishop, J. and Strack, O., 2011, *IJNME*, 38, 279- 306

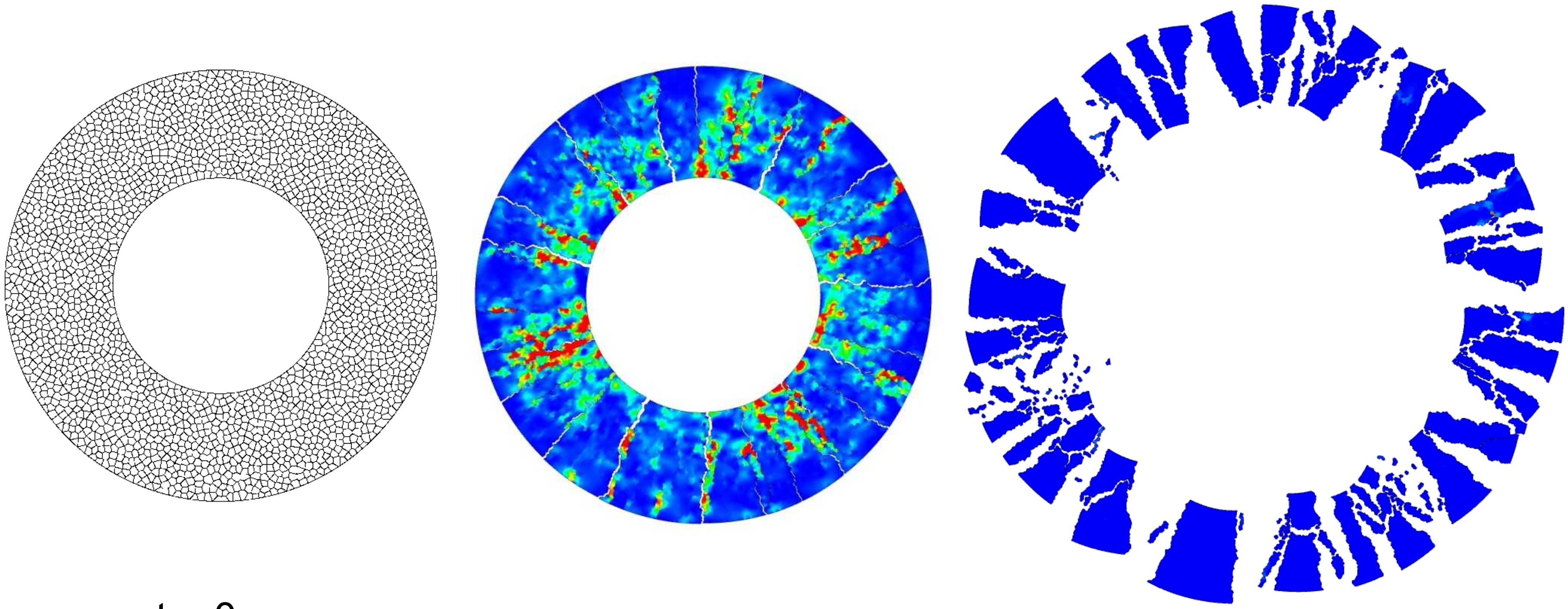

t = 0

t = 2 ms

t = 20 ms

Explosively loaded cylinder

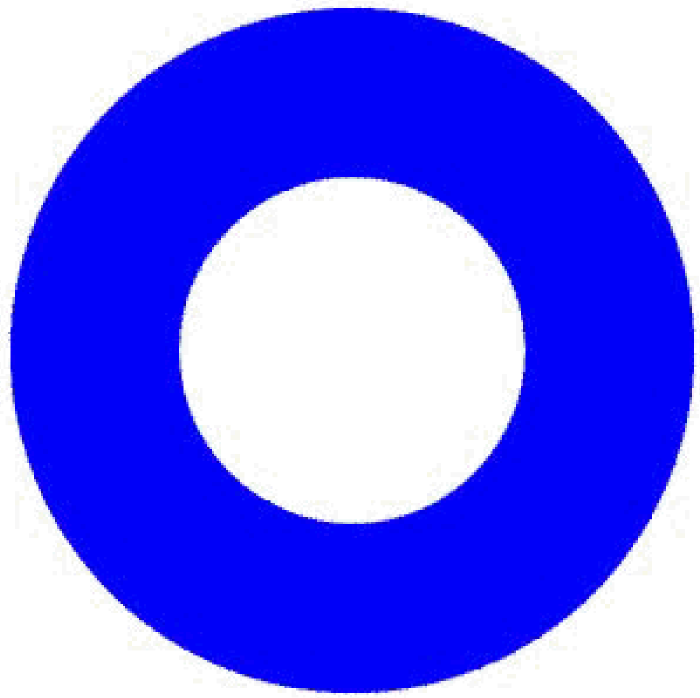

Hydraulic Fracture Simulation

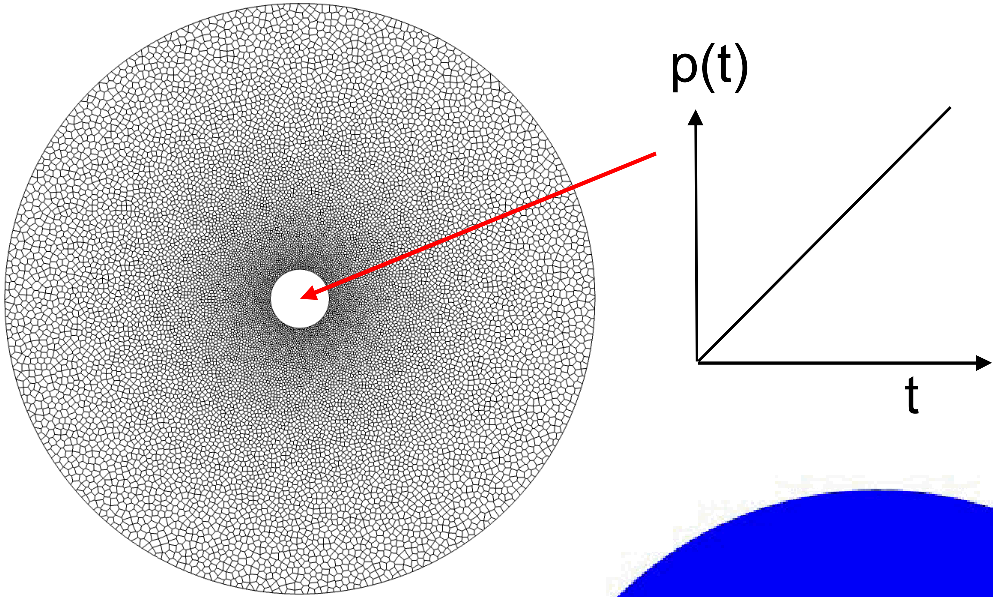

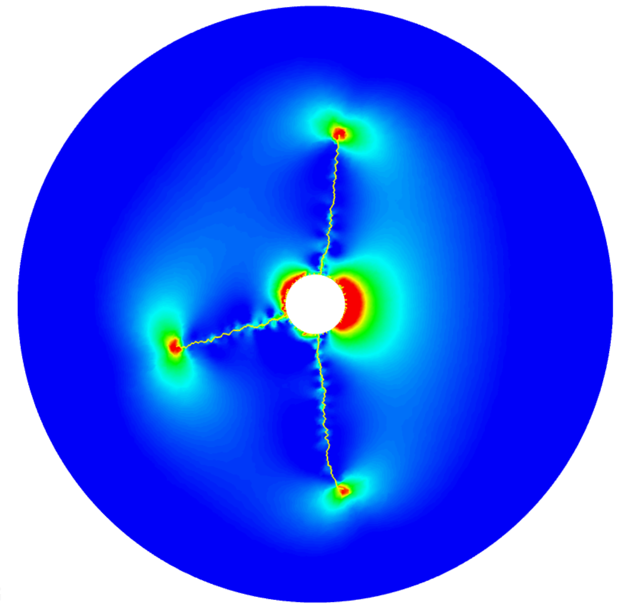

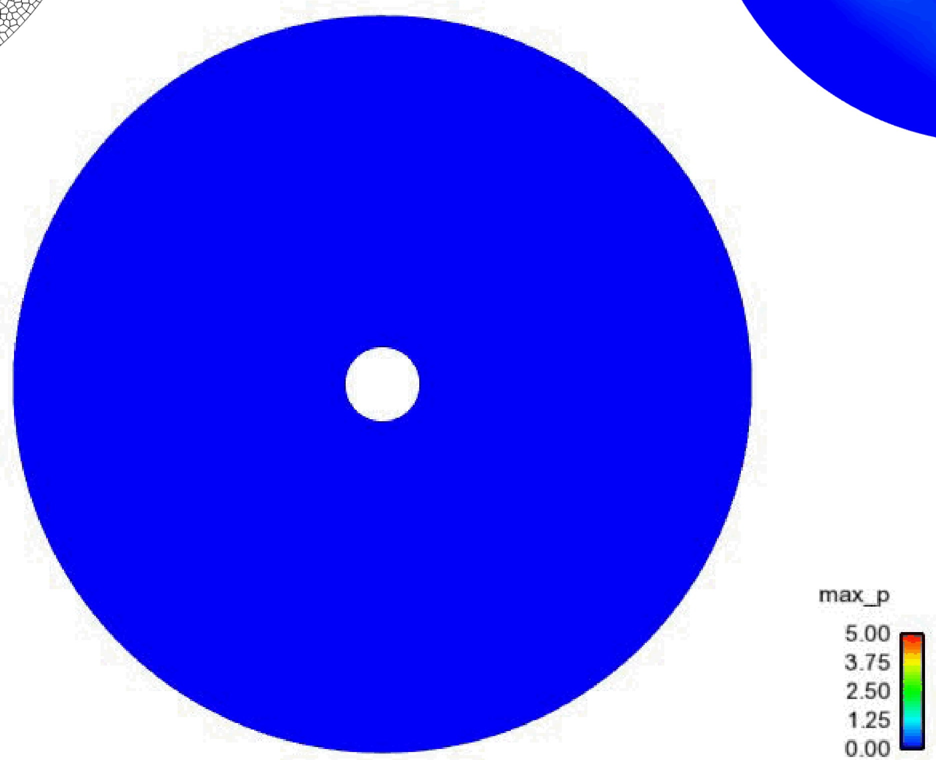

Coupled fluid flow in fracture networks

Lots of Recent Literature on Polygonal or Polyhedral Finite Elements

- Rashid, M.M. and P.M. Gullett, "On a finite element method with variable element topology." *Computer Methods in Applied Mechanics and Engineering*, 2000. 190(11-12): p. 1509-1527.
- Sukumar, N. and A. Tabarraei, "Conforming polygonal finite elements." *International Journal for Numerical Methods in Engineering*, 2004. 61(12): p. 2045-2066.
- Rashid, M.M. and M. Selimotic, "A three-dimensional finite element method with arbitrary polyhedral elements." *International Journal for Numerical Methods in Engineering*, 2006. 67(2): p. 226-252.

  Going to adopt integration rule from here.
- Wicke, M., M. Botsch, and M. Gross, "A Finite Element Method on Convex Polyhedra." *Computer Graphics Forum*, 2007. 26(3): p. 355-364.
- Martin, S., et al., "Polyhedral Finite Elements Using Harmonic Basis Functions." *Computer Graphics Forum*, 2008. 27(5): p. 1521-1529.

  Going to adopt use of harmonic shape functions from here.
- Bishop, J., "Simulating the pervasive fracture of materials and structures using randomly close packed Voronoi tessellations." *Computational Mechanics*, 2009. 44(4): p. 455-471.
- Mousavi, S.E., H. Xiao, and N. Sukumar, "Generalized Gaussian quadrature rules on arbitrary polygons." *International Journal for Numerical Methods in Engineering*, 2010. 82(1): p. 99-113.
- Joshi, P., et al., "Harmonic coordinates for character articulation." *ACM Trans. Graph.*, 2007. 26(3): p. 71.

  and here

Polyhedral Grids in Other Fields

Mimetic Finite Difference

- Brezzi, F., K. Lipnikov, and V. Simoncini, “A family of mimetic finite difference methods on polygonal and polyhedral meshes.” *Math. Models Methods Appl. Sci.*, 2005. 15: p. 1533-1553.
- Brezzi, F., et al., “A new discretization methodology for diffusion problems on generalized polyhedral meshes.” *Computer Methods in Applied Mechanics and Engineering*, 2007. 196(37-40): p. 3682-3692.
- Lipnikov, K., M. Shashkov, and I. Yotov, “Local flux mimetic finite difference methods.” *Numerische Mathematik*, 2009. 112(1): p. 115-152.

Finite Volume

(CD-Adapco, thermal, fluid-structure interaction)

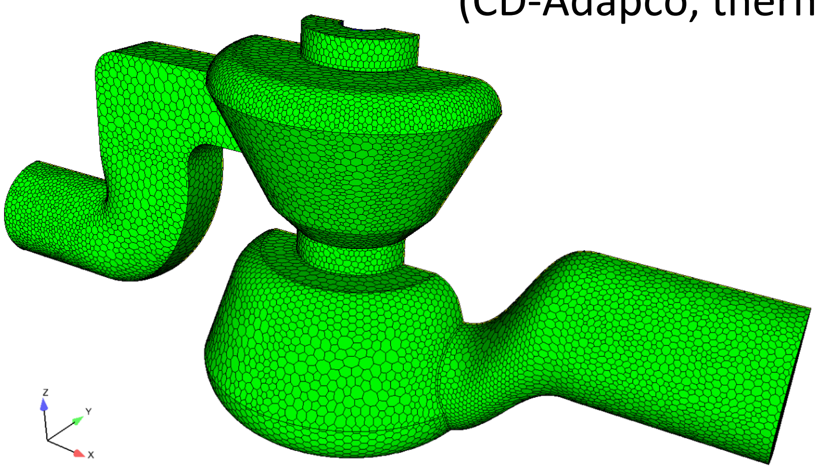

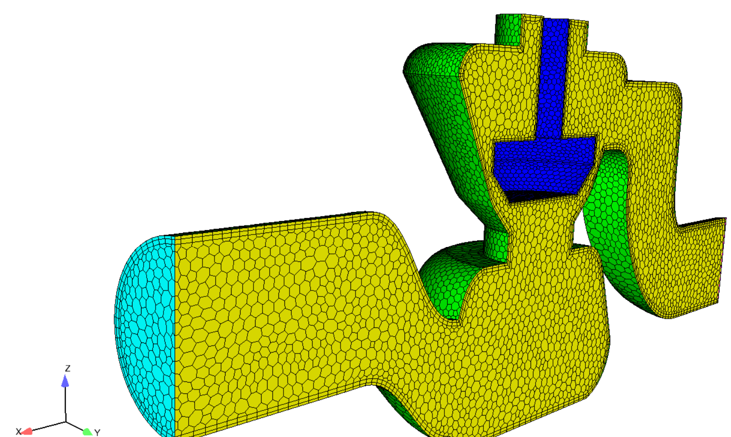

Polyhedral Finite-Element Formulation

Bishop, J., 2014, "A displacement-based finite element formulation for general polyhedra using harmonic shape functions," *IJNME*, (DOI: 10.1002/nme.4562)

- Developed for nonlinear solid mechanics (minimize number of integration points while avoiding artificial stabilization).
- General polyhedra: non-convex with non-planar faces
- Uses harmonic shape functions defined in the original configuration
- Uses total-Lagrangian formulation
- Mean-dilation formulation for nearly-incompressible materials
- Compatible with standard trilinear hexahedron

Star Convexity

For ease of construction, present formulation assumes star-convexity with respect to vertex-averaged centroid.

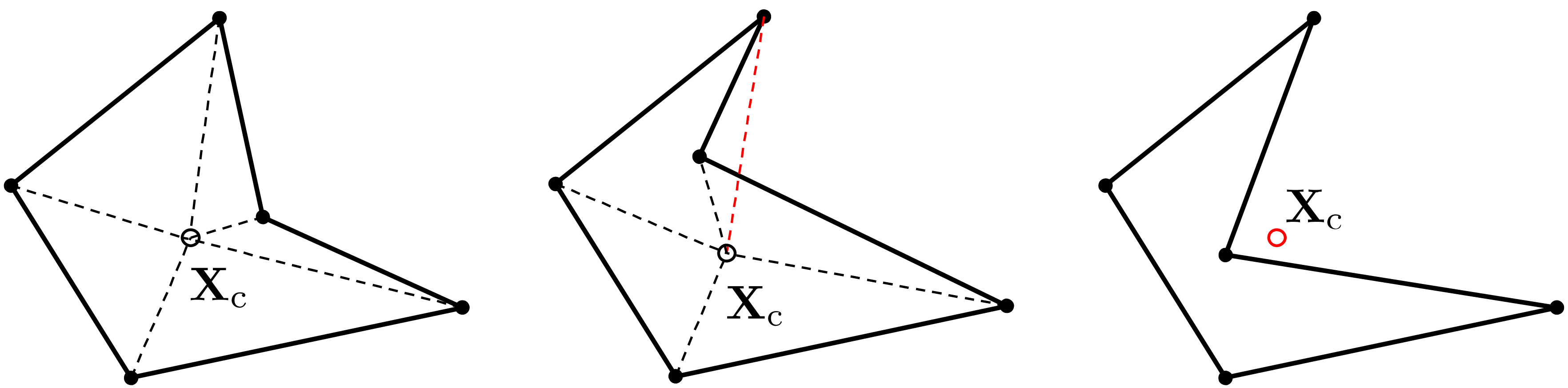

star convex | not star convex | not star convex

How to Fully Specify Face Geometry?

- Use vertex-averaged face centroid.
- Could also use a bilinear mapping for quadrilateral faces.
- Could also use any barycentric mapping.

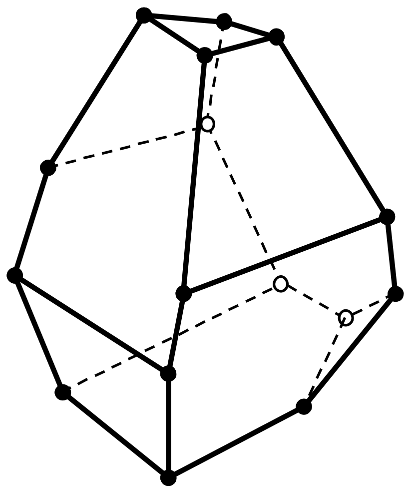

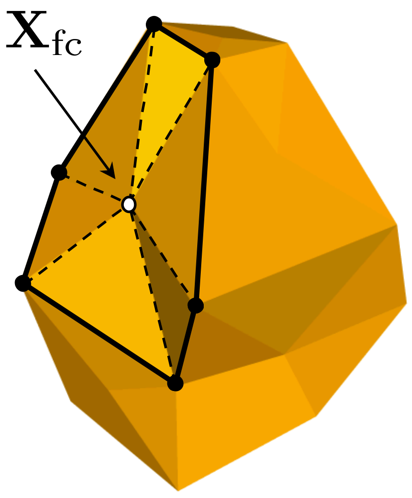

Define Shape Functions Directly on Initial Configuration

Standard trilinear hexahedral mapping using a parent c.s.

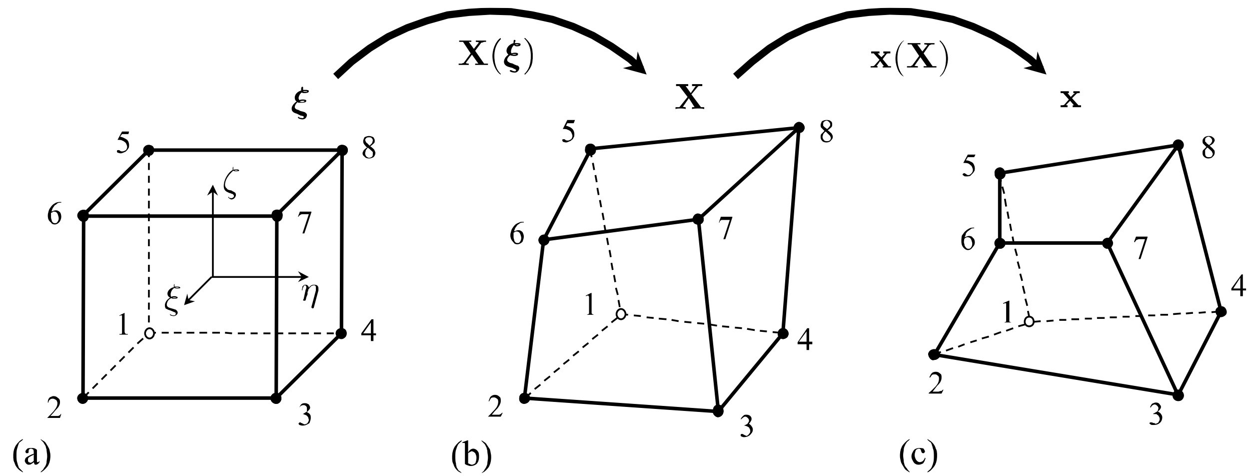

Present formulation defines shape functions directly on initial configuration.

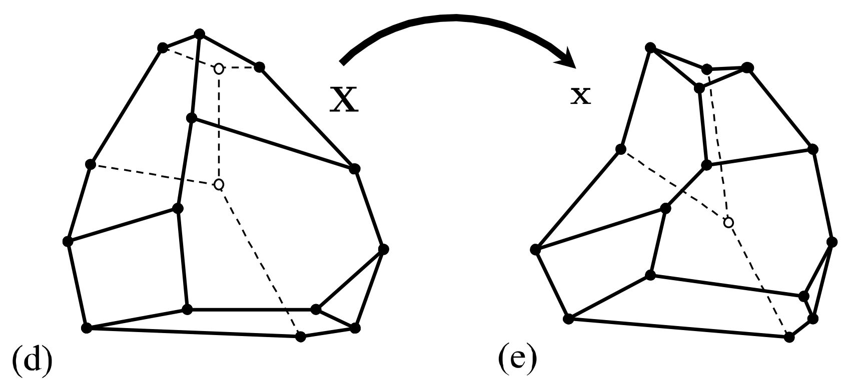

Harmonic Shape Functions

A harmonic function is a solution of Laplace's equation (with appropriate boundary conditions).

$$\nabla^2 \psi = 0$$

Can solve efficiently using BEM, or can just use FEM.

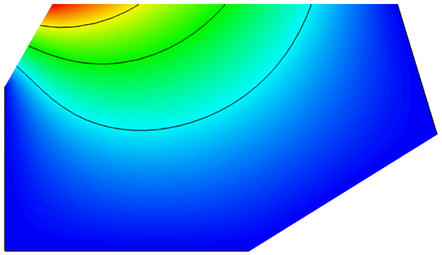

example in 2D

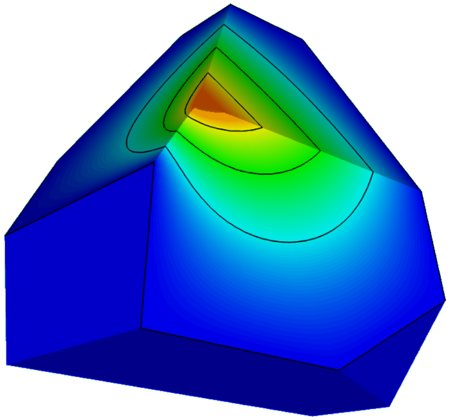

example in 3D

Note: Only need to store shape function values and derivatives at the quadrature points.

Harmonic Shape Function Examples

Sandia National Laboratories

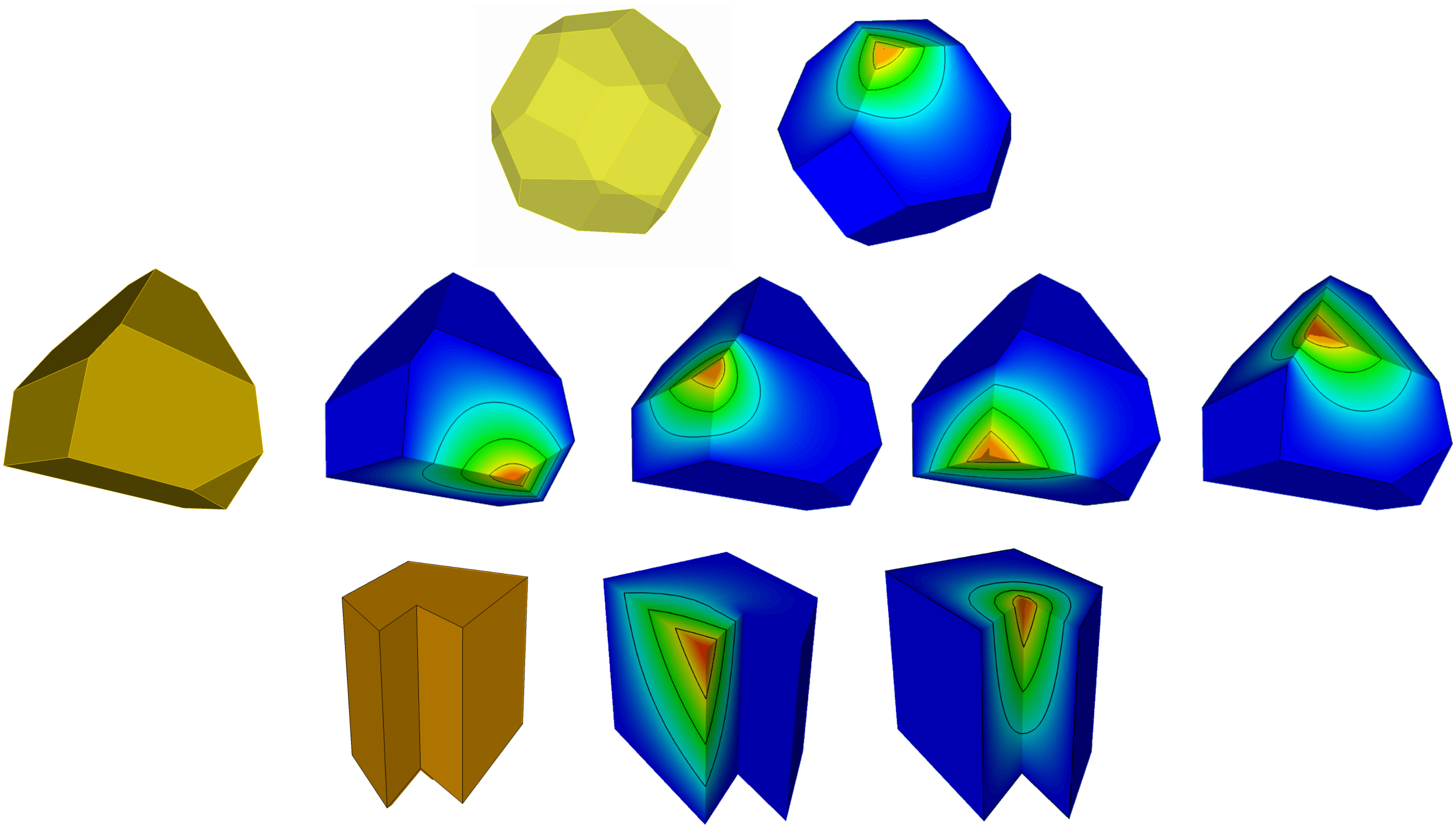

Harmonic Shape Function Properties

$$\sum_{a=1}^{N_\mathrm{v}} \psi^a(\mathbf{X}) = 1\,, \quad \mathbf{X} \in \Omega_\mathrm{e}$$

partition of unity

$$\sum_{a=1}^{N_\mathrm{v}} \psi^a(\mathbf{X})\,\mathbf{X}^a = \mathbf{X}\,, \quad \mathbf{X} \in \Omega_\mathrm{e}$$

reproduce linear fields

$$\psi^a(\mathbf{X}^b) = \delta_{ab}$$

Kronecker-delta property at nodes

Hierarchical Construction of Harmonic Shape Functions

(Joshi, 2007)

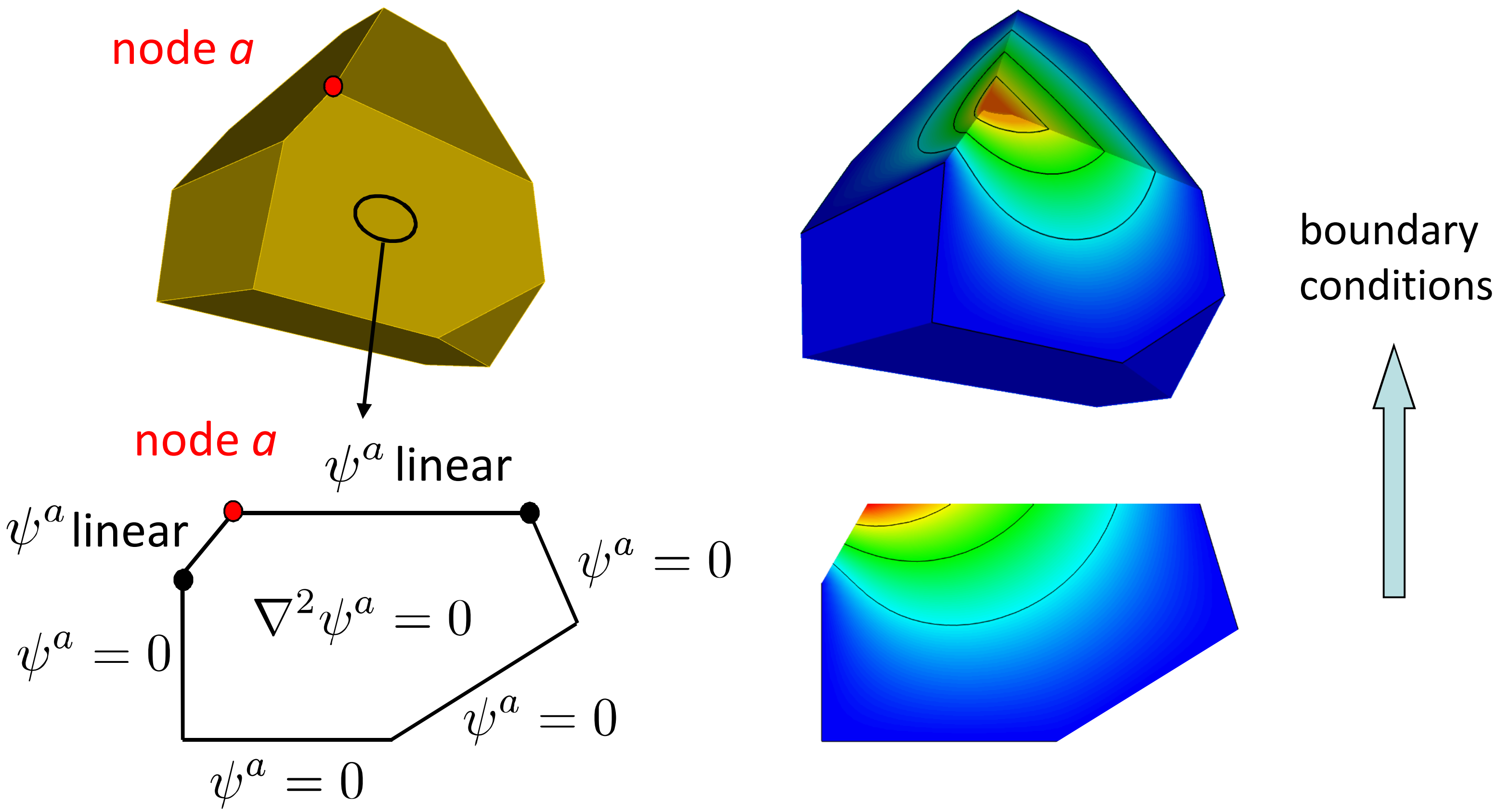

Harmonic Shape Functions for Non-planar Faces

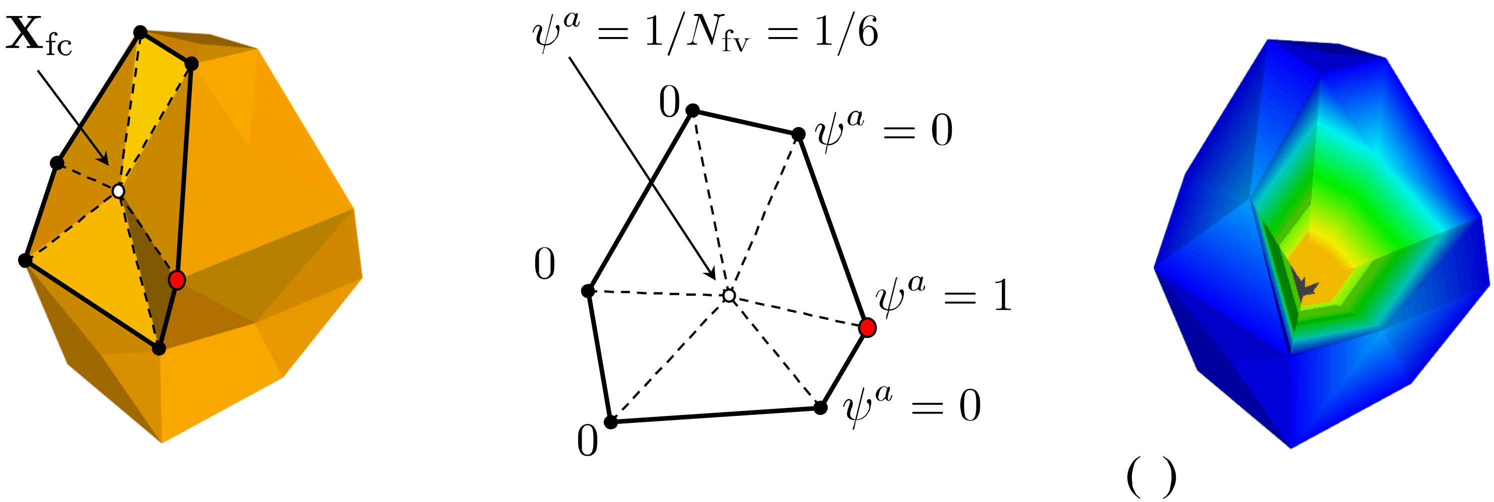

Can also use other barycentric face mappings.

How to Solve for Harmonic Shape Functions using FEA

Use a temporary tetrahedral submesh.

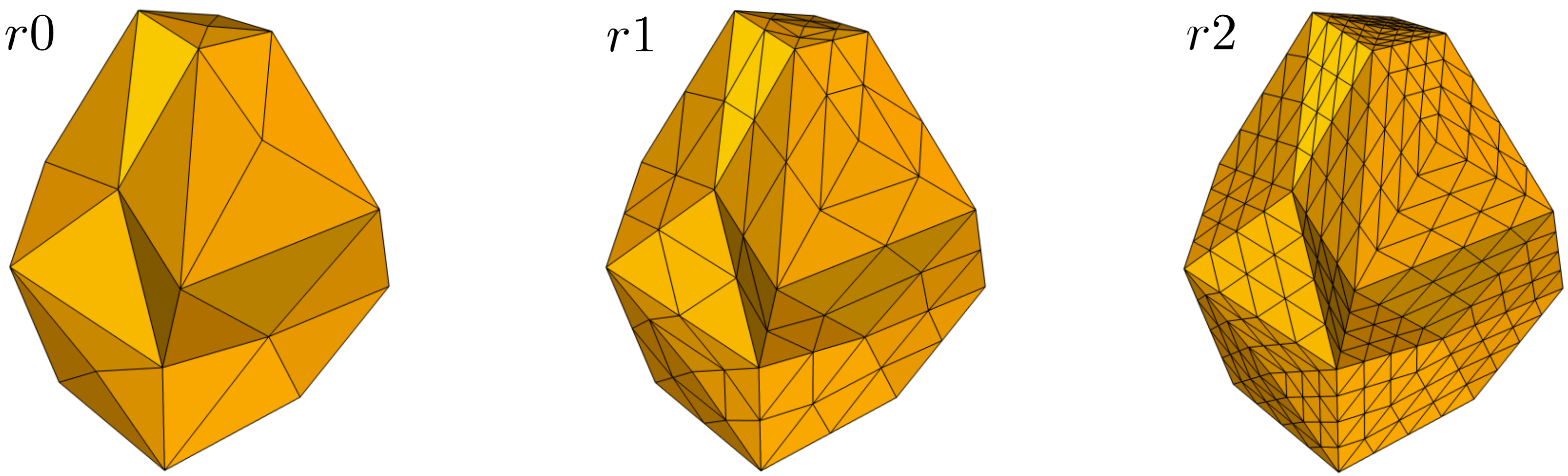

Accuracy of Harmonic Shape Functions?

Base tetrahedral subdivision

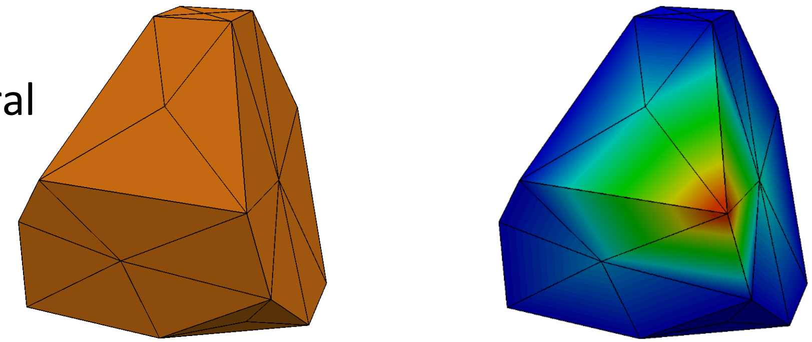

R0

Note: Only one unknown to solve for.

1 : 8 subdivision

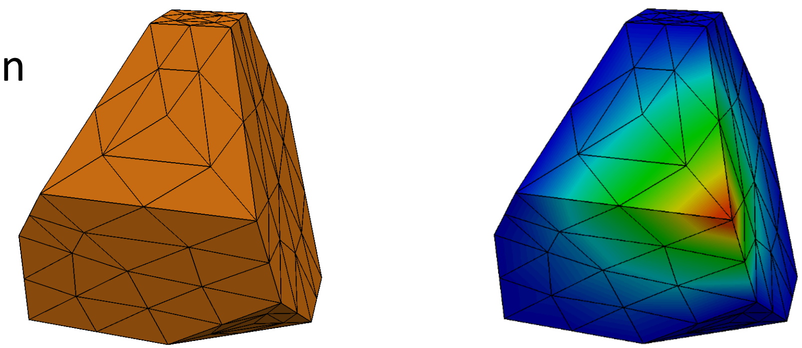

R1

Number of unknowns to solve for = $N_\mathrm{v} + N_\mathrm{f} + 1$

1 : 8 subdivision

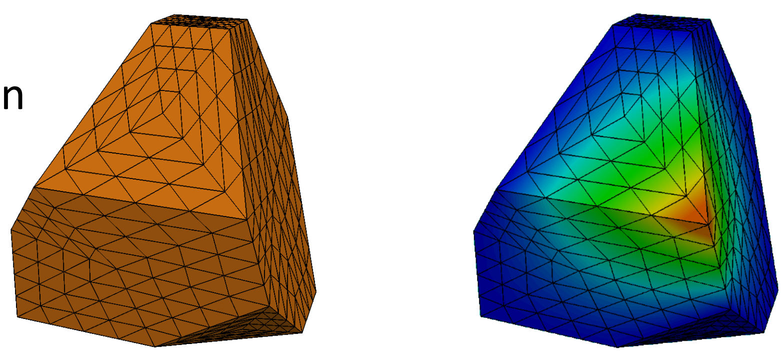

R2

Numerical Precision in Reproducing Properties

subdivision	Partition of Unity $\max\limits_{k\in\{1,\ldots,N_{\text{i.p.}}\}} \left[\sum_{a=1}^{N_\text{v}} \psi^a(\mathbf{X}^k) - 1 \right]$	Reproduction of Linear Fields $\max\limits_{\substack{k\in\{1,\ldots,N_{\text{i.p.}}\} \\ j\in\{1,2,3\}}} \left[\sum_{a=1}^{N_\text{v}} \psi^a(\mathbf{X}^k) X_j^a - X_j^k \right]$
$r0$	3.33×10^{-16}	5.55×10^{-16}
$r1$	6.66×10^{-16}	5.55×10^{-16}
$r2$	1.55×10^{-15}	5.55×10^{-16}

Element Integration

- Due to computational expense of plasticity models, want to minimize the number of quadrature points.
- Follow approach of Rashid and Selimotec, 2006.
- Each node is associated with a "tributary" volume.
- Number of quadrature points is equal to the number of vertices.
- Quadrature weight = volume of tributary volume.
- First-order accurate, but quadrature weights are positive (avoids Runge's phenomenon)

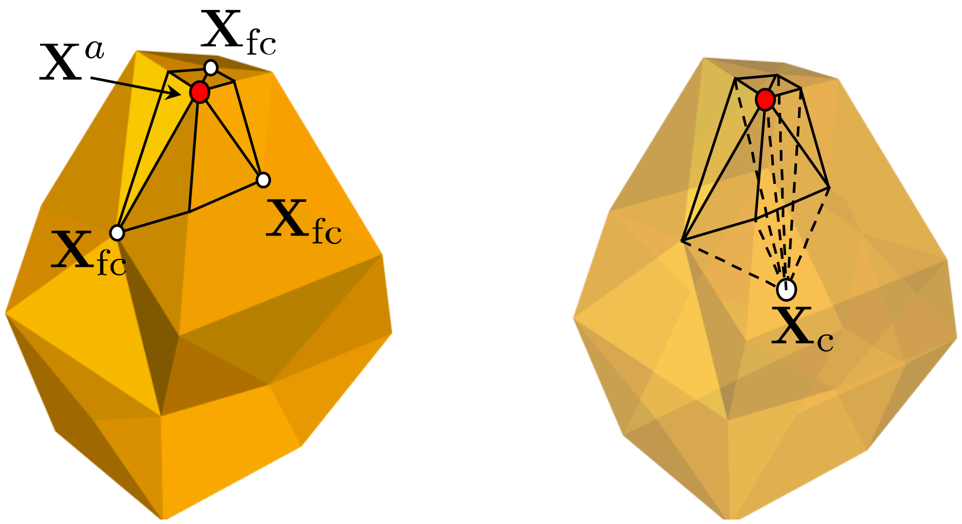

Patch Test

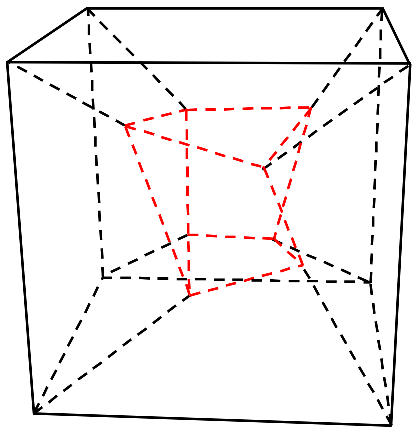

distorted hex patch

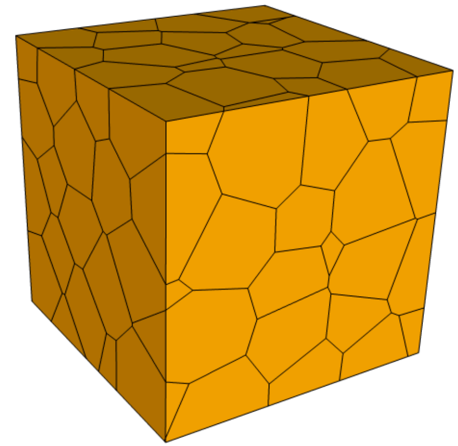

random close-packed Voronoi patch

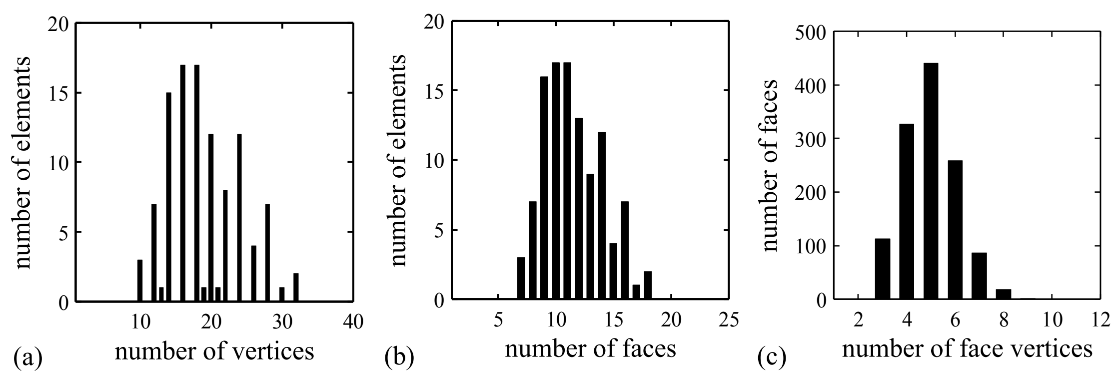

Patch Test

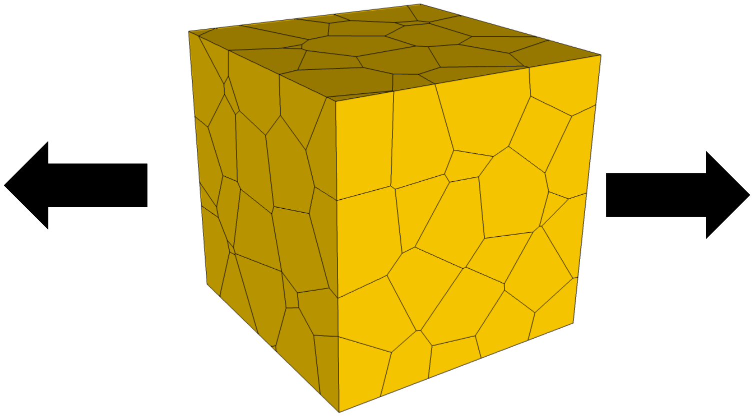

patch of elements

Failed patch test!

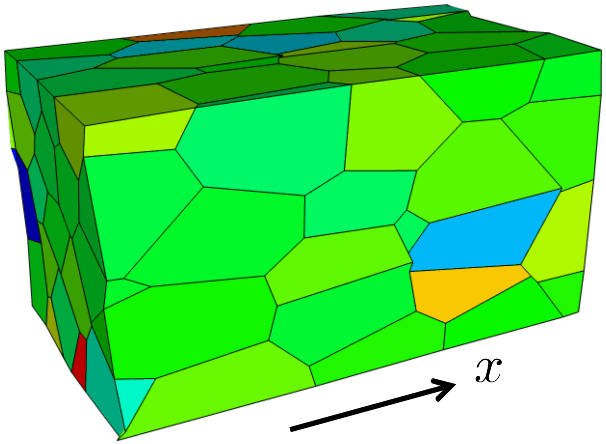

stress error > 10%

Patch Test and Integration Consistency

(Krongauz & Belytschko, 1997; Chen, 2001)

Divergence theorem

$$\int_{\Omega_e} \psi^a_{,i} \, d\Omega = \int_{\Gamma_e} \psi^a \, n_i \, d\Gamma \,, \quad a = 1, \ldots, N_v \,, \quad i = 1, 2, 3$$

Discrete divergence theorem

$$\sum_{k=1}^{N_{\mathrm{i.p.}}} w_k \psi^{ak}_{,i} = \sum_{l=1}^{N^{\Gamma}_{\mathrm{i.p.}}} w^{\Gamma}_l \, \psi^{al} n^l_i \,, \quad a = 1, \ldots, N_v \quad i = 1, 2, 3$$

Maximum error in integration constraint

subdivision	before derivative correction	after derivative correction
$r0$	0.0609	2.77×10^{-17}
$r1$	0.0138	2.77×10^{-17}
$r2$	0.0106	2.77×10^{-17}

(error over all shape functions and coordinate directions)

Derivative Correction to Pass the Patch Test

- "Tweak" the shape function derivatives to satisfy the integration consistency condition.
- Maintain the reproducing properties of the derivatives.
- Minimize the difference between the new derivatives and the old.
- Local solve at the element level; performed once.
- Performed for each direction and shape function independently.

$$\min_{\xi^k \in \Re} \sum_{k=1}^{N_{\mathrm{i.p.}}} w_k \left(\xi^k - \psi^{ak}_{,i}\right)^2 \text{ subject to the constraints } \sum_{k=1}^{N_{\mathrm{i.p.}}} w_k \xi^k - \sum_{l=1}^{N^{\Gamma}_{\mathrm{i.p.}}} w^{\Gamma}_l \, \psi^{al} n^l_i = 0$$

Derivative Correction to Pass the Patch Test

Maximum error in integration constraint

subdivision	before derivative correction	after derivative correction
$r0$	0.0609	2.77×10^{-17}
$r1$	0.0138	2.77×10^{-17}
$r2$	0.0106	2.77×10^{-17}

(error over all shape functions and coordinate directions)

Patch Test: Before and After

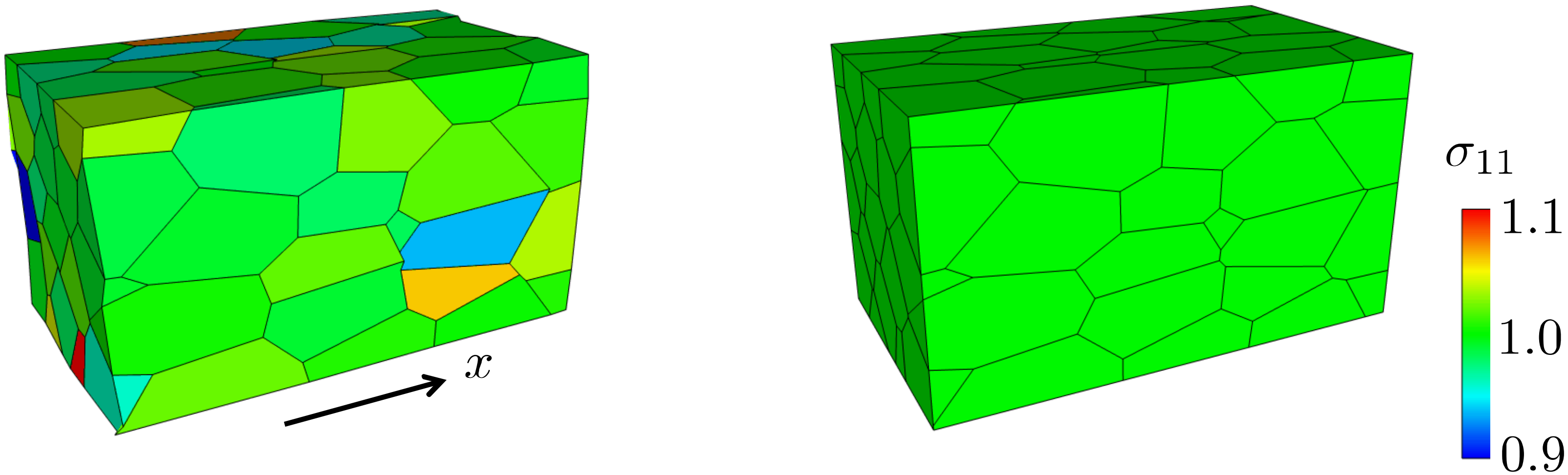

failed patch test

successful patch test

case	without derivative correction	with derivative correction
hex patch, trilinear formulation	1.11×10^{-15}	–
hex patch, poly formulation	0.0863	5.55×10^{-16}
hex patch, trilinear and poly	0.0152	8.88×10^{-16}
random Voronoi patch	0.1844	1.41×10^{-12}

Patch Test with Non-Convex Elements

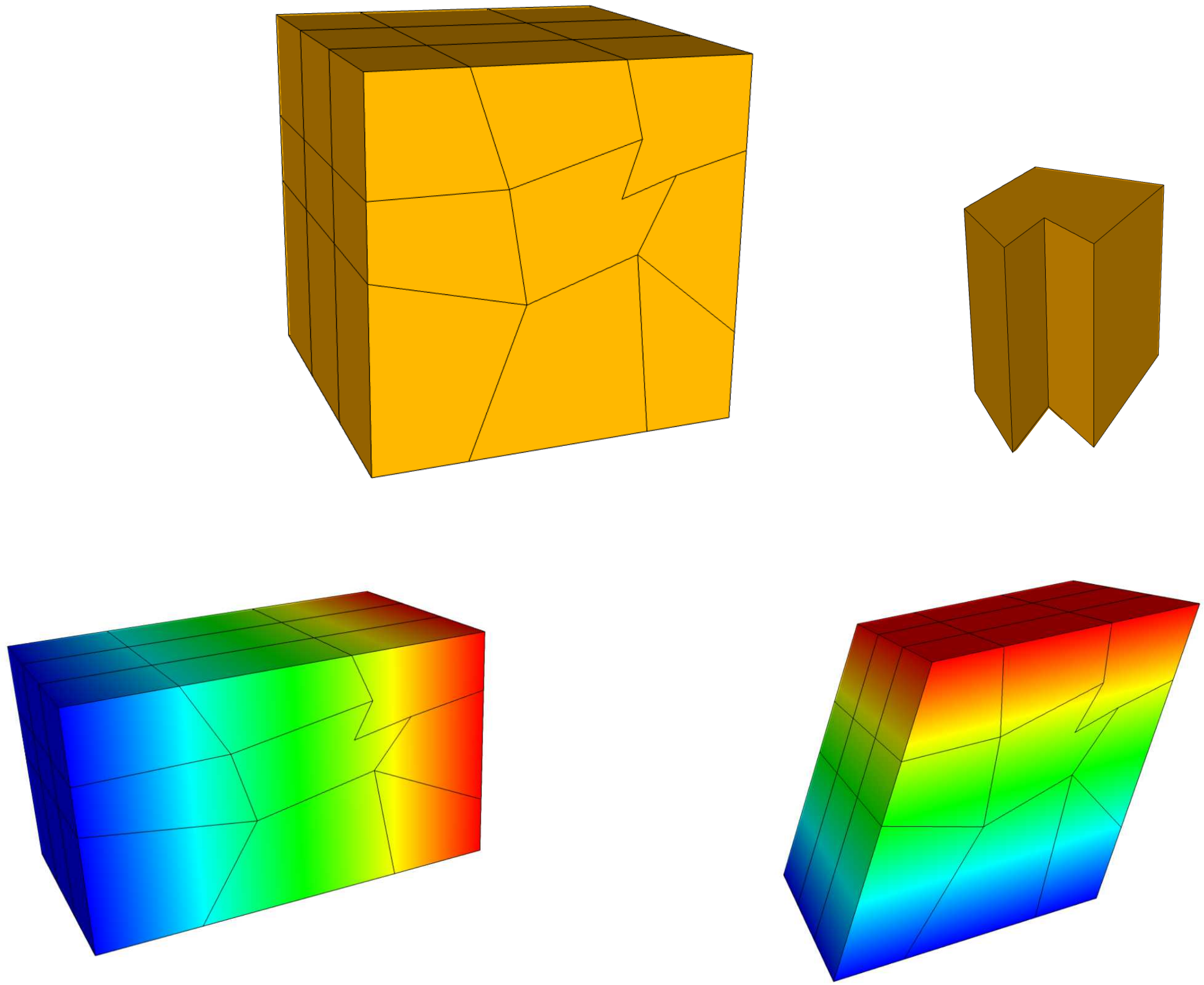

Verification Tests

<u>loading</u>: 3D beam bending with end shear load (have exact solution)

<u>meshes and element formulations</u>:

1. perfect hex mesh, trilinear vs. poly formulation
2. distorted hex mesh, trilinear vs. poly formulation
3. Voronoi mesh, poly formulation

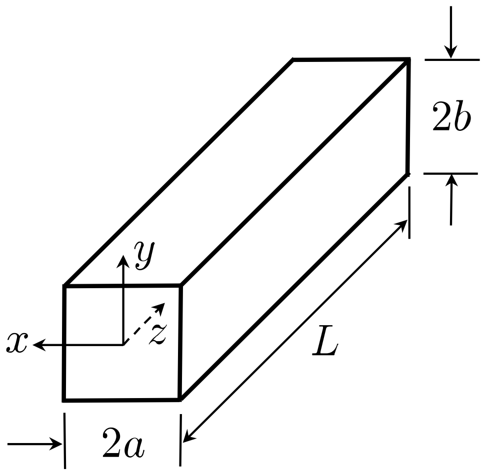

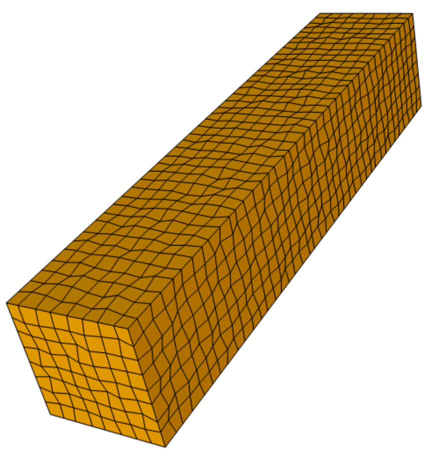

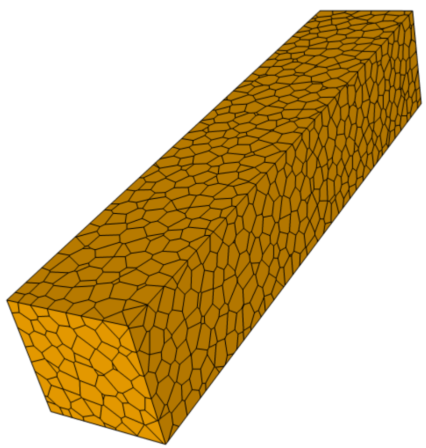

Verification Test: Beam Bending with Shear Load

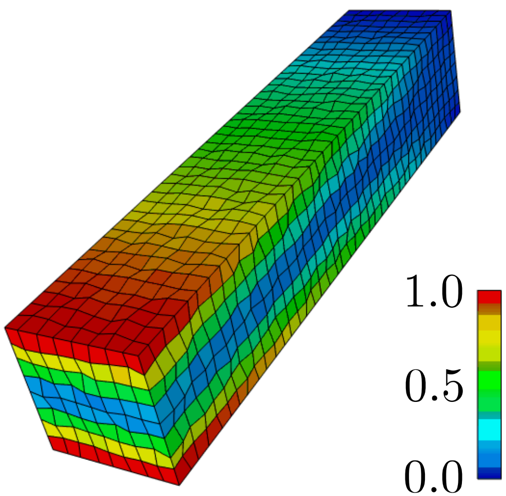

trilinear hex formulation

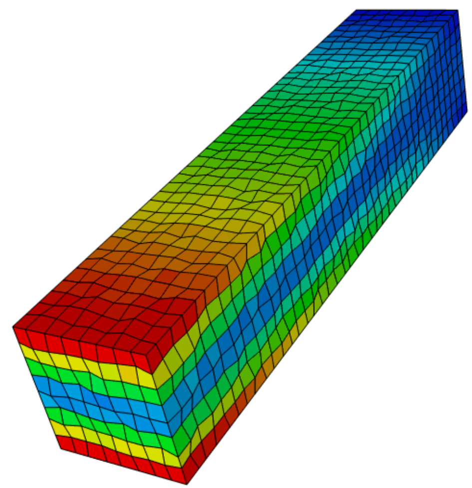

poly formulation

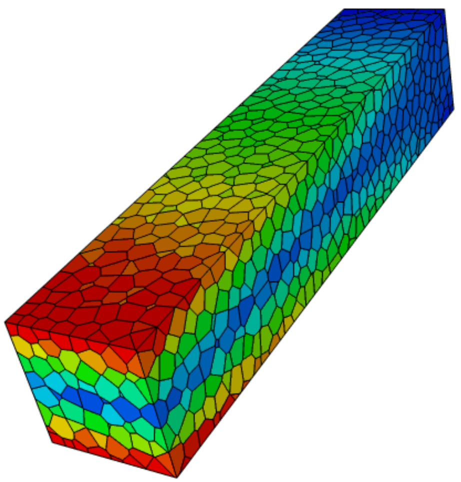

poly formulation

Beam Bending with Shear Load

(perfect hex mesh)

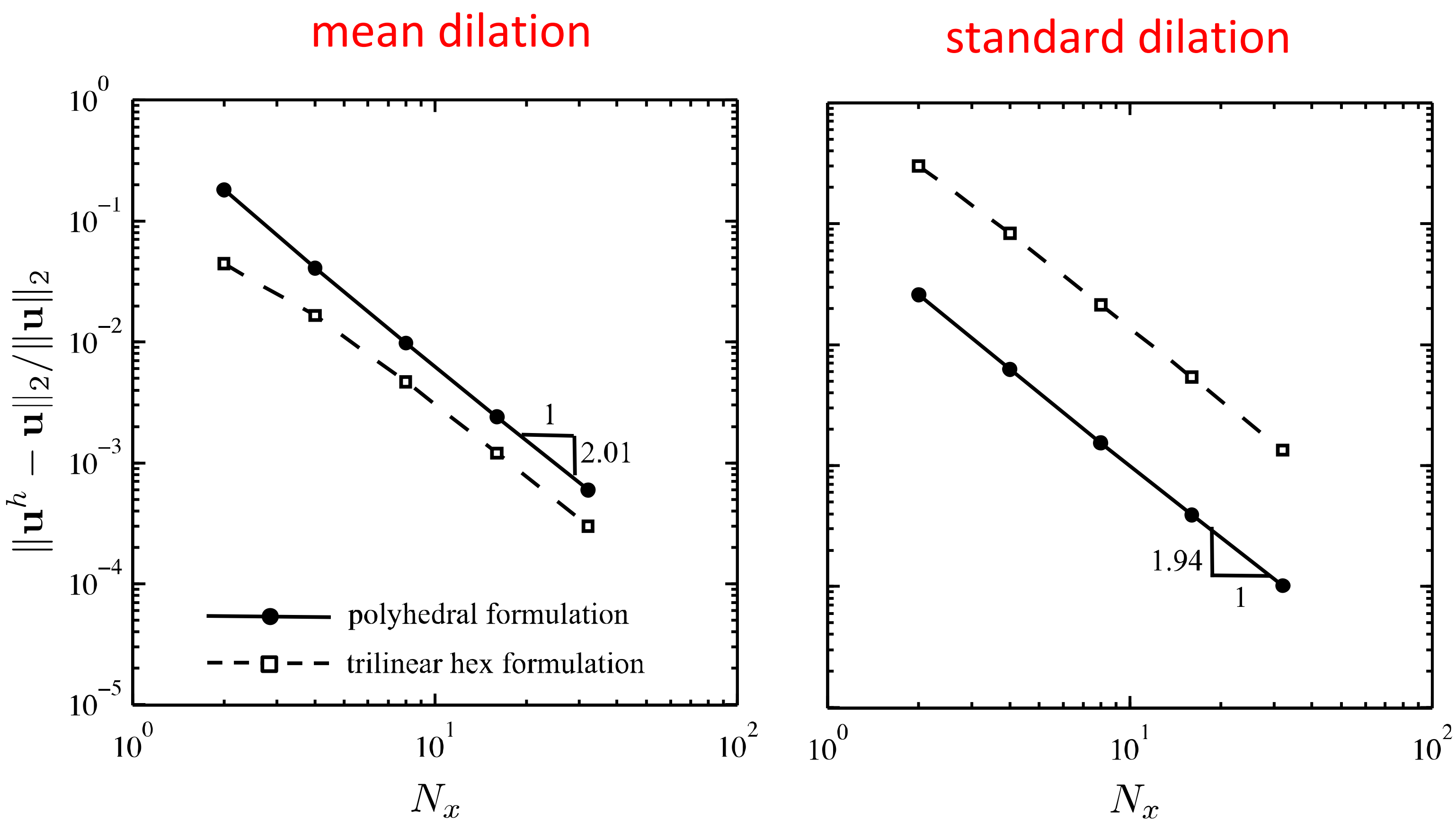

Energy Norm

(perfect hex mesh)

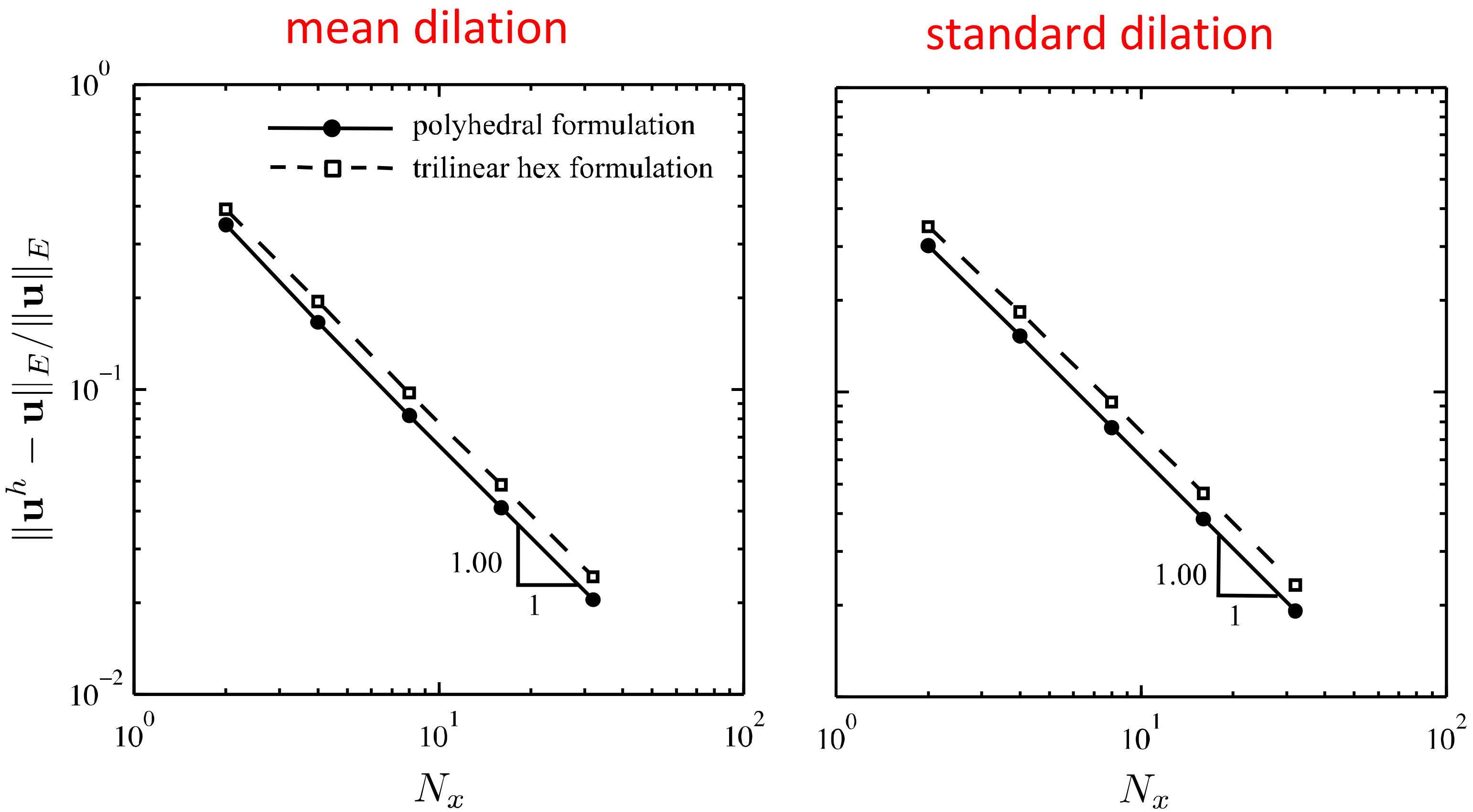

Random Hex Mesh (20 realizations)

(mean dilation)

L2 norm

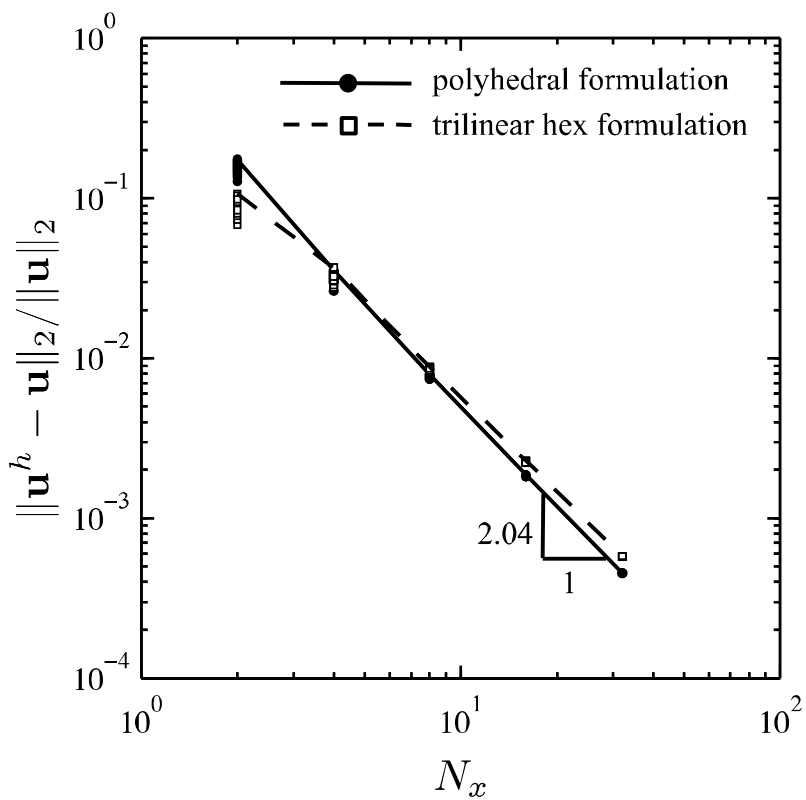

Energy Norm

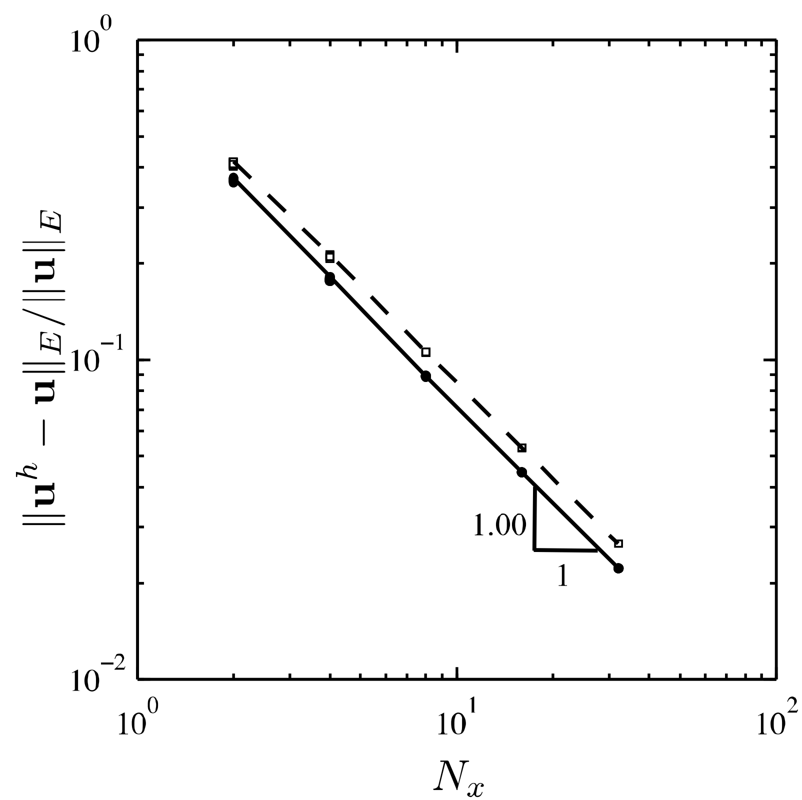

Random Voronoi Mesh (20 realizations)

(mean dilation)

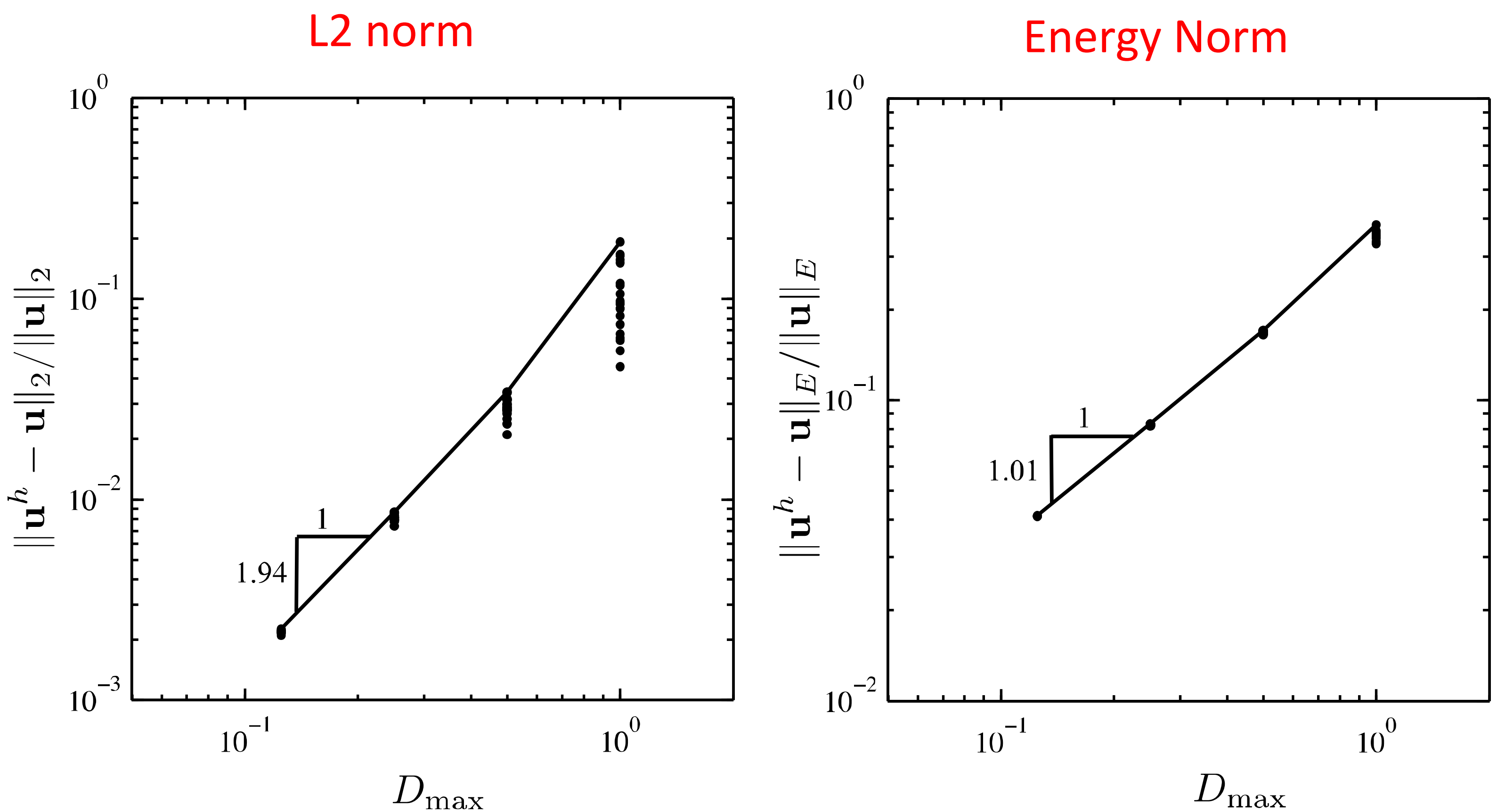

Near Incompressibility

(mean dilation, worst case Voronoi mesh at each refinement)

L2 norm

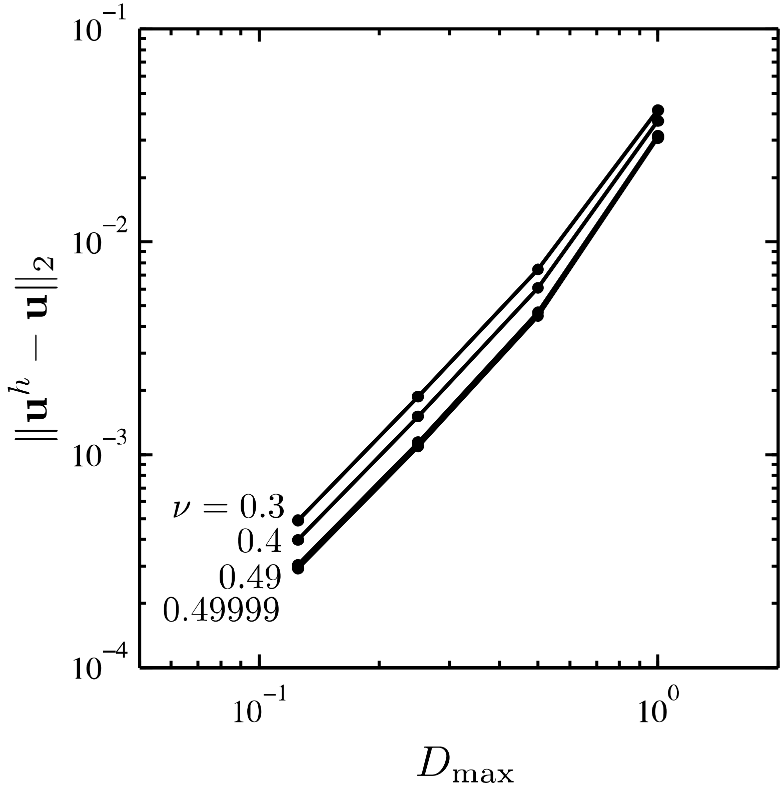

Energy Norm

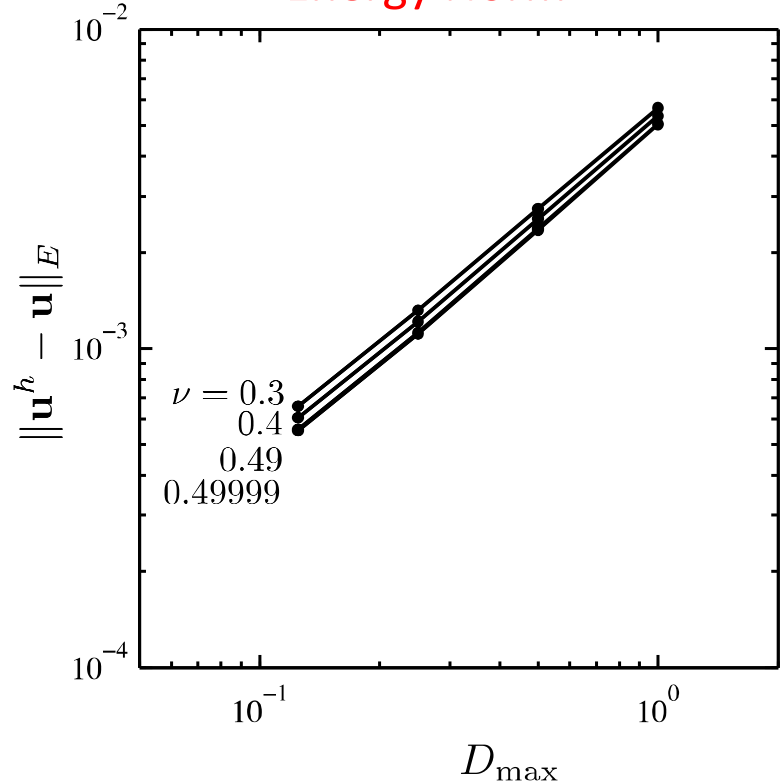

Effect of Shape Function Accuracy

(worst case Voronoi mesh at each refinement)

L2 norm

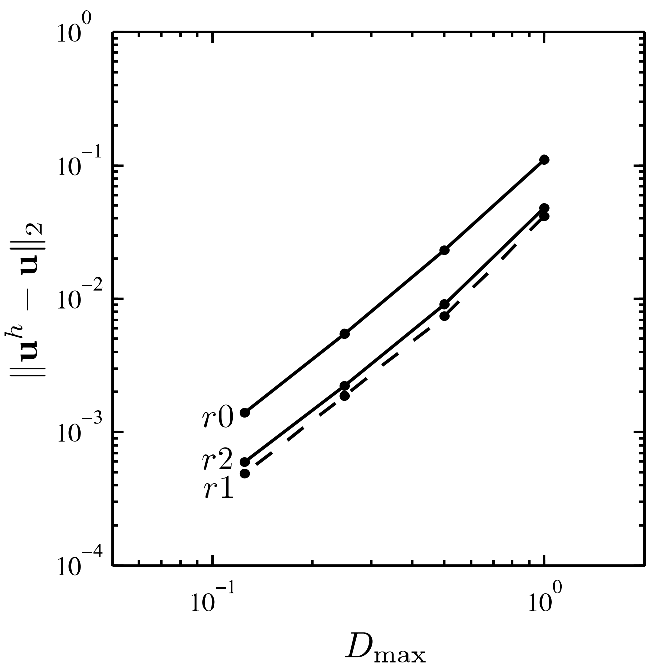

Energy Norm

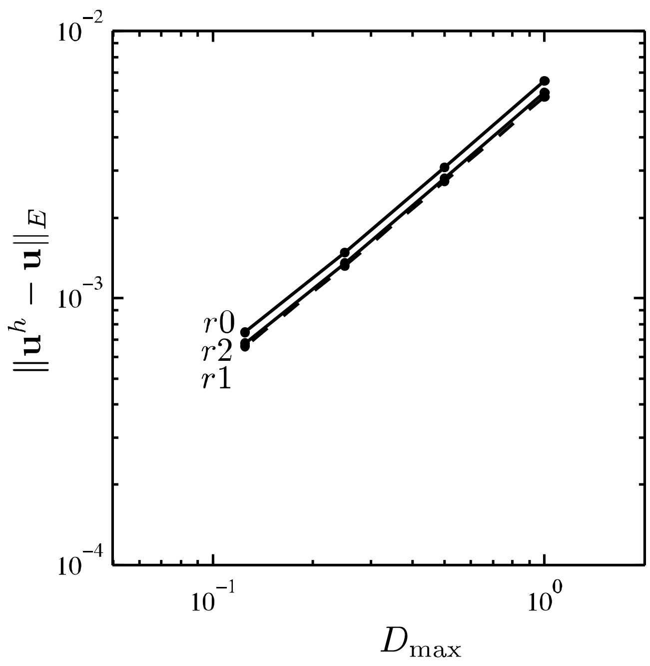

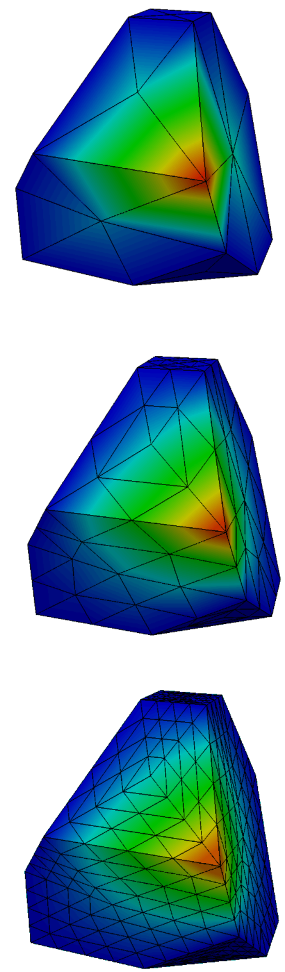

R0

R1

R2

Sandia National Laboratories

Summary

1. Presented a polyhedral finite-element formulation based on harmonic shape functions.
2. Applicable to non-convex elements with non-planar faces.
3. Adopted quadrature scheme of Rashid (number of quadrature points = number of vertices, total-Lagrangian formulation)
4. In order to pass the patch test, needed to use “pseudo-derivatives”.

Future Work

1. Nonlinear examples (plasticity, large deformation)
2. Try this element formulation using other barycentric coordinates (e.g. maxEnt)
3. Remove restriction of star-convexity (used for convenience)

Outline

1. Polyhedral finite elements
   - motivation
   - harmonic shape functions
   - patch test
   - verification
   - future work
2. Multiscale modeling and material variability
   - review of homogenization theory
     a. weak convergence
     b. effective vs. apparent material properties
     c. type 1 and type 2 material variability
   - direct numerical simulations
3. Summary

Goals / Questions

- What is material variability?
- How do we “consistently” include material variability in our macroscale simulations?
- When is material variability significant?
- How does material variability impact engineering quantities of interest?

Homogenization

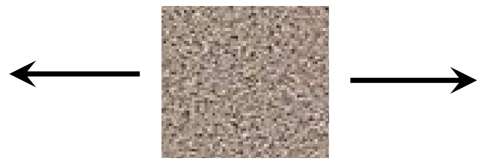

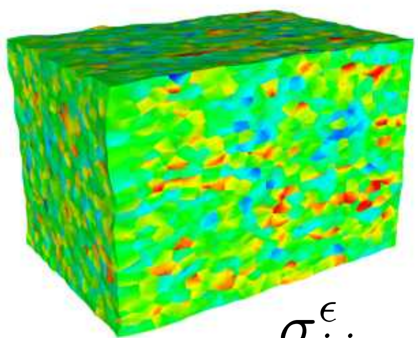

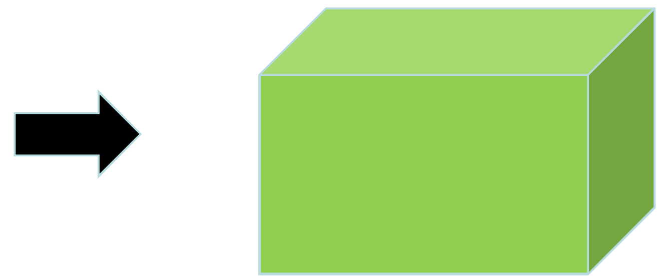

σ_{ij}^{ϵ}

fine-scale fluctuations

$\sigma_{ij} = \langle \sigma_{ij}^{\epsilon} \rangle$

replaced with mean behavior

This equivalence is defined in an energy sense: $\sigma_{ij}\varepsilon_{ij} = \langle \sigma_{ij}^{\epsilon} \rangle \langle \varepsilon_{ij}^{\epsilon} \rangle$

Constitutive models map average strain to average stress:

$$\varepsilon_{ij} = \langle \varepsilon_{ij}^{\epsilon} \rangle \longrightarrow \sigma_{ij} = \langle \sigma_{ij}^{\epsilon} \rangle$$

Apparent vs. Effective Material Properties

Huet, C. (1990). "Application of variational concepts to size effects in elastic heterogeneous bodies." *Journal of the Mechanics and Physics of Solids,* 38(6): 813-841.

$C =$ stiffness tensor

finite RVE, apparent

infinite RVE, effective

$$C_{\sigma}^{\text{app}}(\omega) \leq C \leq C_{\varepsilon}^{\text{app}}(\omega)$$

SUBC — stochastic

deterministic

KUBC — stochastic

partial ordering defined in an energetic sense:

$B < A$ iff $\varepsilon : (A - B) : \varepsilon > 0$ for all $\varepsilon \neq 0$

Apparent vs. Effective Material Properties

Huet, C. (1990). "Application of variational concepts to size effects in elastic heterogeneous bodies." *Journal of the Mechanics and Physics of Solids,* 38(6): 813-841.

$$C^{\mathrm{app}}_{\sigma,L} \leq C^{\mathrm{app}}_{\sigma,2L} \leq C^{\mathrm{app}}_{\sigma,4L} \leq \cdots \leq C^{\mathrm{app}}_{\sigma,\infty} = C$$

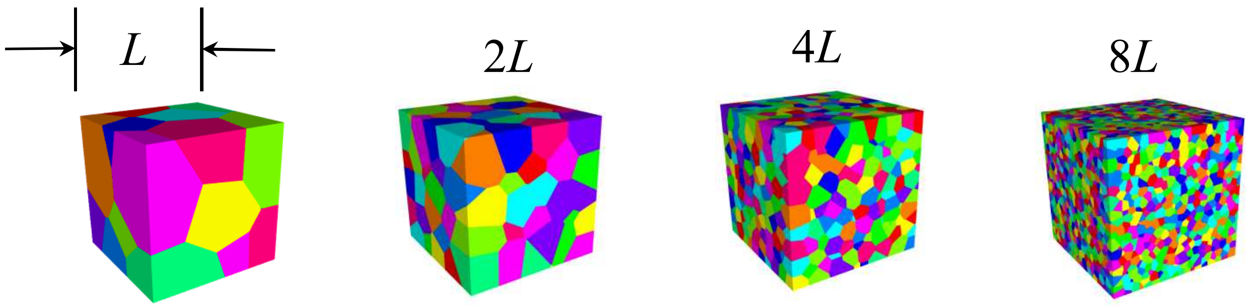

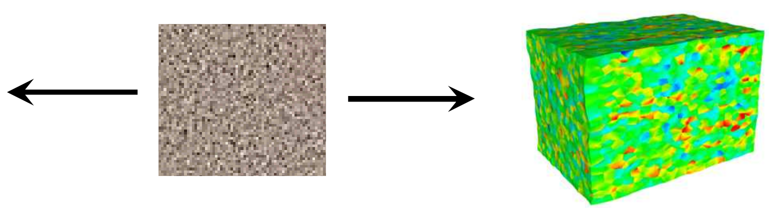

Apparent vs. Effective Material Properties

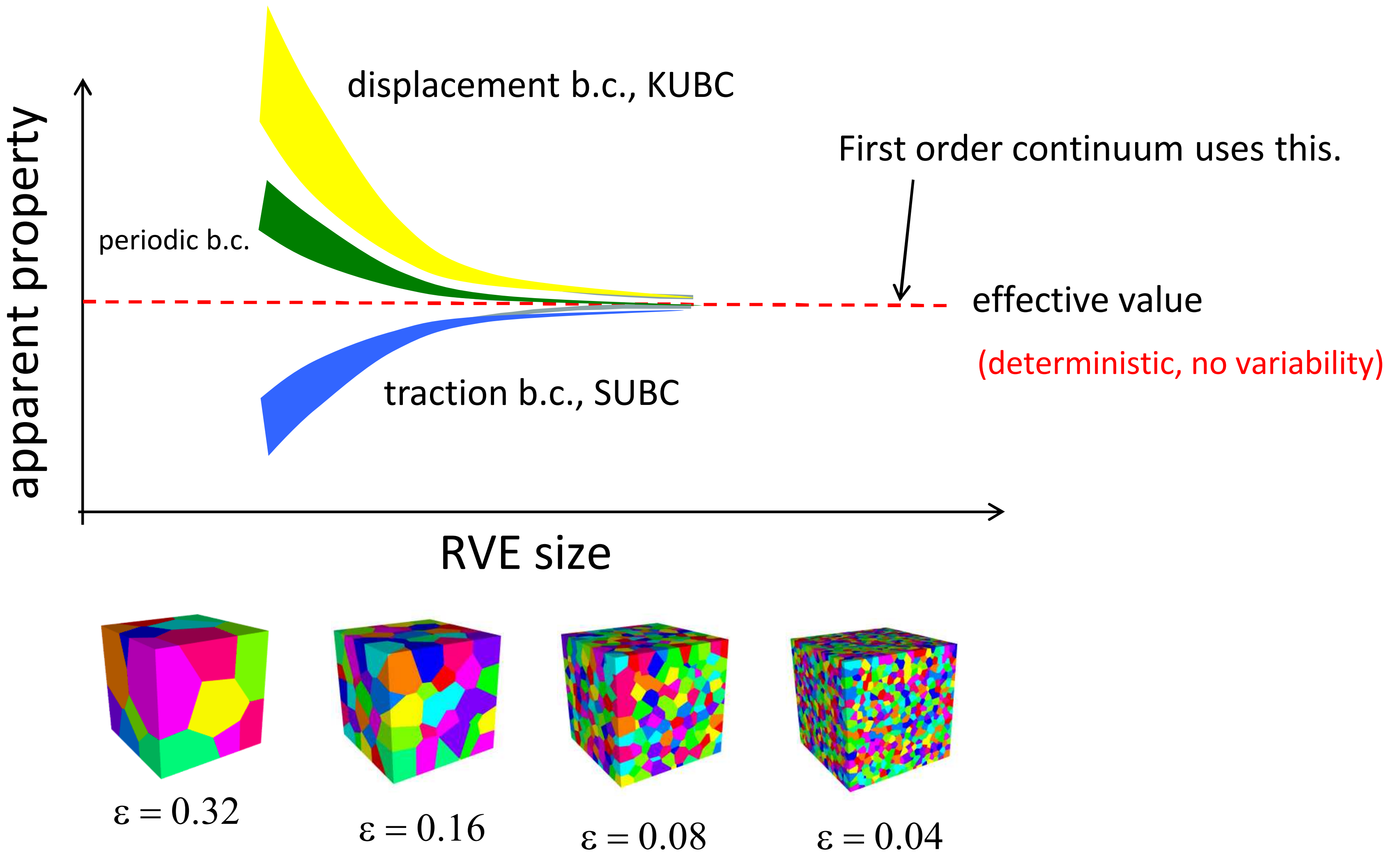

What about the Governing PDE?

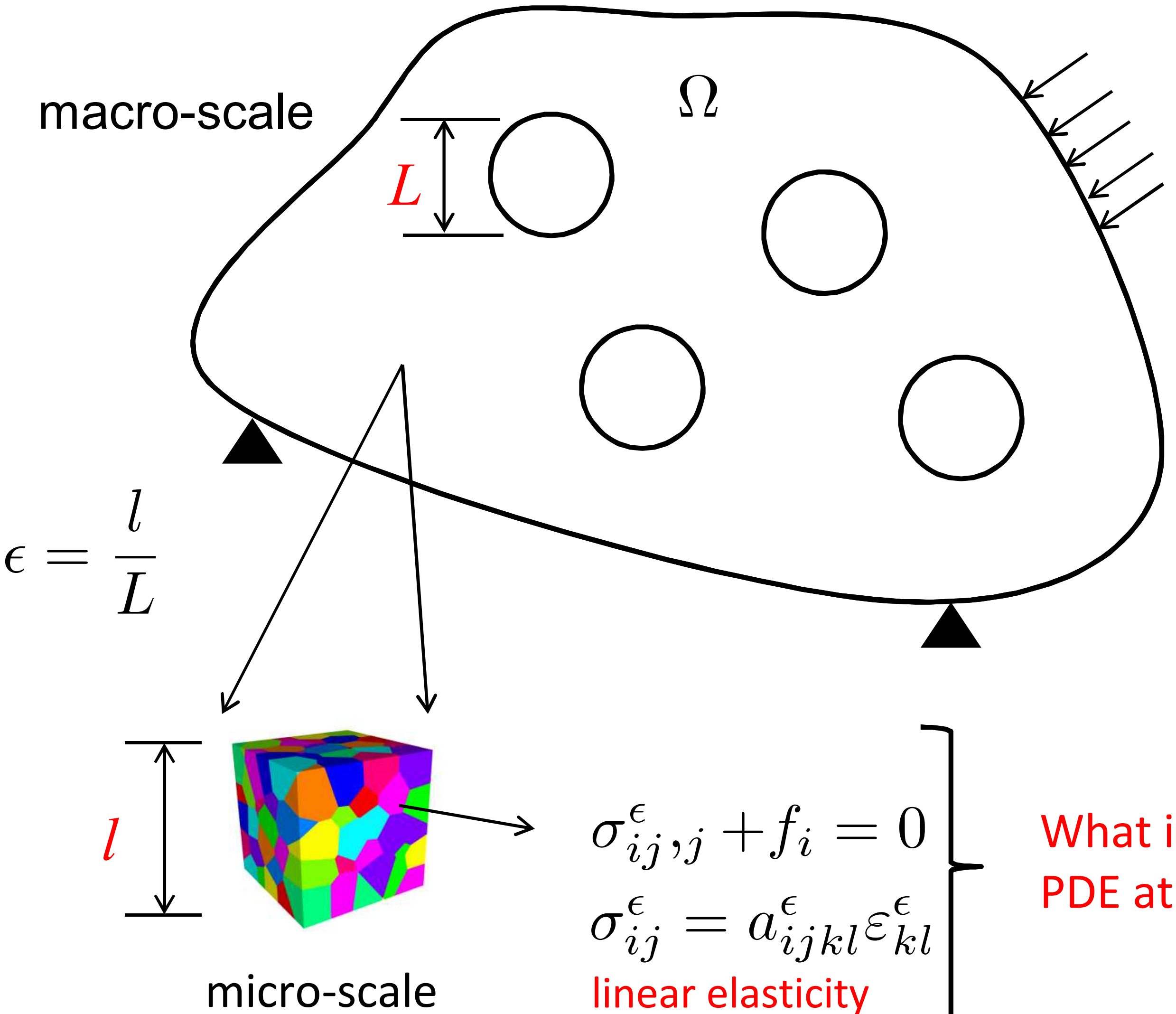

$$\sigma^{\epsilon}_{ij},_{j} + f_i = 0$$

$$\sigma^{\epsilon}_{ij} = a^{\epsilon}_{ijkl}\varepsilon^{\epsilon}_{kl}$$

linear elasticity

What is the governing PDE at the macroscale?

Strong and Weak Convergence

A sequence of functions (u_n), $u_n \in L^2$ is **strongly** convergent to $u \in L^2$ if

$$\lim_{n \to \infty} \|u_n - u\|_{L^2} = 0$$

A sequence of functions (u_n), $u_n \in L^2$ is **weakly** convergent to $u \in L^2$ if

$$\lim_{n \to \infty} \langle u_n, v \rangle = \langle u, v \rangle \quad \text{for all } v \in L^2$$

These are the modes of convergence in which homogenization is defined.

Weak Convergence

Example: The sequence of functions $u_n = \sin(n\pi x)$ in $L^2[0,1]$ converges weakly to $u = 0$.

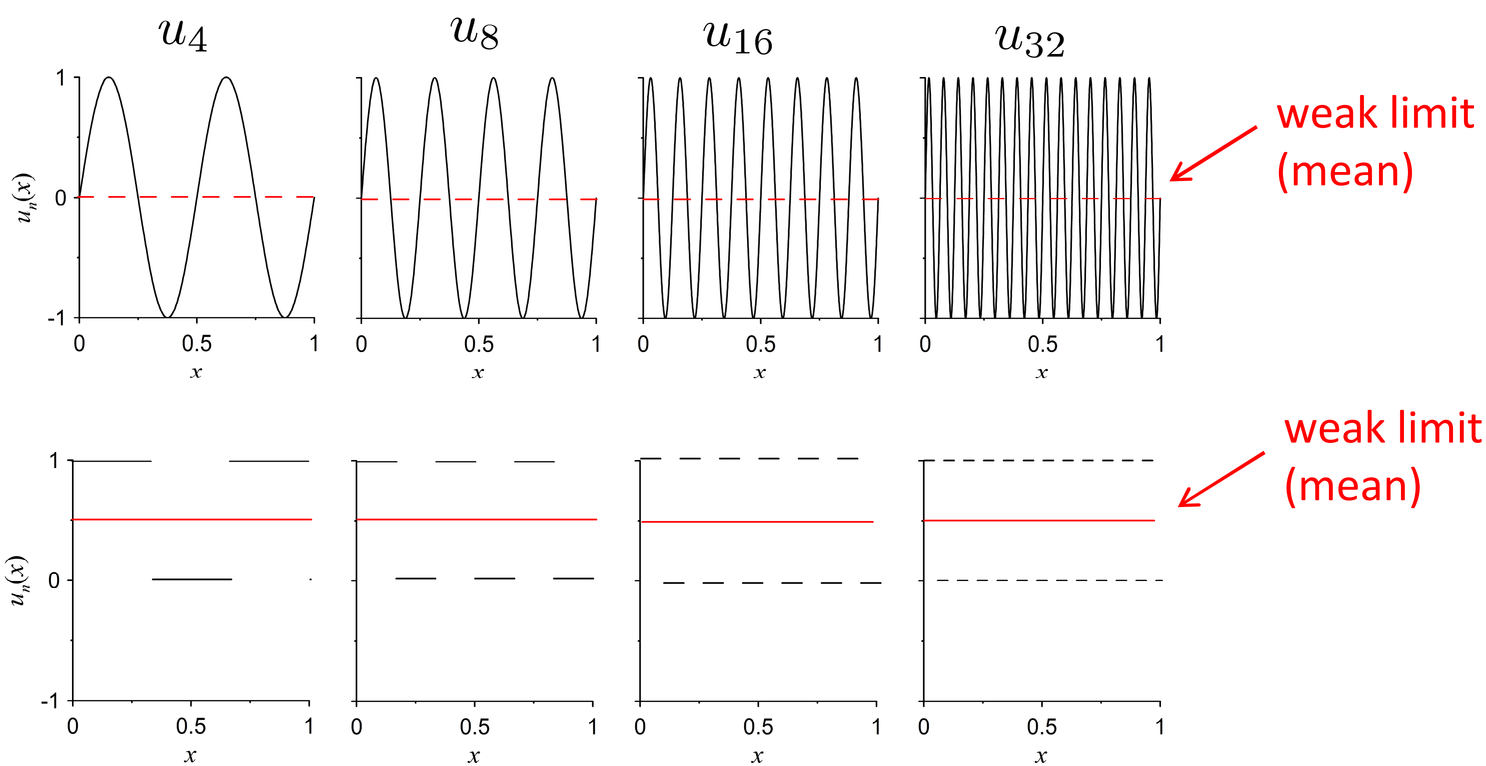

Theorem: Any sequence of periodic functions converges weakly to the mean as the period approaches zero.

Definitions of Statistical Convergence

almost sure convergence

$$\Pr\left(\lim_{h\to 0} x_h = x\right) = 1$$

convergence in r-mean

$$\lim_{h\to 0} E\left(\left|x_h - x\right|^r\right) = 0$$

convergence in probability

$$\lim_{h\to 0} \Pr\left(\left|x_h - x\right| > \varepsilon\right) = 0$$

convergence in distribution

$$\lim_{h\to 0} F_h(x) = F(x)$$

increasing strength

Asymptotic Expansion

(Cioranescu and Donato, 1999, *An Introduction to Homogenization.*)

$$\mathbf{u}^{\epsilon}(\mathbf{x}) = \mathbf{u}_0(\mathbf{x},\mathbf{y}) + \epsilon\mathbf{u}_1(\mathbf{x},\mathbf{y}) + \epsilon^2\mathbf{u}_2(\mathbf{x},\mathbf{y}) + \cdots$$

$\mathbf{u}_j(\mathbf{x},\mathbf{y})$ are periodic in $\mathbf{y}$

$\mathbf{y} = \mathbf{x}/\epsilon$ is the `fast' variable

$\mathbf{x}$ is the `slow' variable

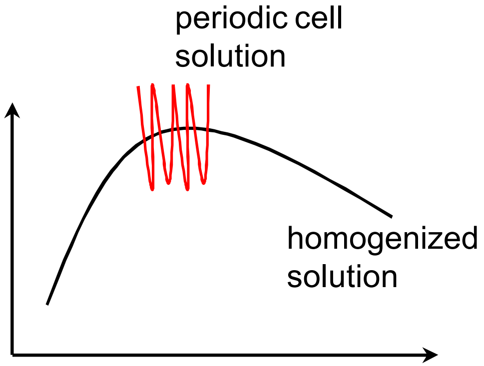

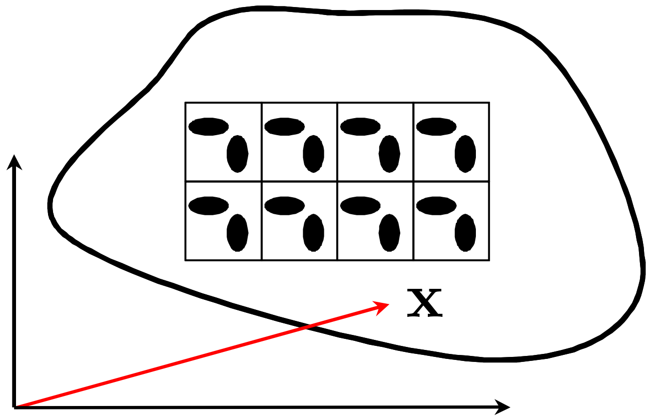

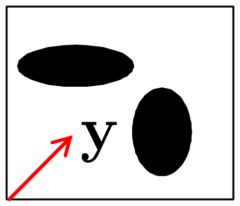

Linear Homogenization Results

$$\mathbf{u}^{\epsilon}(\mathbf{x}) = \mathbf{u}_0(\mathbf{x},\mathbf{y}) + \epsilon\mathbf{u}_1(\mathbf{x},\mathbf{y}) + \epsilon^2\mathbf{u}_2(\mathbf{x},\mathbf{y}) + \cdots$$

substitute

$$\sigma^{\epsilon}_{ij},_j + f_i = 0$$

$$\sigma^{\epsilon}_{ij} = a^{\epsilon}_{ijkl}\varepsilon^{\epsilon}_{kl}$$

RESULT: $$\mathbf{u}^{\epsilon}(\mathbf{x}) = \mathbf{u}_0(\mathbf{x}) - \epsilon\chi(\mathbf{y}) \cdot \nabla\mathbf{u}_0 + \epsilon^2\theta(\mathbf{y}) : \nabla\nabla\mathbf{u}_0 + \cdots$$

homogenized solution does not depend upon ϵ!

first-order corrector

second-order corrector

Observations:

- In the limit as $\epsilon \to 0$, get a first-order continuum (homogenized).
- For $\epsilon \neq 0$ need gradient terms (higher-order continuum)

Linear Homogenization Results

(Cioranescu and Donato, 1999, *An Introduction to Homogenization.*)

$$\mathbf{u}^\epsilon \rightarrow \mathbf{u} \;\; \text{strongly in} \;\; L^2$$
$$\mathbf{u}^\epsilon \rightarrow \mathbf{u} \;\; \text{weakly in} \;\; H^1$$
$$\sigma^\epsilon \rightarrow \sigma \;\; \text{weakly in} \;\; L^2$$
$$W^\epsilon \rightarrow W \;\; \text{strongly in} \;\; \Re$$

For random media:

$$\int_\Omega \langle ||\mathbf{u}^\epsilon - \mathbf{u}||^2 \rangle d\Omega \rightarrow 0 \quad \text{as} \quad \epsilon \rightarrow 0$$

or

$$\mathbf{u}^\epsilon(\omega) \rightarrow \mathbf{u} \quad \text{in mean square}$$

Homogenization

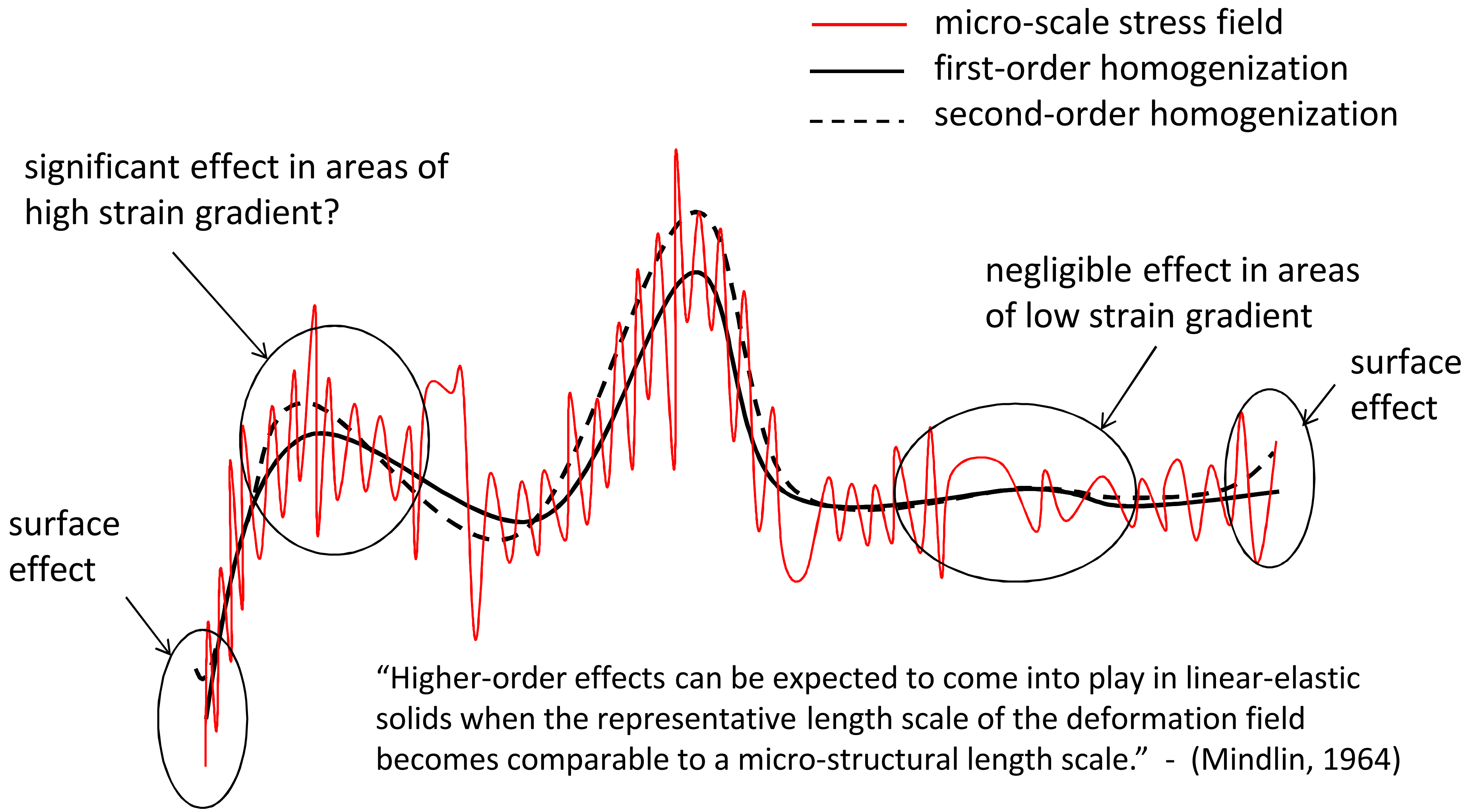

“Higher-order effects can be expected to come into play in linear-elastic solids when the representative length scale of the deformation field becomes comparable to a micro-structural length scale.” - (Mindlin, 1964)

Identify Two Types of Material Variability

(Type 1) 1. Spatial variability of homogenized material constants

- size of microstructure $\varepsilon = 0$
- first-order homogenization, first-order PDE
- spatial correlation at the macro-scale
- elastic isotropy assumption holds regardless of scale

(Type 2) 2. Higher-order terms in the PDE itself (Type 2)

- micro-structure is finite $\varepsilon \neq 0$
- higher-order PDE
- spatial correlation at the micro-scale only
- anisotropic fluctuations

Direct Numerical Simulations

- Perform direct numerical simulations (DNS) of macroscopic boundary-value problems with microstructure and compare with the solution from the homogenized PDE.
- Identify any evidence of Type-2 material variability.
- Propose/investigate a higher-order continuum theory for Type-2 material variability.

Voronoi Microstructure from MPS Seeding

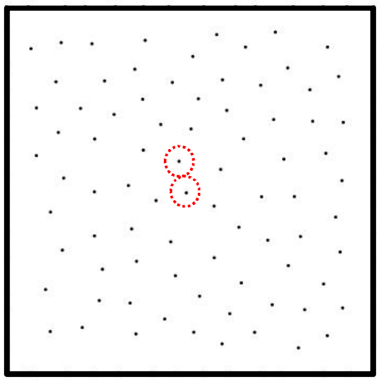

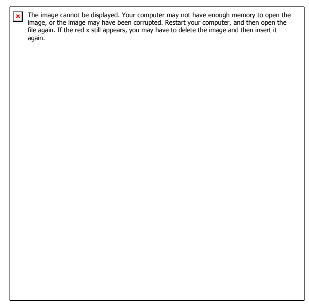

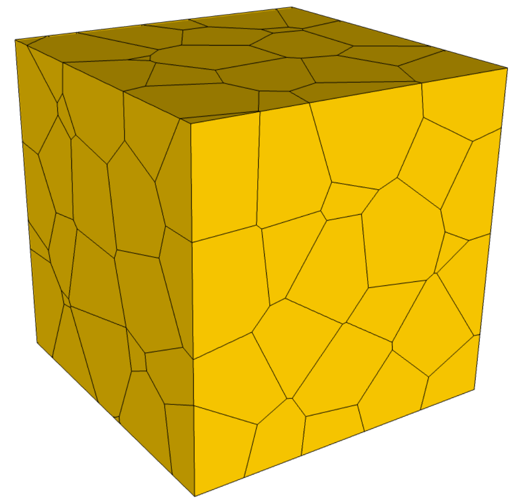

Maximal Poisson Sampling

- constraint on min. dist.
- seed until ‘max’ packing
- Ebeida/Mitchell Algorithm (1400)

Voronoi Overlay of Hexahedral Mesh

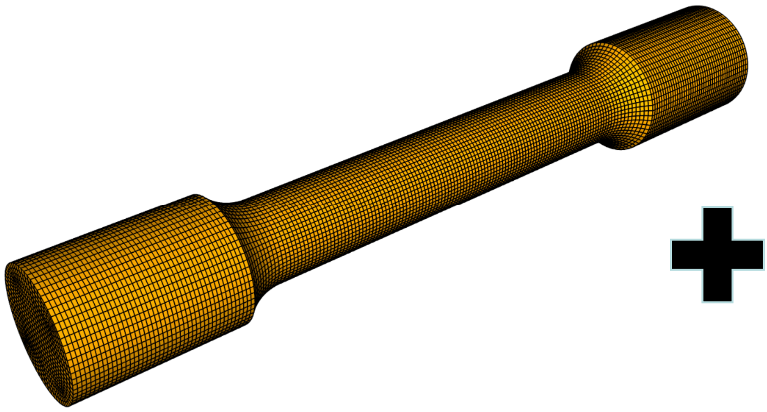

+

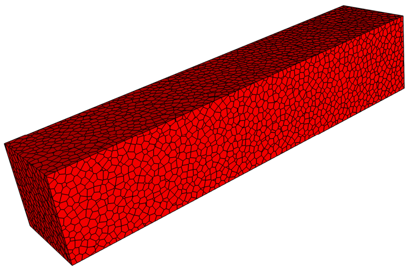

=

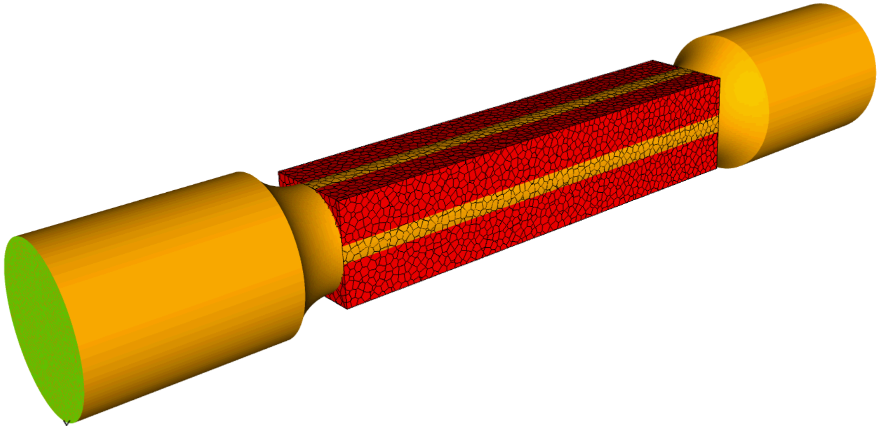

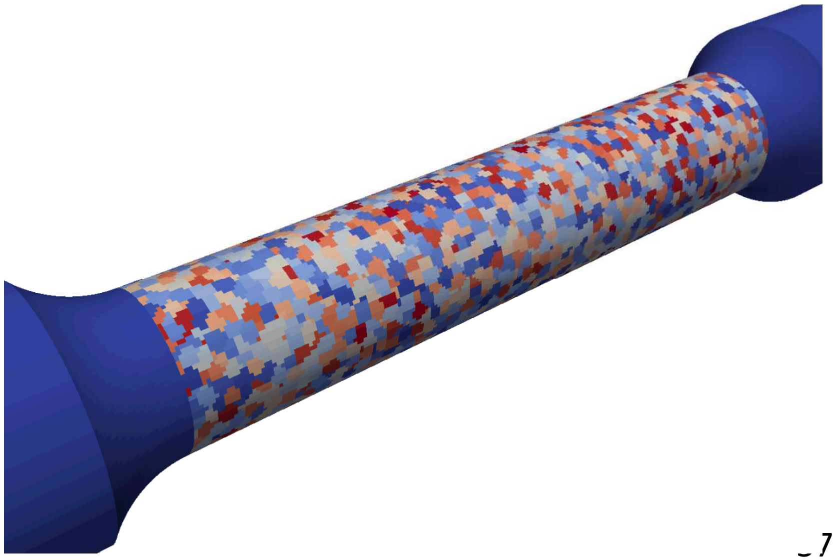

Hierarchy of Hexahedral Meshes

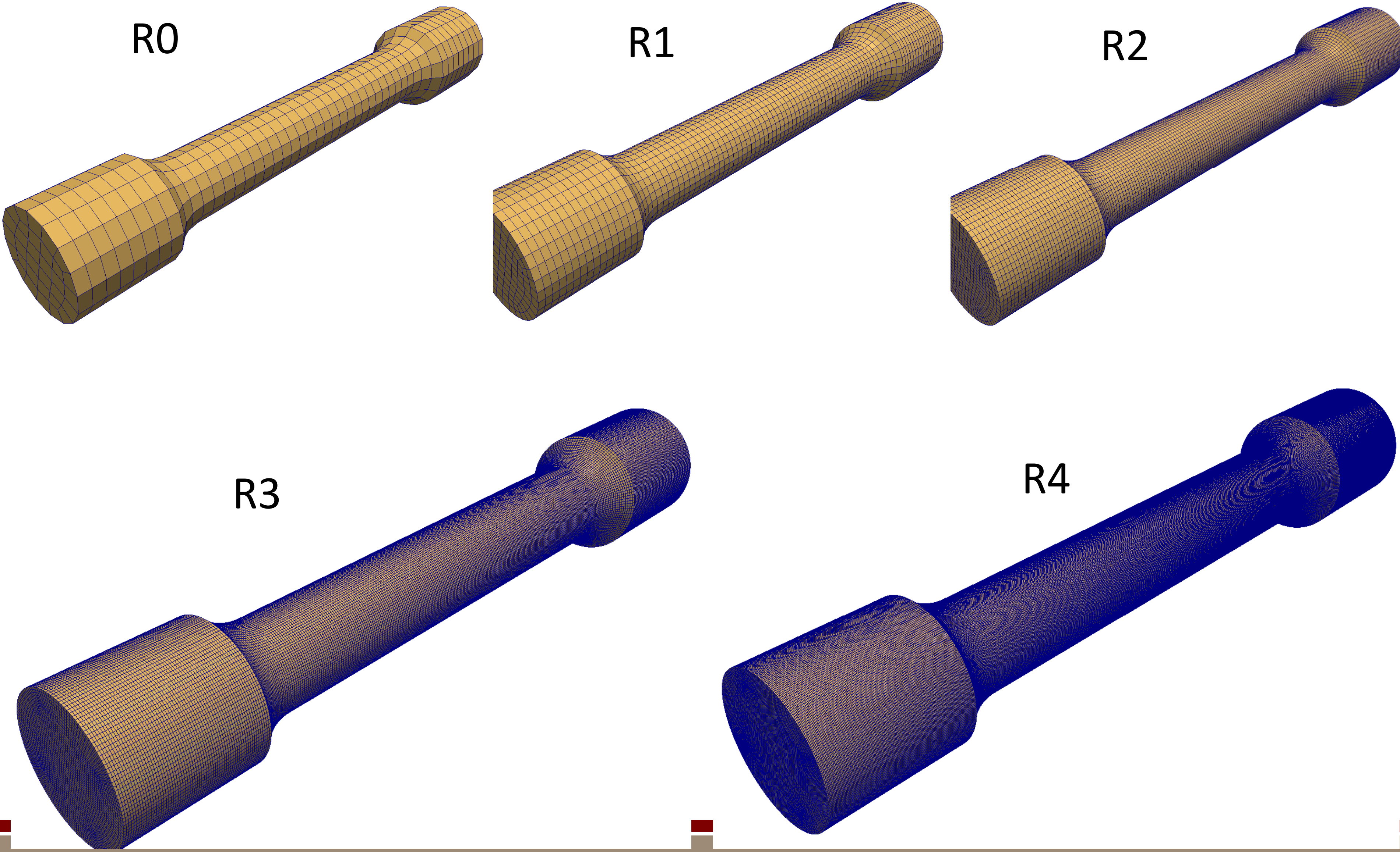

Voronoi Overlay of Hierarchy of Hexahedral Meshes

- One grain realization with ~ 6 grains through the diameter (~ 940 grains)
- Hierarchy of hexahedral meshes
- Pixelation decreases with mesh refinement

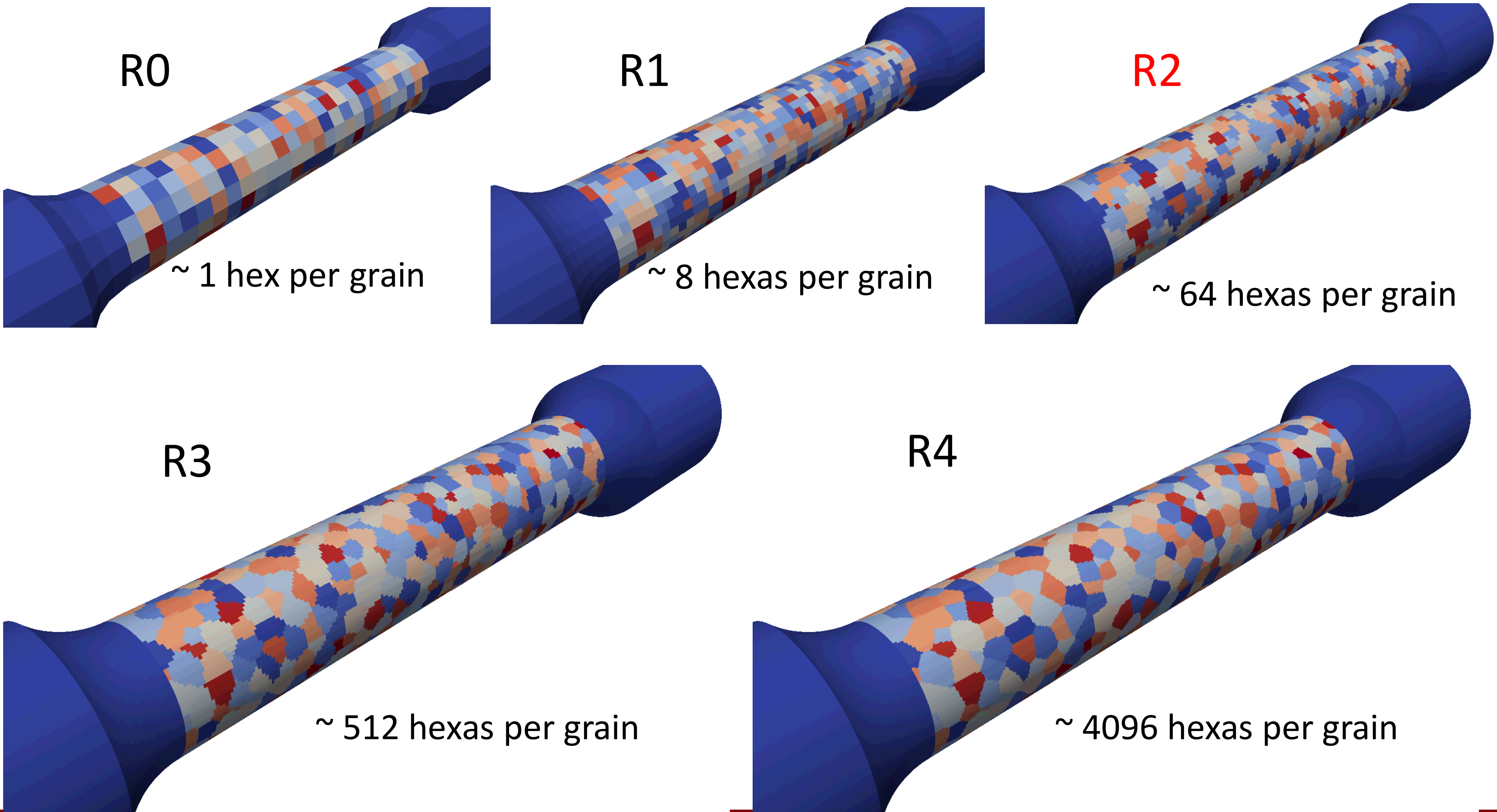

Voronoi Overlay of Hierarchy of Hexahedral Meshes

One grain realization with ~ 12 grains through the diameter (~ 6200 grains)

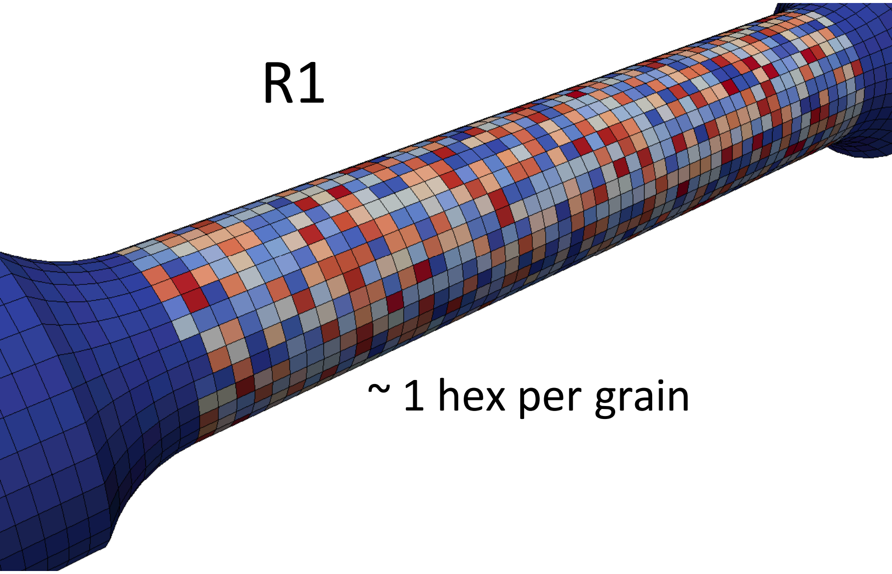

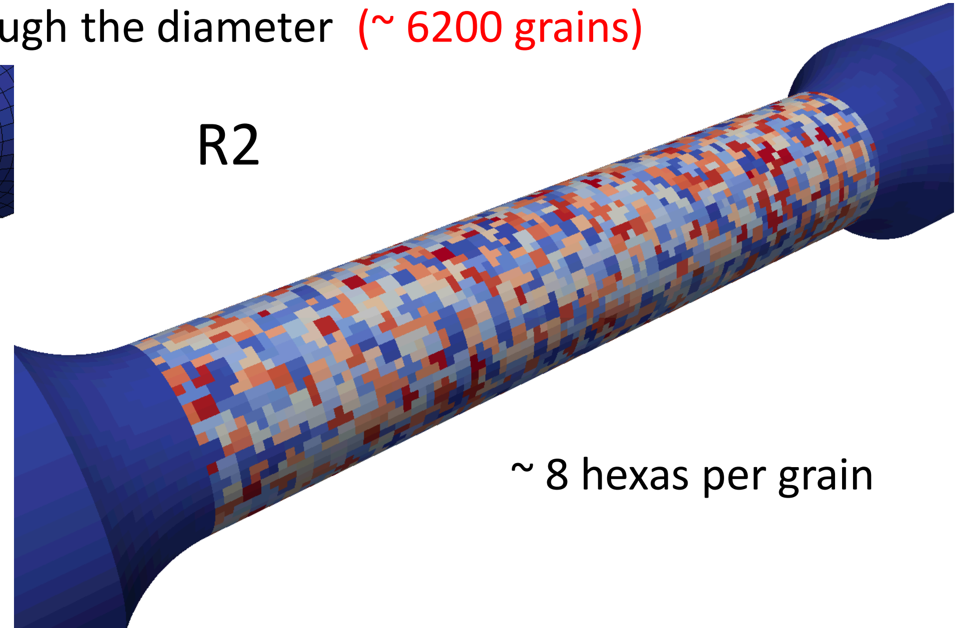

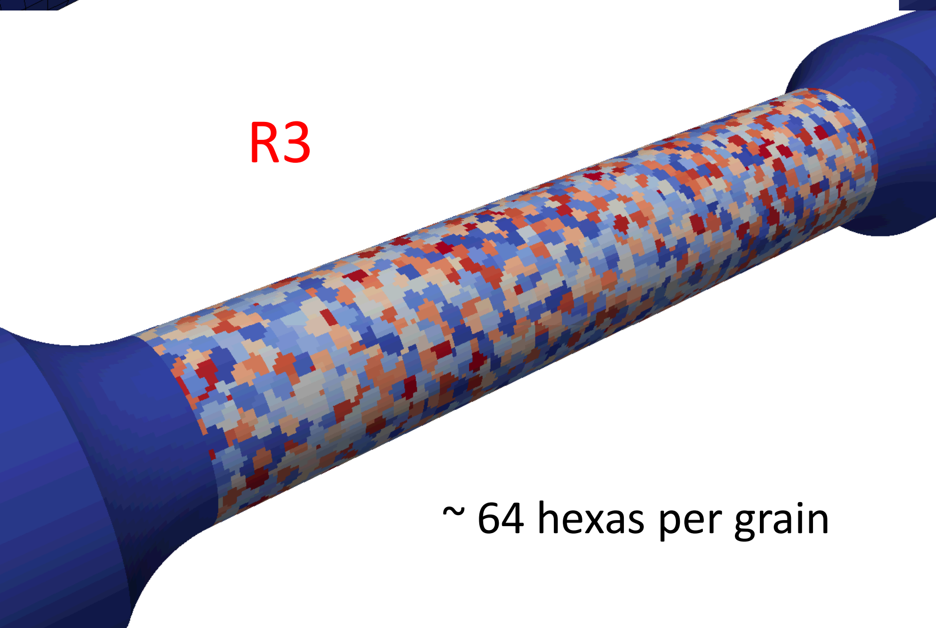

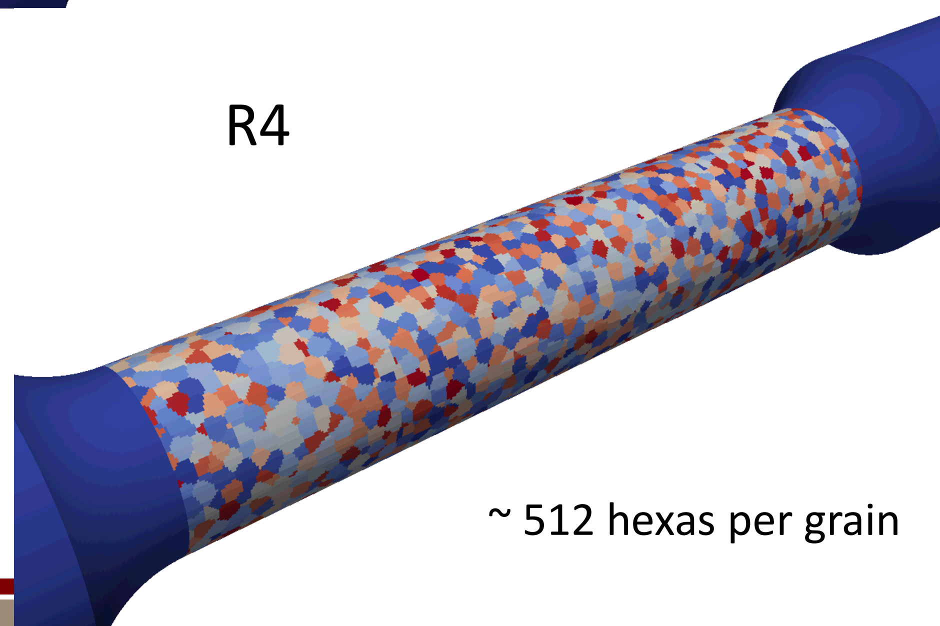

304L Single Crystal Elasticity Constants

(Ledbetter, 1984)

single crystal elastic constants (cubic symmetry)

$$C_{11} = 204.6 \ \text{GPa}$$
$$C_{12} = 137.7 \ \text{GPa}$$
$$C_{44} = 126.2 \ \text{GPa}$$

anisotropy ratio,

$$A = \frac{2C_{12}}{C_{11} - C_{44}} = 3.5$$

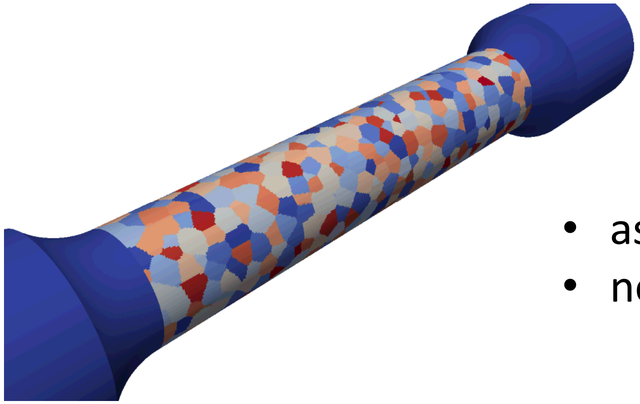

- assume random crystallographic orientations
- no correlation between grains (no texture)

RPI Crystal Plasticity Model

(Dave Littlewood, John Emery, Chris Weinberger)

plastic velocity gradient: $L^p = \sum_{\alpha=1}^{N} \dot{\gamma}^\alpha P^\alpha$ (sum over slip systems)

Schmid tensor: $P^\alpha = m^\alpha \otimes n^\alpha$

slip system slip rates: $\dot{\gamma}^\alpha = \dot{\gamma}_o \frac{\tau^\alpha}{g^\alpha} \left| \frac{\tau^\alpha}{g^\alpha} \right|^{1/m-1}$

slip system hardening: $g = g_o + (g_{so} - g_o) \left[1 - \exp \left(- \frac{G_o}{g_{so} - g_o} \gamma \right) \right]$

$$\gamma = \sum_{s=1}^{N} |\gamma^s|$$

How to Get Homogenized Material Model?

- Ideally, would use computational homogenization (FE^2) for nonlinear homogenization
- Since this is not available, use a simple power-law hardening plasticity model.
- Use RVE techniques to get isotropic elasticity constants

number of grains	apparent Young's Modulus (GPa)	apparent Poisson's ratio
~8^3 grains	177.2	0.317
~16^3 grains	180.6	0.312
~32^3 grains	182.4	0.310
∞	184.1	0.309

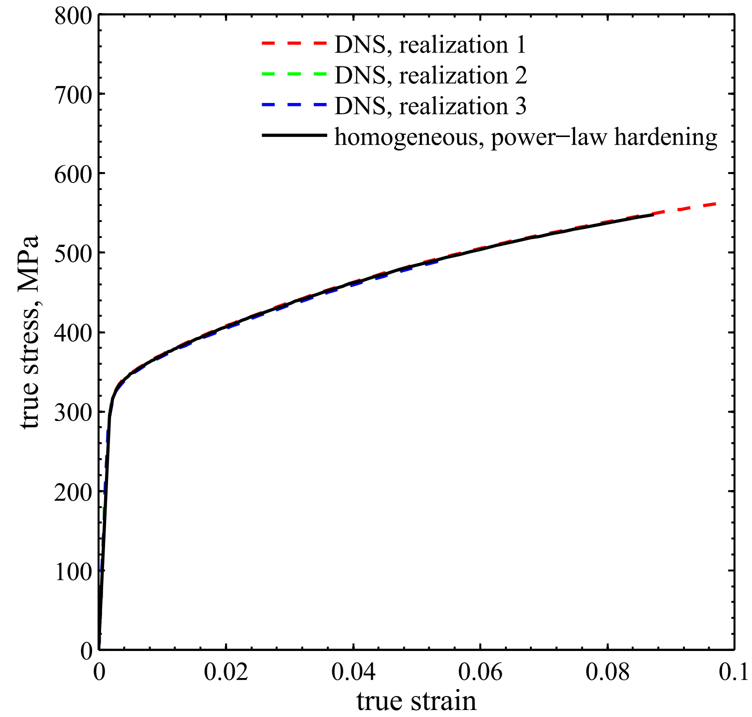

I-Beam Example

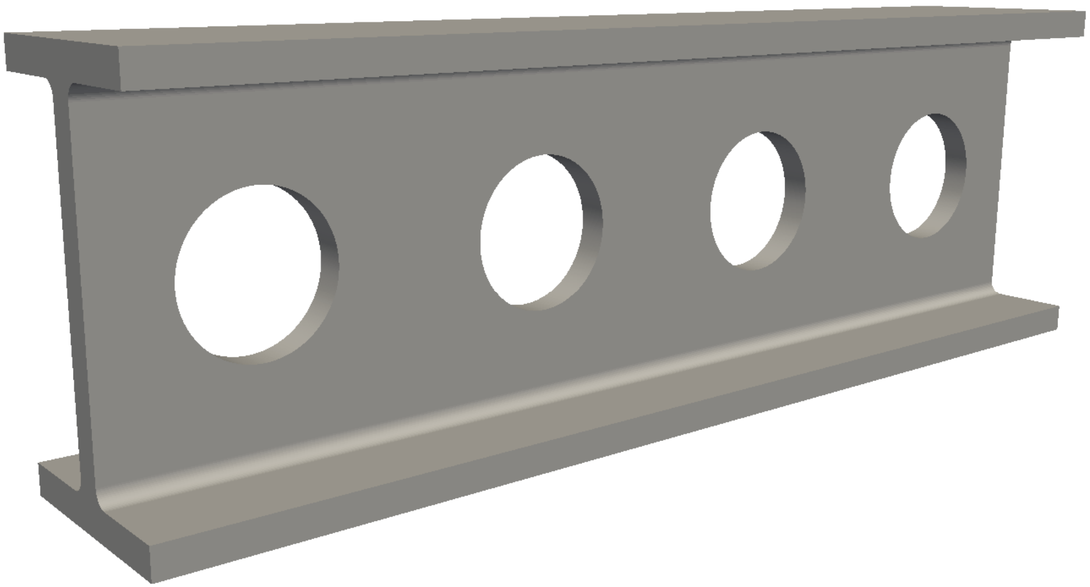

- tension
- bending
- torsion

Hierarchy of Hexahedral Meshes

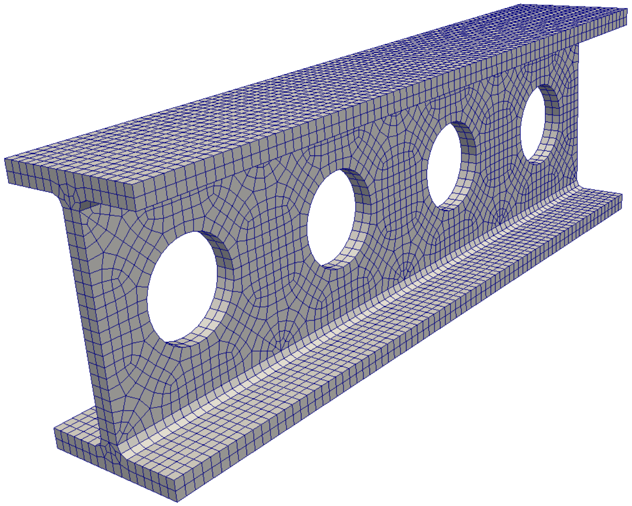

- R0
- 8,576 hexas

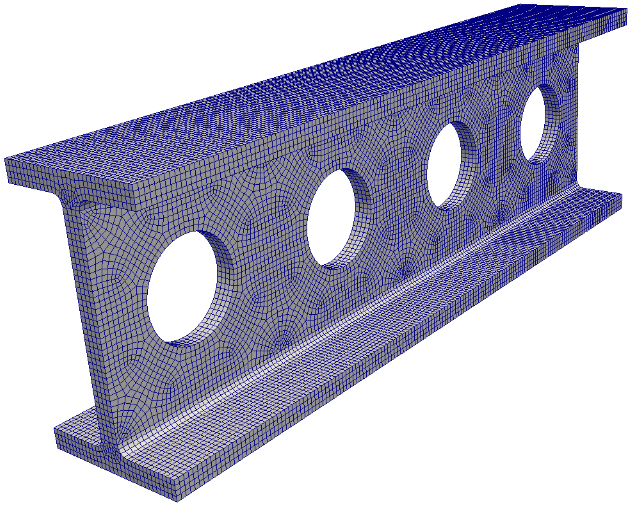

- R1
- 69K hexas

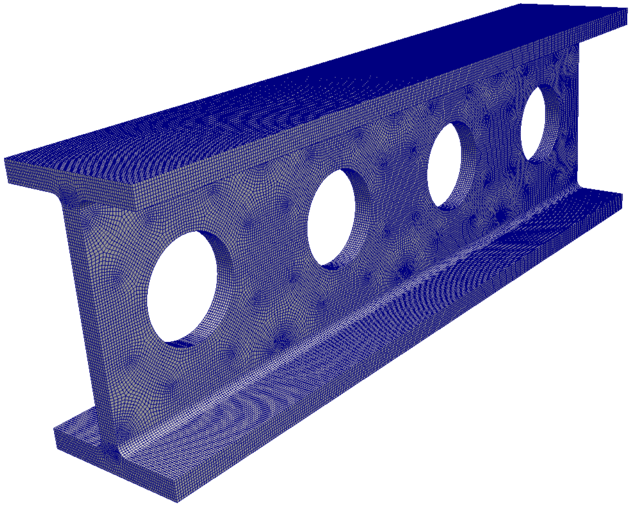

- R2
- 549K hexas

- R3
- 4.4M hexas

- R4
- 35M hexas

Thickness/grain-ratio = 8

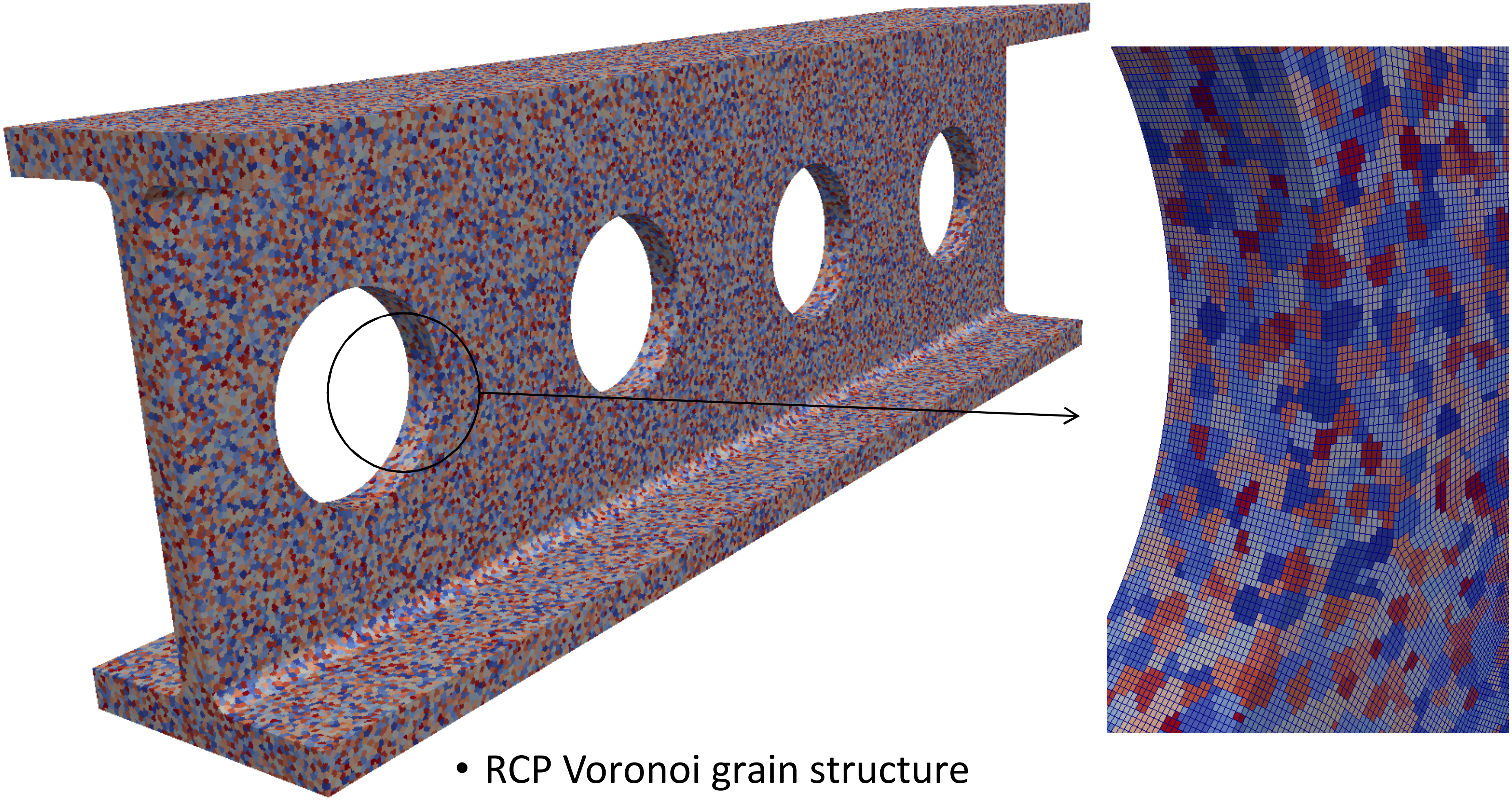

- RCP Voronoi grain structure
- 420K grains
- hex mesh overlay = R4 (35M elements)

Homogenized solution

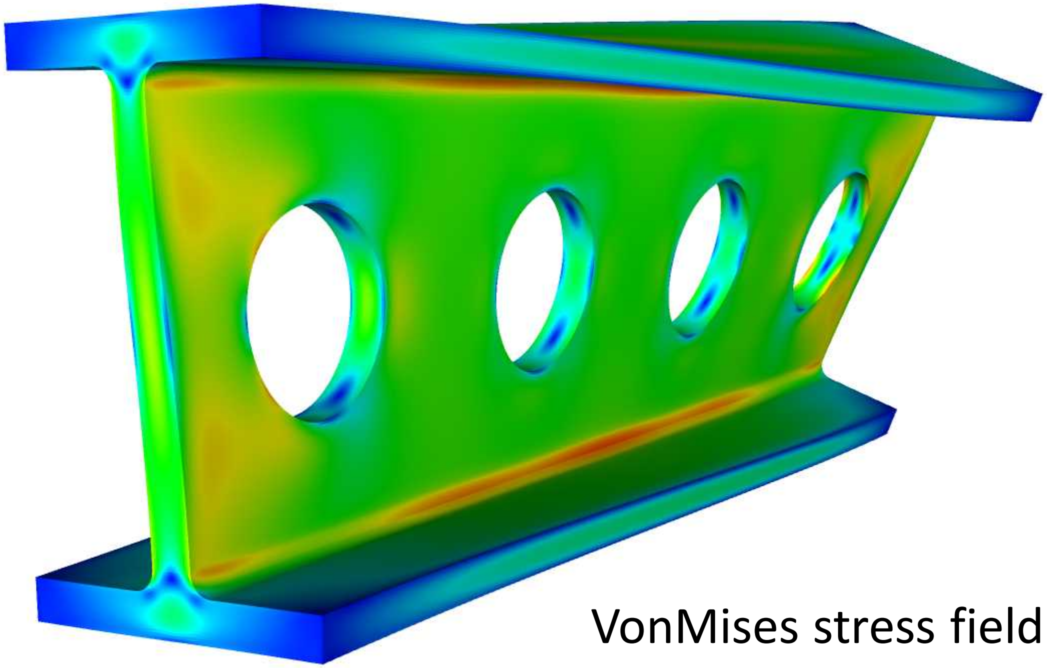

VonMises stress field

Direct numerical simulation

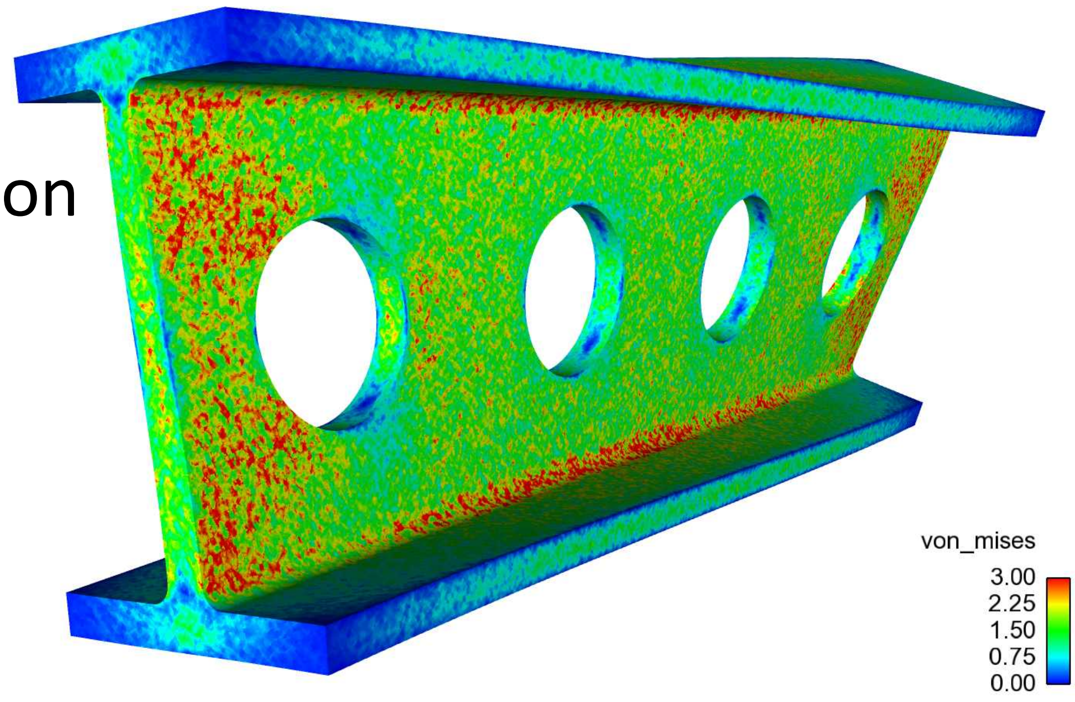

Homogenized Solution vs. Direct-Numerical Simulation

Stress magnitude along lower fillet

realization 1

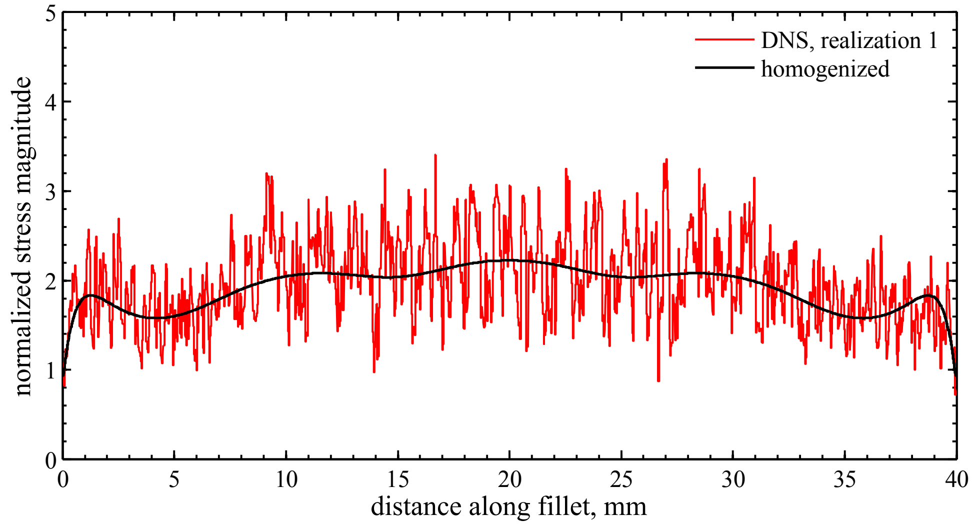

realization 2

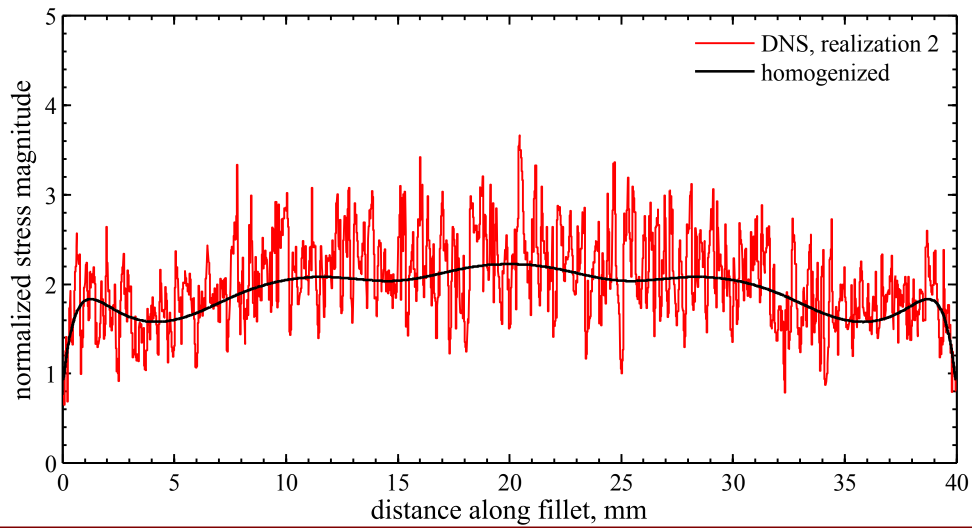

Homogenized Solution vs. Ensemble Average

Beran and McCoy (1970) showed that the governing equation for the mean field is nonlocal.

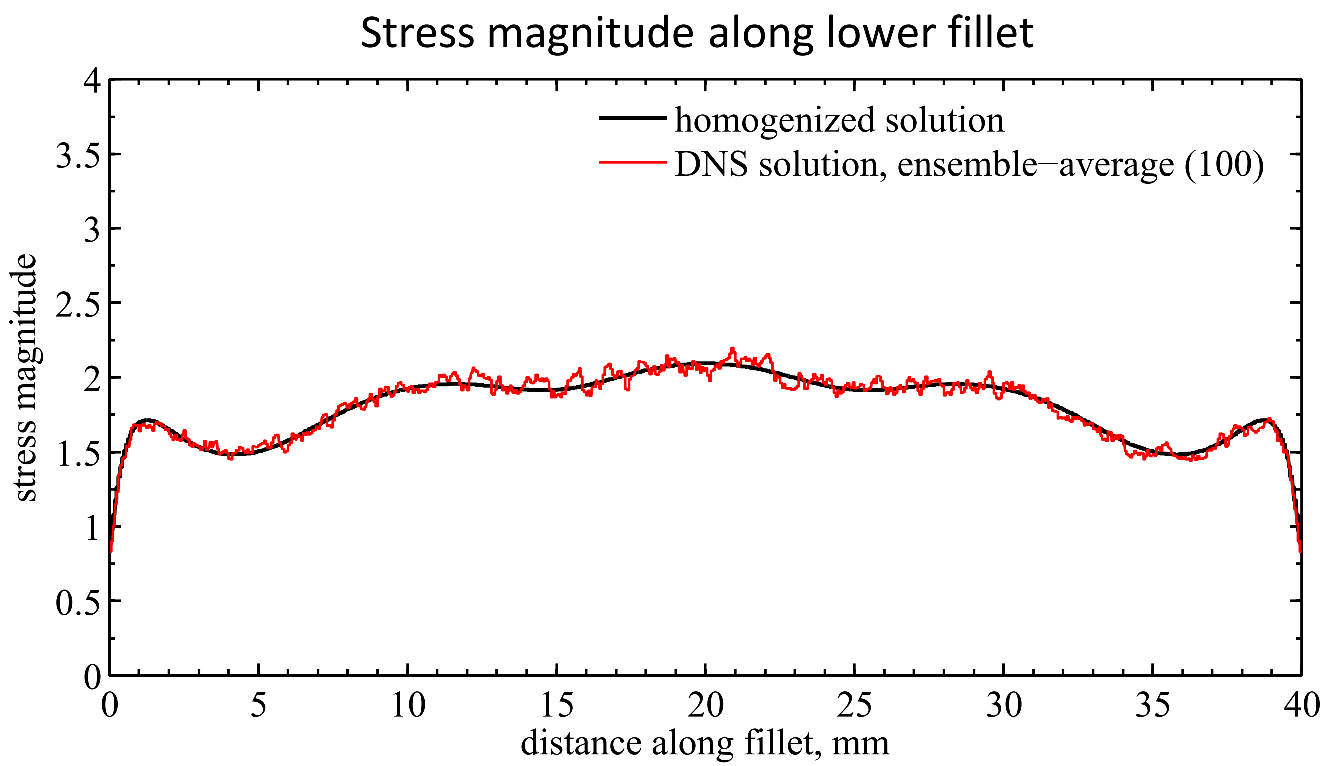

See no evidence for nonlocality here.

Homogenized Solution vs. Direct-Numerical Simulation

Stress magnitude around hole

realization 1

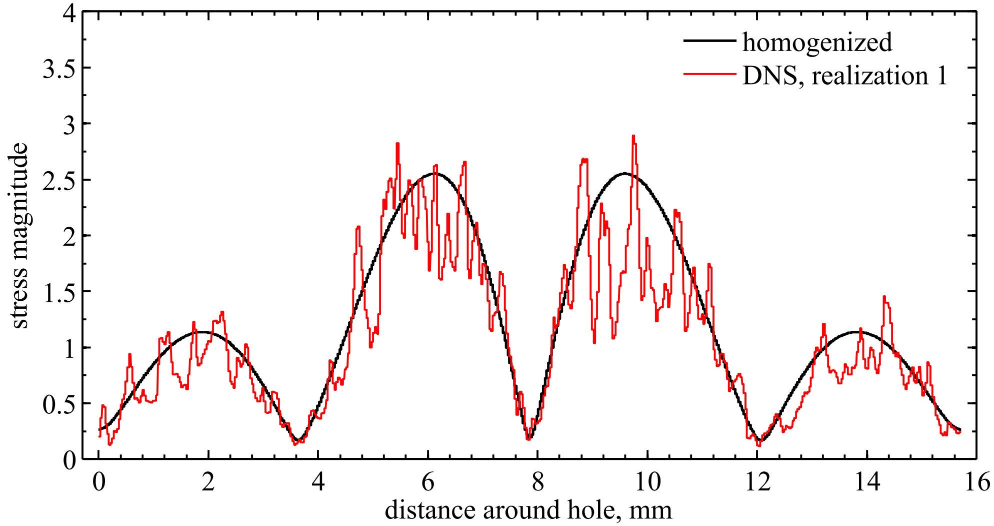

realization 2

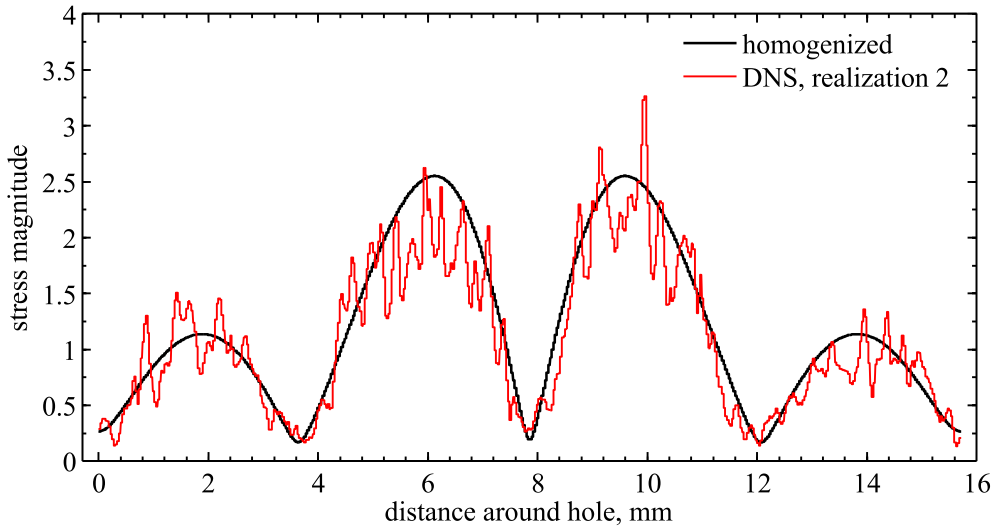

Homogenized Solution vs. Ensemble Average

Stress magnitude around hole

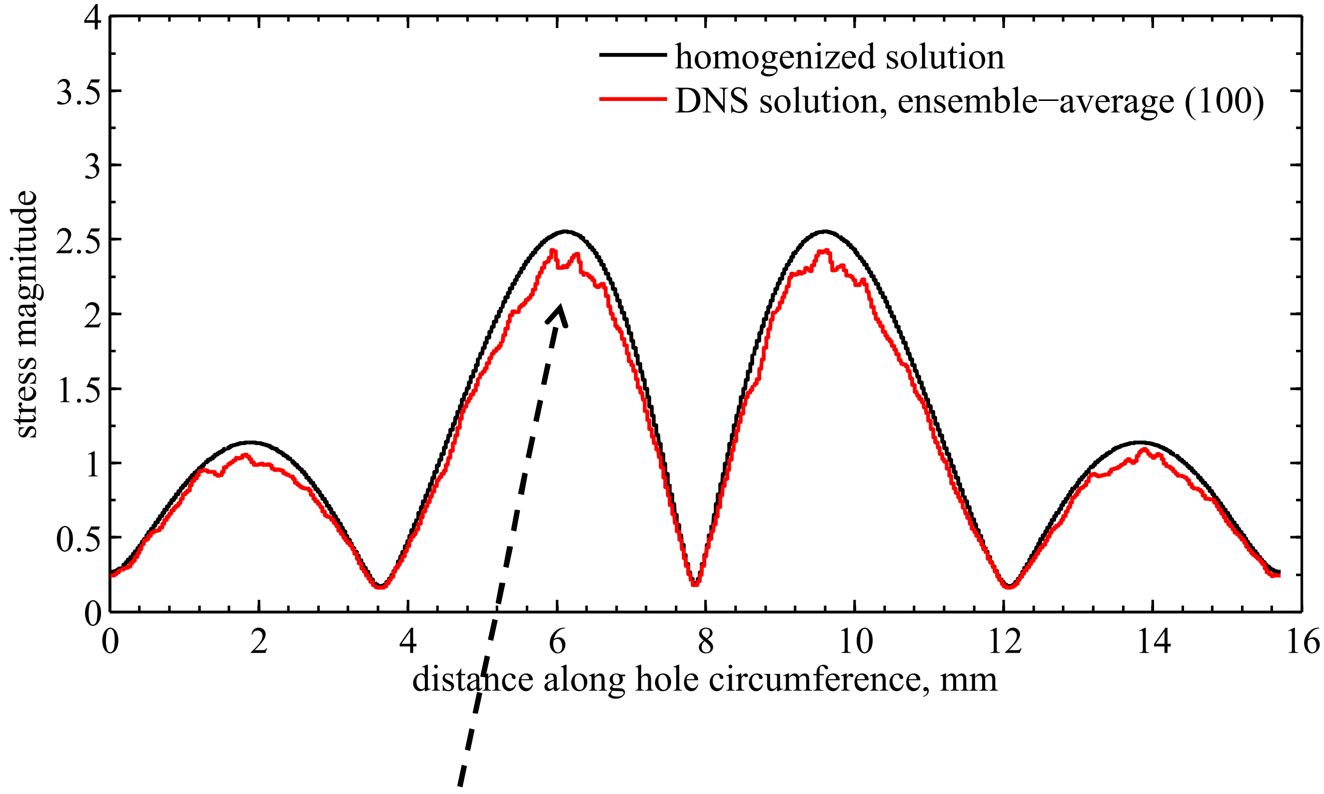

See some evidence for nonlocality here.

3D Moving Average using Gaussian Filter

Sandia National Laboratories

convolution

$$\hat{\sigma}_{ij}(\mathbf{x}) = \gamma_\alpha(\mathbf{x}) * \sigma_{ij}(\mathbf{x}) = \int_{\Omega_\infty} \gamma_\alpha(\mathbf{x}-\mathbf{y})\sigma_{ij}(\mathbf{y})d\mathbf{y}$$

$$\gamma_\alpha(\mathbf{x}-\mathbf{y}) = A\, e^{-\frac{||\mathbf{x}-\mathbf{y}||^2}{\alpha^2}}$$

A = normalization constant to reproduce constant functions

cutoff frequency $\omega_c = \frac{\sqrt{2\ln 2}}{\alpha} = \frac{1.1774}{\alpha}$

Gaussian Kernel

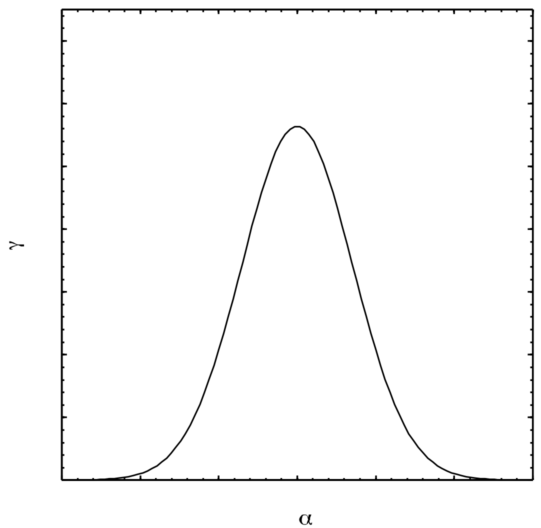

Gain vs. spatial frequency

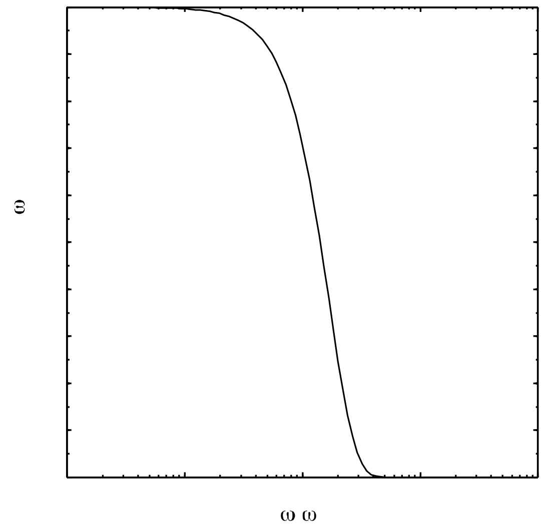

3D Moving Average using Gaussian Filter

unfiltered

filtered

$\alpha = 1.0\,\mathrm{mm}$

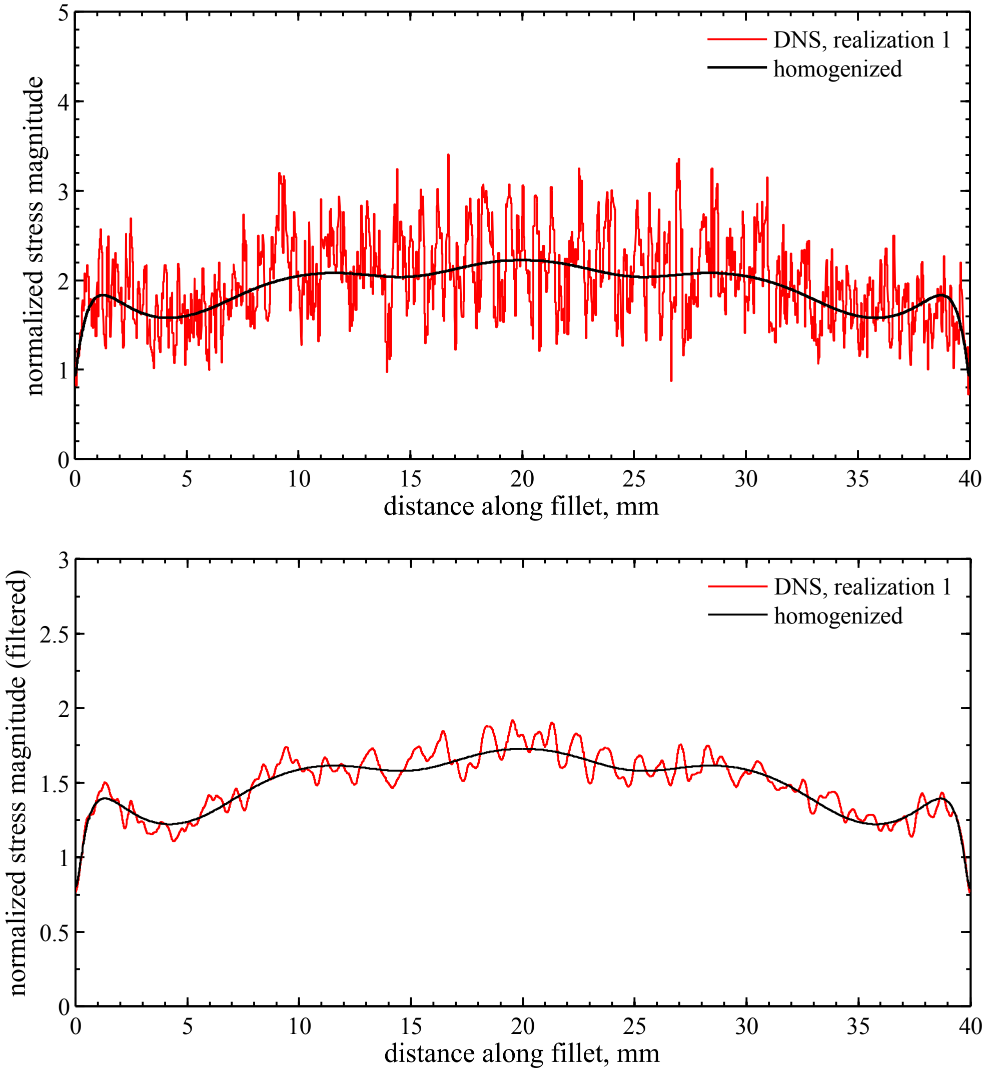

Homogenized solution is a surprisingly good approximation.

Stainless-steel Tube under Combined Tension-Torsion

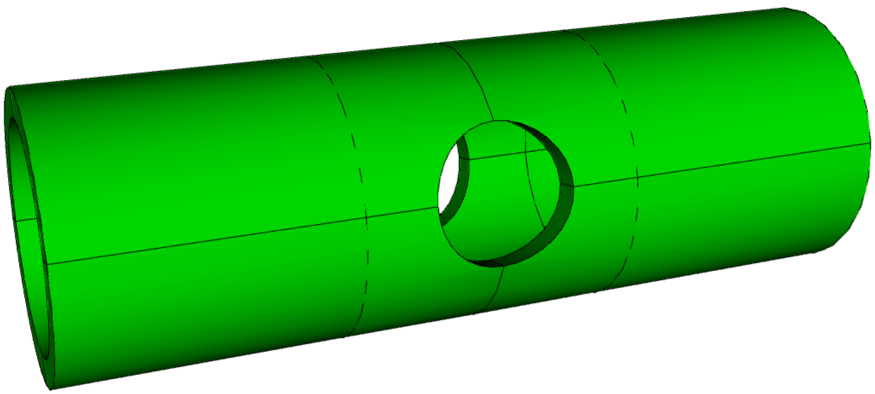

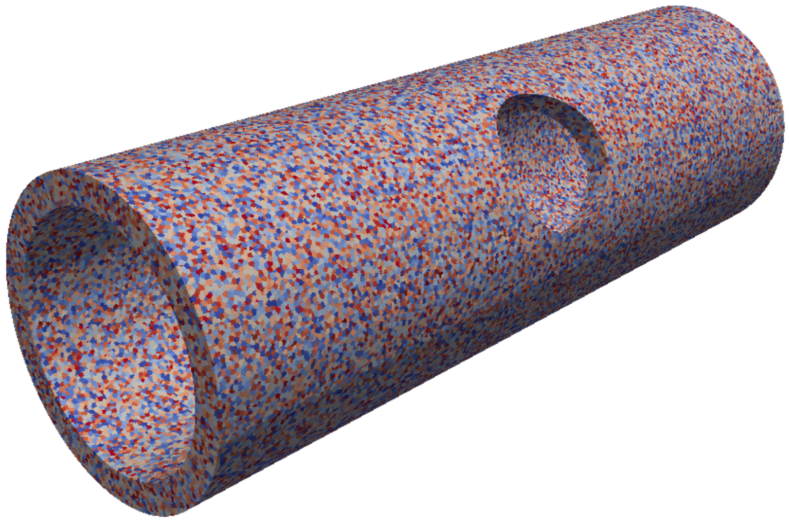

Axial Load

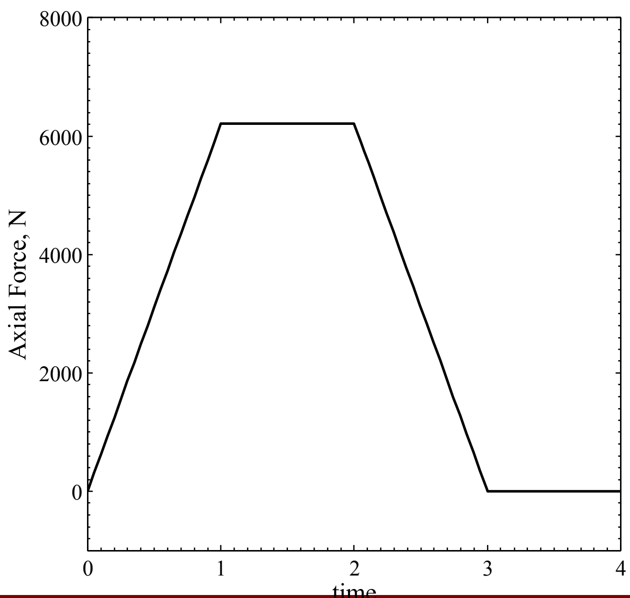

Torque

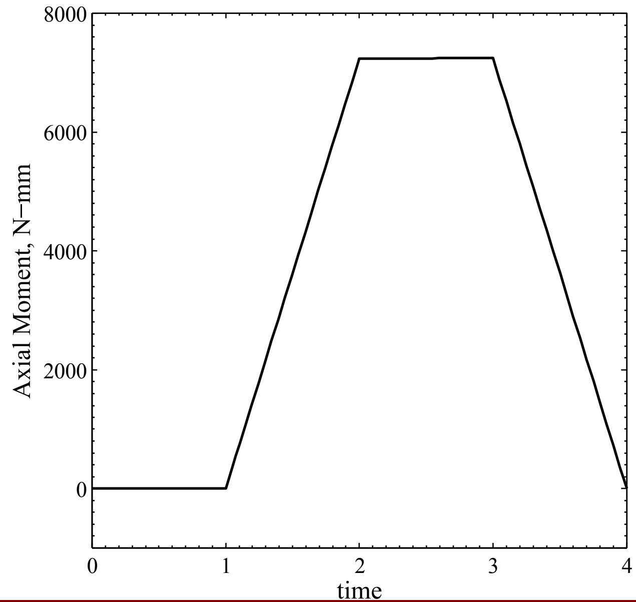

Strain under Combined Tension-Torsion

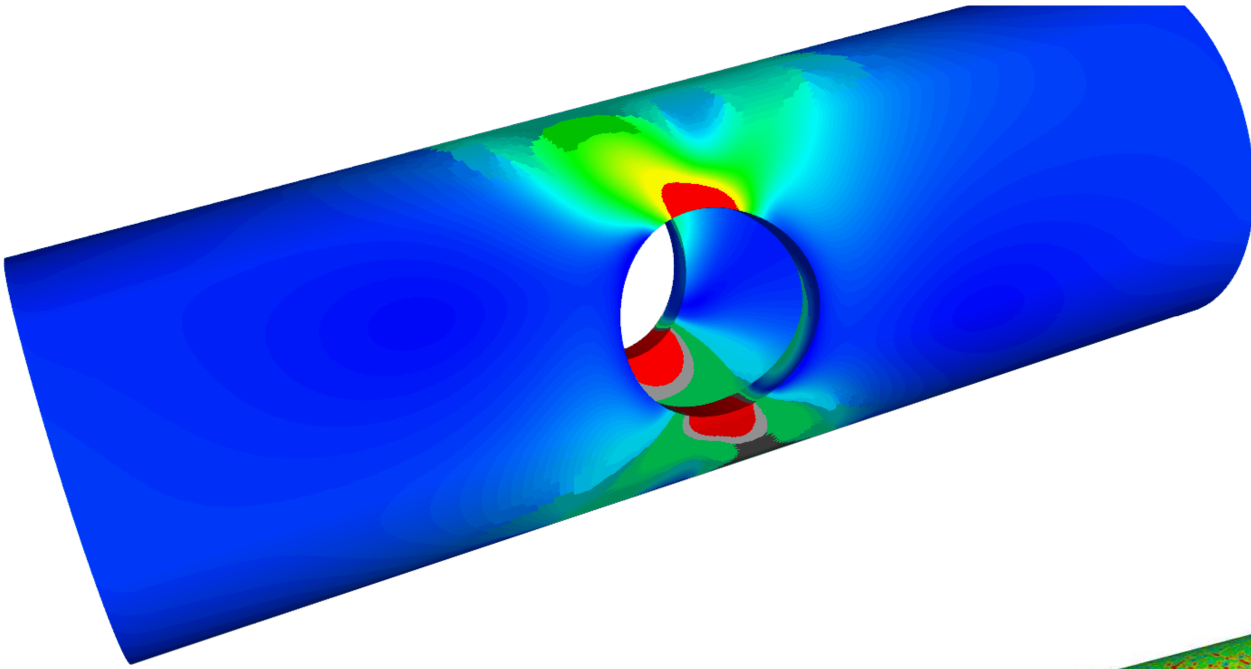

- homogenized isotropic power-law hardening plasticity model

- direct numerical simulation
- crystal plasticity model
- 352,000 grains
- 8 grains through the thickness

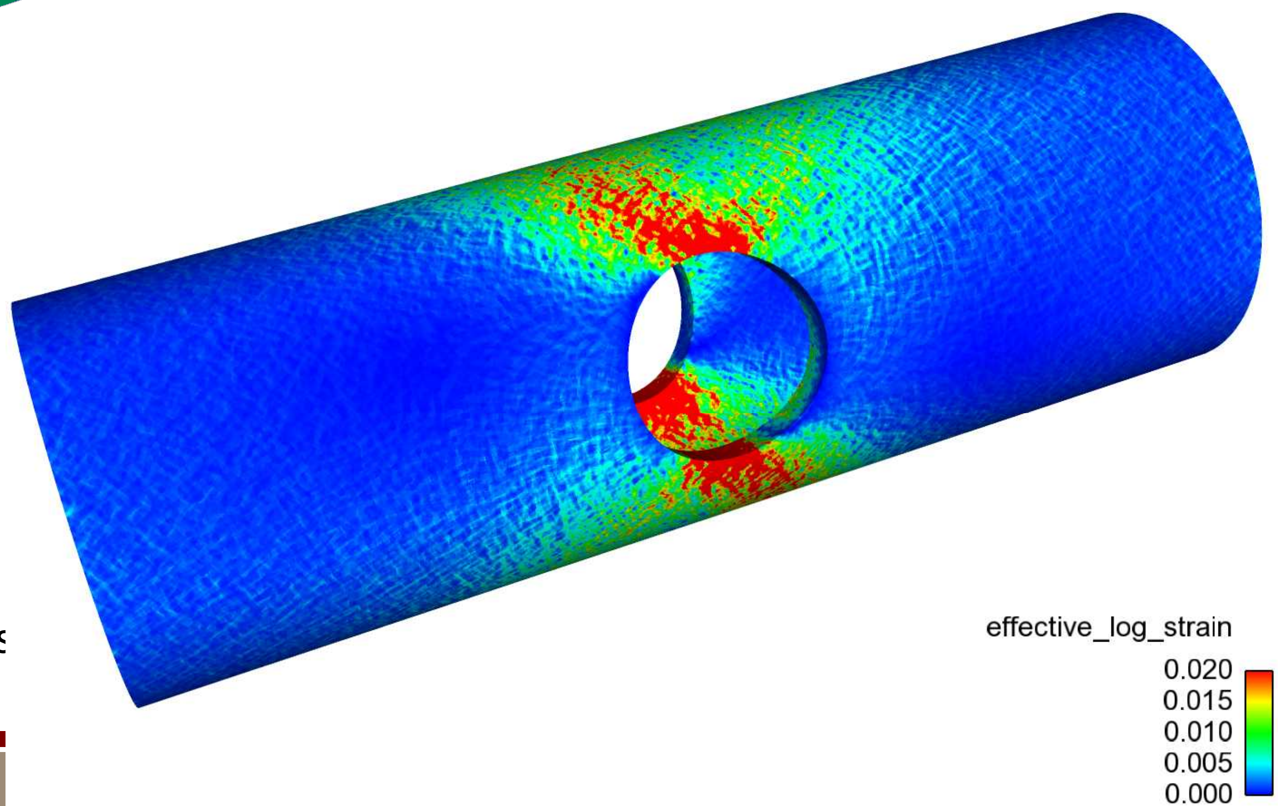

Axial Load Only

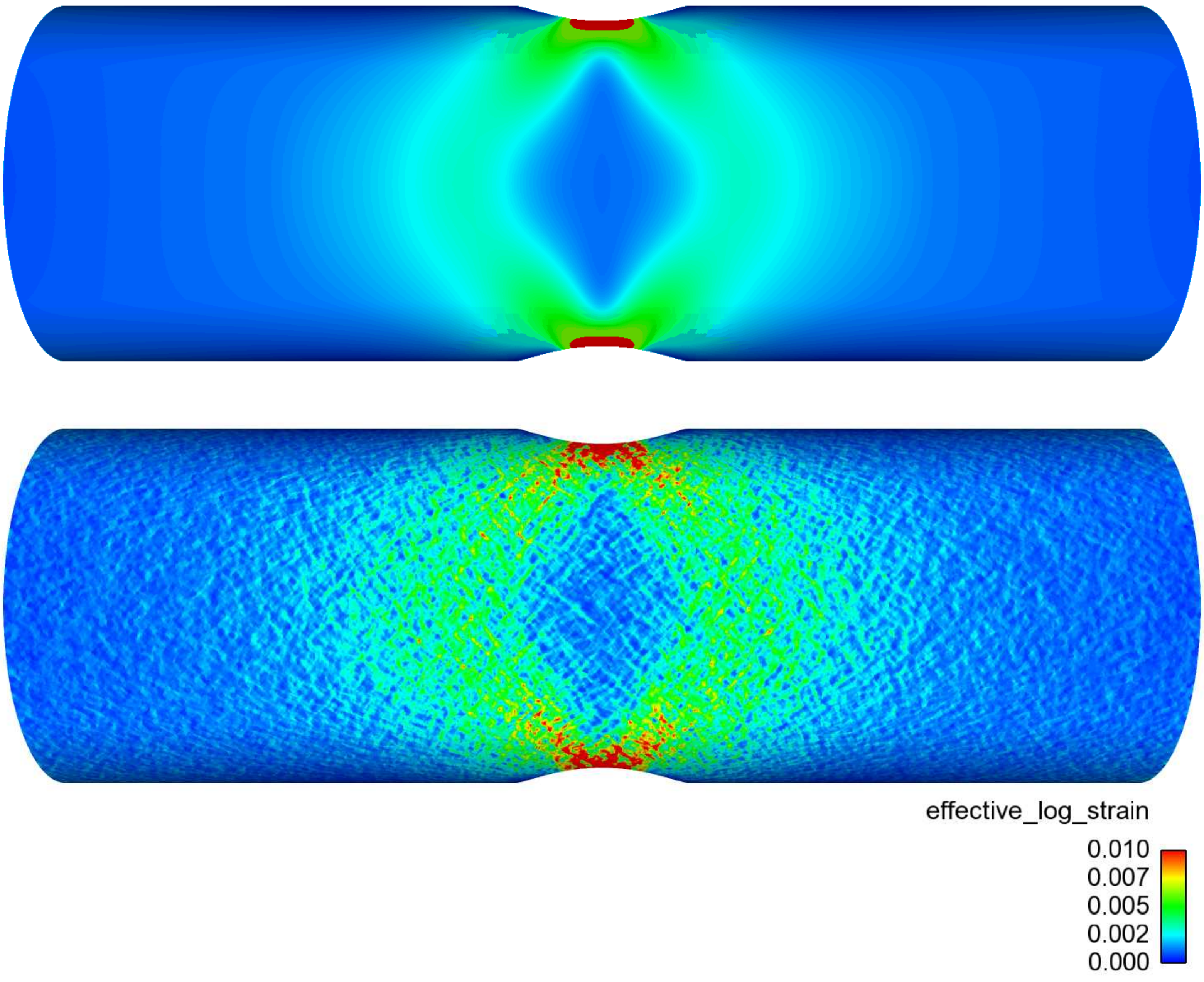

Axial Load + Torsion

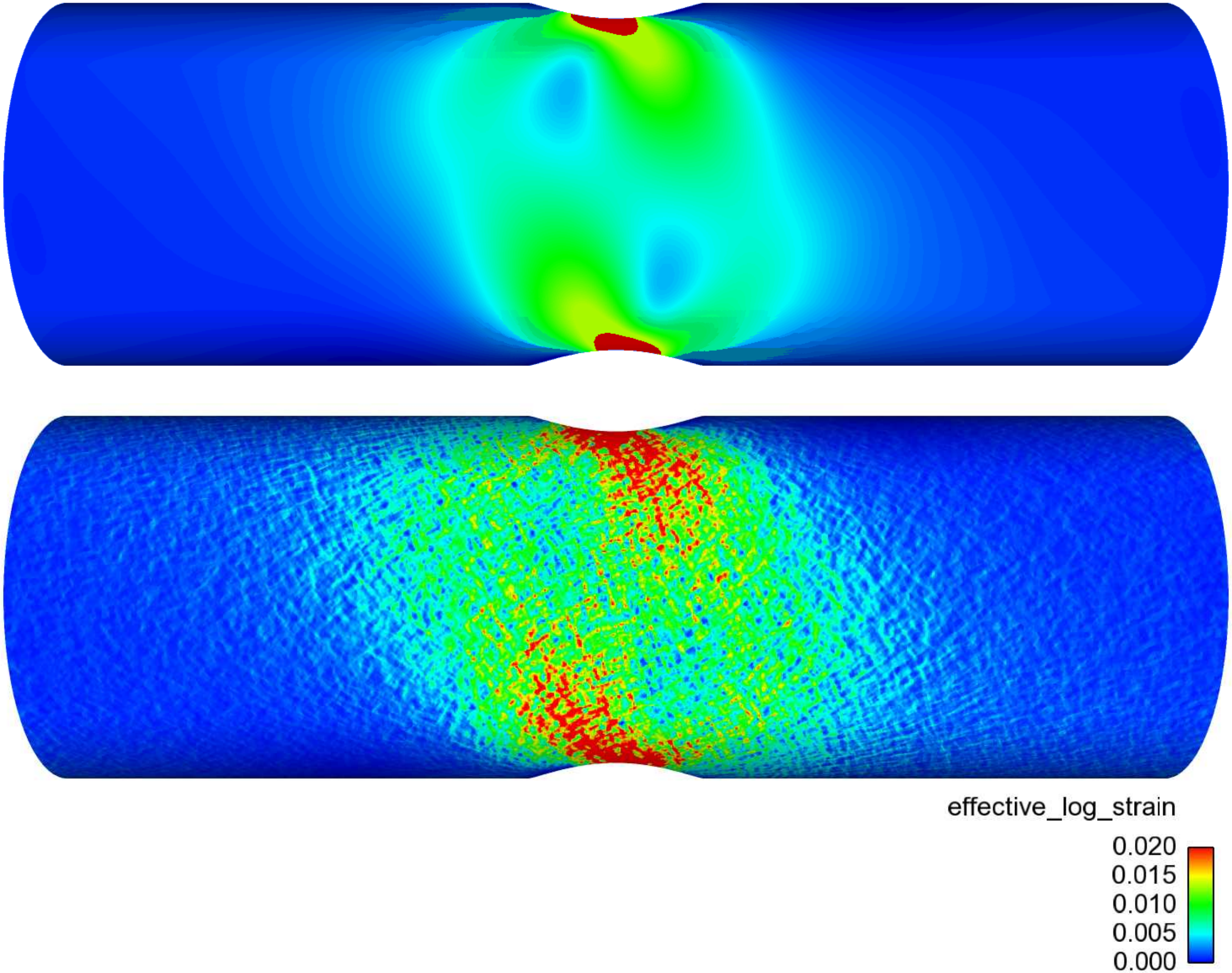

Strain magnitude along length of tube

(midsection between holes, combined tension-torsion)

unfiltered

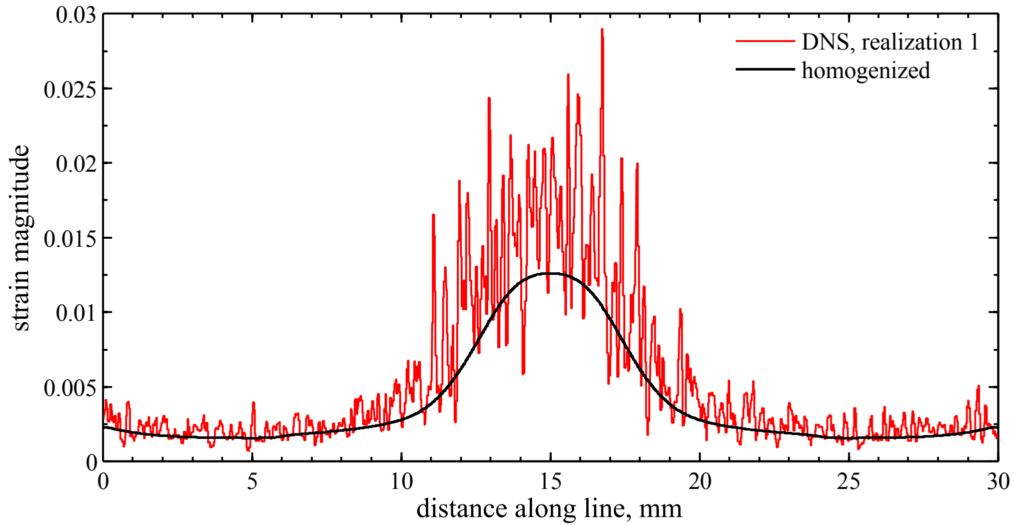

filtered

$\alpha = 1.0\,\mathrm{mm}$

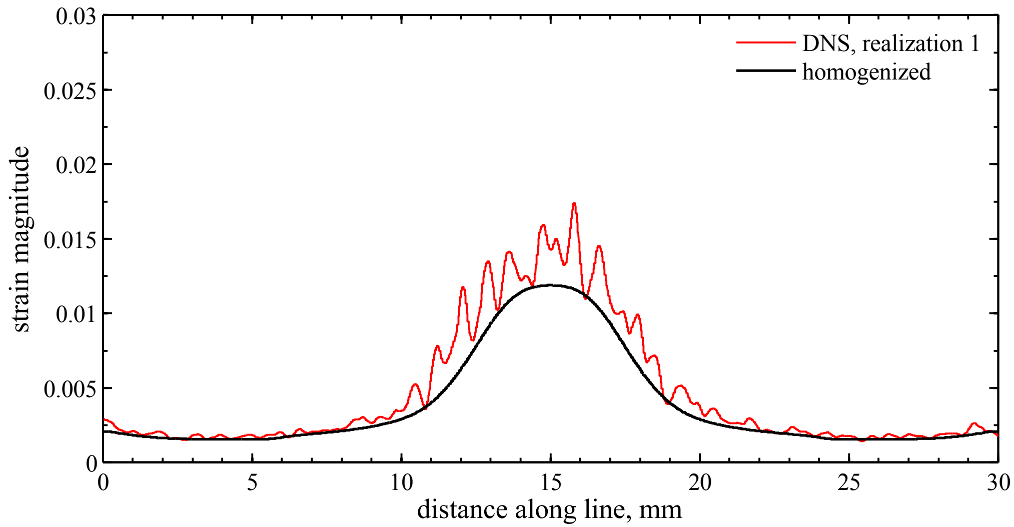

Homogenized solution is a surprisingly good approximation to the filtered response.

Strain magnitude around hole

(inside circumference, combined tension-torsion)

unfiltered

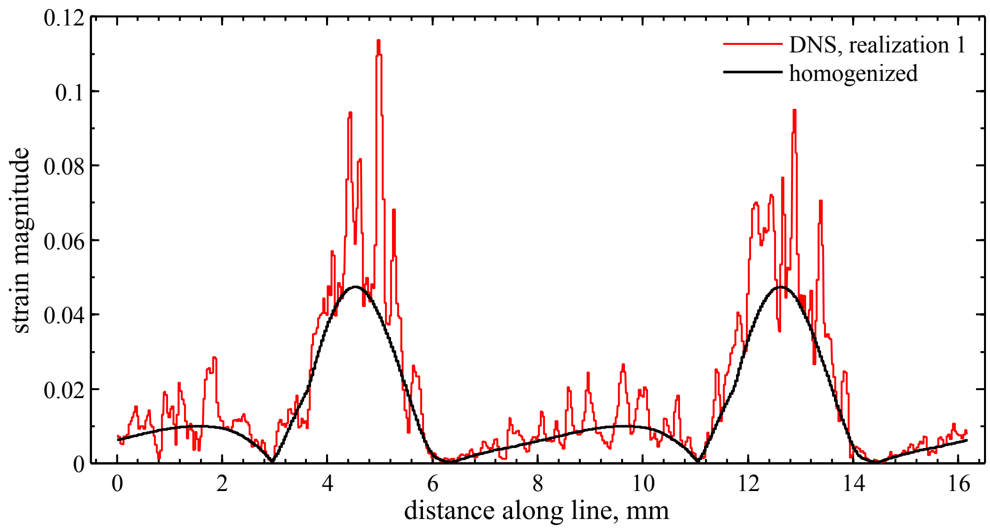

filtered

$\alpha = 1.0\,\mathrm{mm}$

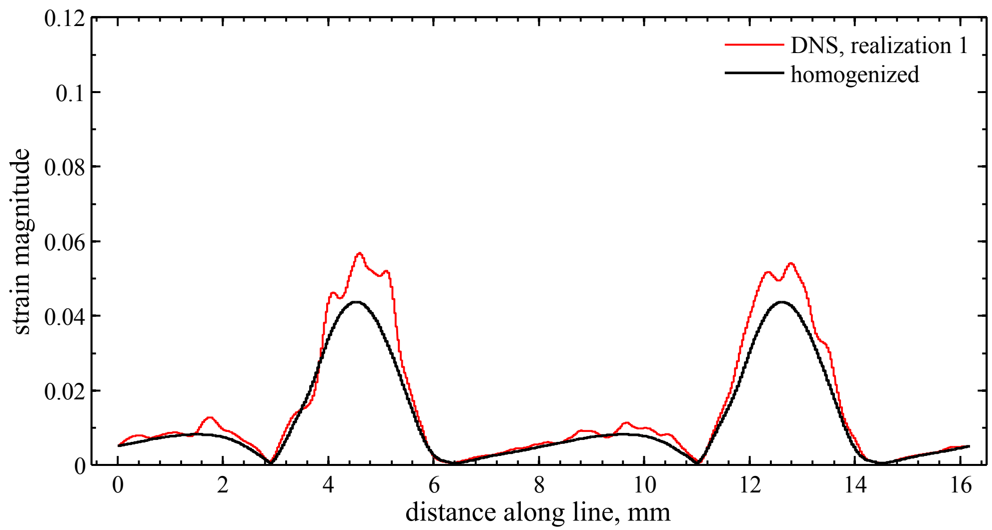

Homogenized solution is a surprisingly good approximation to the filtered response.

Global Stretch and Rotation of Tube

axial stretch

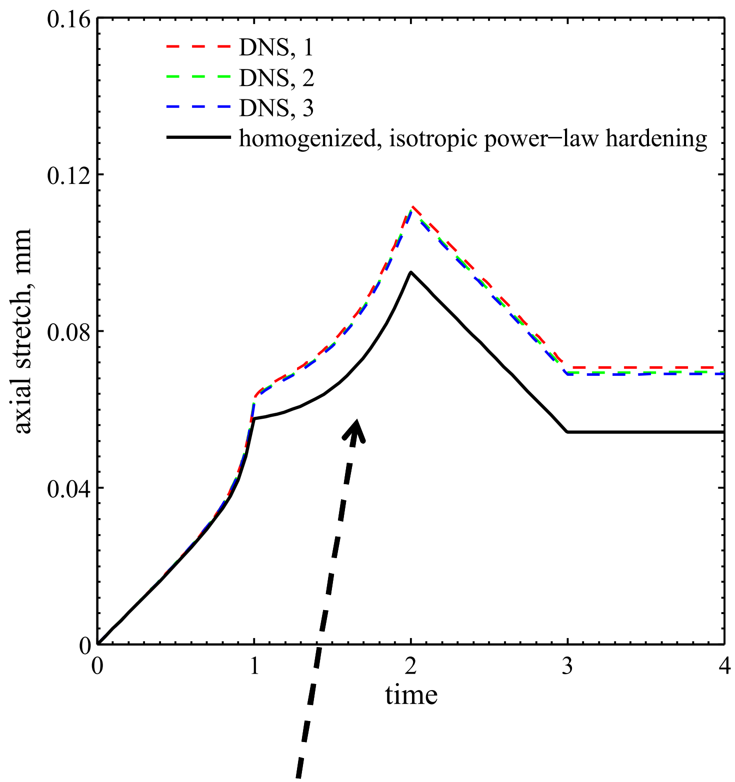

rotation

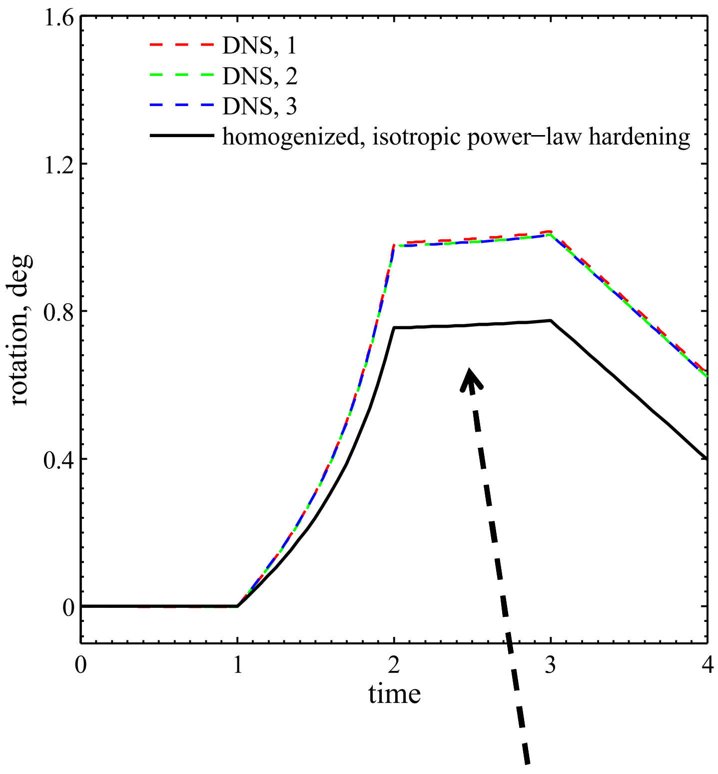

Homogenized solution good in tension-only region but less accurate in combined tension-torsion.

Summary

- Identified two types of material variability; Type-1 is “classical” while Type-2 arises from higher-order effects (gradient, surface, nonlocal).
- Used Direct Numerical Simulations of macroscale boundary value problems containing microstructure to investigate Type-2 material variability.
- Found little evidence of higher-order effects for this material and these BVPs.

Future Work

- Investigate DNS mesh resolution (~280M element model requires 3-level FETI solver on ~16000 cores)
- Investigate the use of "Filter" multiscale scheme (Yvonnet & Bonnet, 2014) for incorporating microscale variability in macroscale models.

Extra

Stochastic Volume Elements

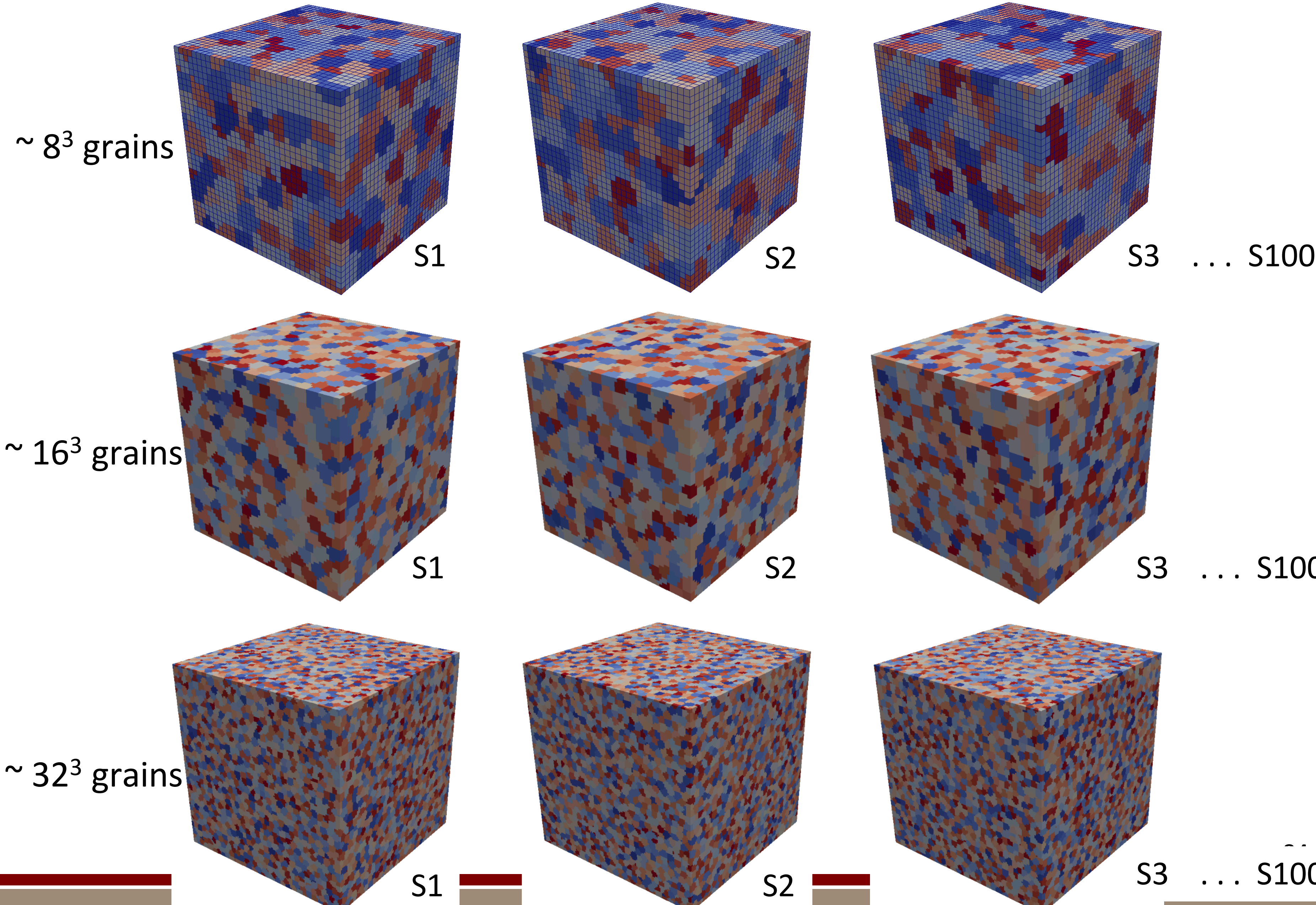

Stochastic Volume Elements

- traction boundary conditions corresponding to uniaxial stress state
- recover average strain field
- calculate apparent moduli
- 100 realizations at each grain level
- take average

Von Mises stress field

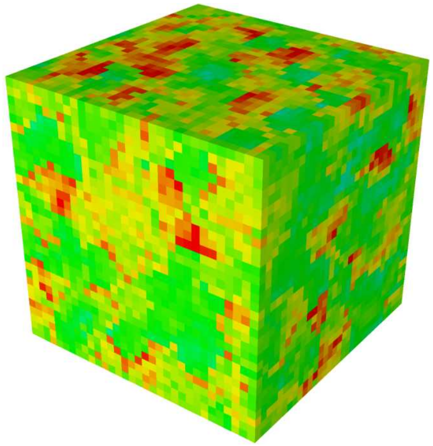

~ 8^3 grains

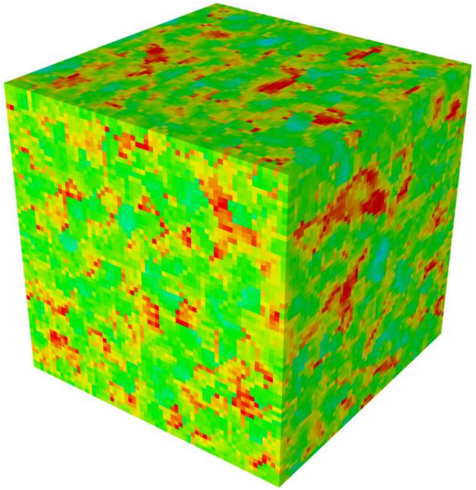

~ 16^3 grains

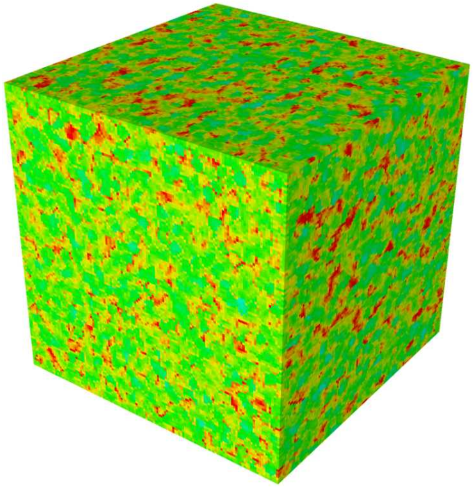

~ 32^3 grains

Convergence to Effective Isotropic Properties

- mean of 100 simulations at each "grain level"
- rational function extrapolation to ∞
- first order convergence rate

number of grains	apparent Young's Modulus (GPa)	apparent Poisson's ratio
~8^3 grains	177.2	0.317
~16^3 grains	180.6	0.312
~32^3 grains	182.4	0.310
∞	184.1	0.309

These values will be used as the homogenized, isotropic properties.